Spark Ignition Energy Measurements in Jet A

Joseph E. Shepherd, J. Christopher Krok, and Julian J. Lee

Graduate Aeronautical Laboratories
California Institute of Technology
Pasadena, CA 91125

May 3, 1999 **Revised January 24, 2000**

Explosion Dynamics Laboratory Report FM97-9

Prepared for and supported by the National Transportation Safety Board
Under Order NTSB12-97-SP-0127

Abstract

Experiments have been carried out to measure the spark ignition energy of Jet A vapor in air. A range of ignition energies from 1 mJ to 100 J was examined in these tests. The test method was validated by first measuring ignition energies for lean mixtures of the fuels hexane (C_6H_6) and propane (C_3H_8) in air at normal temperature (295 K) and pressure (1 atm). These results agree with existing data and provide new results for compositions between the lean flame limit and stoichiometric mixtures. Jet A (from LAX, flashpoint 45 – 48°C) vapor mixtures with air have been tested at temperatures between 30 and 60°C at two fuel mass loadings, 3 and 200 kg/m^3, in an explosion test vessel with a volume of 1.8 liter. Tests at 40, 50, and 60°C have been performed at a mass loading of 3 kg/m^3 in an 1180-liter vessel. Experiments with Jet A have been carried out with initial conditions of 0.585 bar pressure to simulate altitude conditions appropriate to the TWA 800 explosion.

Ignition energies and peak pressures vary strongly as a function of initial temperature, but are a weak function of mass loading. The minimum ignition energy varies from less than 1 mJ at 60°C to over 100 J at 30°C. At temperatures less than 30°C, ignition was not possible with 100 J or even a neon sign transformer (continuous discharge). The peak pressure between 40 and 55°C was approximately 4 bar. Peak pressures in the 1180-liter vessel were slightly lower and the ignition energy was higher than in the 1.8-liter vessel.

The following conclusions were reached relative to the TWA 800 crash: (a) spark ignition sources with energies between 5 mJ and 1 J are sufficient to ignite Jet A vapor, resulting in a propagating flame; (b) the peak pressure rise was between 1.5 and 4 bar (20 and 60 psi). (c) a thermal ignition source consisting of a hot filament created by discharging electrical energy into a metal wire is also sufficient to ignite Jet A vapor, resulting in a propagating flame; (d) laminar burning speeds are between 15 and 45 cm/s; and (e) the limited amount of fuel available in the CWT (about 50 gal) did not significantly increase the flammability limit.

The rapid decrease in spark ignition energy with increasing temperature demonstrates that hot fuel tanks are significantly more hazardous than cool ones with respect to spark ignition sources. A systematic effort is now needed in order to utilize these results and apply spark ignition energy measurements to future analyses of fuel tank flammability. Some key issues that need to be addressed in future testing are: (a) effect of flashpoint on the ignition energy-temperature relationship; (b) ignition energy vs. temperature as a function of altitude; (c) effect of fuel weathering on ignition energy; and (d) the effect of ignition source type on ignition limits.

Contents

1 Introduction **1**

2 Spark Ignition **5**
2.1 Jet A Ignition Experiments 7

3 Experimental Apparatus **11**
3.1 Gas Ignition Vessel 11
3.1.1 Vessel 11
3.1.2 Gas-Feed System 11
3.1.3 Electrodes 13
3.1.4 Experimental Procedure 13
3.2 Heated Ignition Vessel 14
3.2.1 Vessel 14
3.2.2 Gas and Liquid Supply System 14
3.2.3 Electrodes 14
3.2.4 Experimental Procedure 15
3.3 The 1180-Liter Vessel 16
3.4 Spark Discharge and Electrode Issues 17
3.4.1 Spark Energy 17
3.4.2 High-Voltage Switching 19
3.4.3 Circuit Reactance 20
3.4.4 Electrode Type 21

4 Validation Tests **23**
4.1 Propane Combustion 23
4.1.1 Ignition Energy 23
4.1.2 Combustion Pressure 24
4.1.3 Flame Speeds 25
4.2 Hexane Combustion 25
4.2.1 Ignition Energy 25
4.2.2 Combustion Pressure 26
4.2.3 Flame Speeds 27

5 Jet A Combustion **31**
5.1 Flashpoint Measurements 31
5.2 Ignition Energy Results 32
5.3 Peak Combustion Pressure 35
5.4 Burning Speed 38
5.5 Ignition in the 1180-Liter Vessel 39

6 Discussion **41**
6.1 Ignition-Energy Prediction 41
6.2 Previous Data 45
6.3 Fuel Mass Loading 46
6.3.1 Fuel Weathering 50
6.4 Pressure Dependence 53
6.5 Miscellaneous Issues 57
6.5.1 Near-Limit Behavior 57
6.5.2 Temperature Nonuniformity 57
6.5.3 Condensation 58
6.5.4 Spark Location 58
6.5.5 Relevance to Airplane Fuel Tanks 59

7 Summary and Recommendations **61**
7.1 Key Results 61
7.2 TWA 800 Crash Investigation 62
7.3 Implications for Fuel-Tank Flammability Reduction 62
7.4 Future Work 64

A Test Conditions **71**

B Hot Filament Ignition of Jet A **77**

List of Figures

1 Classical results on ignition energy by Lewis and von Elbe (1961). 6
2 Composition at MIE vs. molar mass. 6
3 Flammability limits of Jet A in air. 8
4 Ignition energy for Jet A sprays. 10
5 Schematic of the 11.25-liter vessel. 12
6 Schematic of optical arrangement. 12
7 Schematic of the gas-feed system. 13
8 Schematic of the heated ignition vessel. 15
9 Adjustable gap electrodes. 15
10 Schematic of the 1180-liter vessel. 17
11 High voltage mechanical switch spark system. 19
12 Circuit diagram for the trigger spark system. 20
13 Measured ignition energy for propane-air mixtures. 23
14 Pressure histories for propane-air combustion. 24
15 Peak pressure for propane-air mixtures. 25
16 Effective burning speeds for propane-air mixtures. 26
17 Measured ignition energy for hexane-air mixtures. 27
18 Measured pressure histories for hexane-air. 27
19 Measured peak pressure for hexane-air. 28
20 Effective burning speeds for hexane-air. 29
21 Fuel-air mass ratios. 33
22 Measured ignition energy for Jet A, 200 kg/m^3. 34
23 Measured ignition energy for Jet A, 3 kg/m^3. 35
24 Pressure histories for Jet A-air mixtures, 3 kg/m^3. 35
25 Pressure histories for Jet A-air mixtures, 200 kg/m^3. 36
26 Measured peak pressure rise for Jet A-air mixtures. 37
27 Peak pressure rise compared with previous data. 37
28 Peak pressure rise compared with AICC estimates. 38
29 Effective burning speeds in Jet A-air mixtures. 39
30 Pressure histories for Jet A-air mixtures in the 1180-liter vessel. 40
31 Photographs of ignition and growth of a flame. 41
32 Comparison of propane-air ignition energy results with correlations. 44
33 Comparison of present ignition energy results with previously reported data. . . 45
34 Flammability curves for Jet A. 46
35 Ignition energies for Jet A vapor, all mass loadings. 47
36 Vapor pressure vs. temperature. 48
37 Partial pressure vs. number of carbon atoms. 49
38 Molar mass vs. temperature for Reno Jet A (Woodrow and Seiber 1997). 50
39 Mole fraction vs. number of carbon atoms for liquid and vapor. 51
40 Effect of weathering on fuel composition. 52
41 LFL of Jet A, Nestor data. 54

42 Ignition energy vs. mixture pressure for hydrocarbons. 55
43 Ignition energy vs. altitude estimates. 56
44 Pressure and temperature vs. time for 6.9 ml of Jet A sample #5 with air in the 1.8 liter vessel at initial conditions of p_0 = 58.5 kPa, T_0 = 323 K, hot filament ignition. Test 784 of (Kunz 1998). 78
45 Pressure vs. time for 200 ml of Jet A (El Monte) with air in the 1.8 liter vessel at initial conditions of p_0 = 58.5 kPa, T_0 = 323 K Test 776 uses a 40 mJ spark ignition, test 779 uses hot filament ignition (Kunz 1998). 78
46 Video schlieren pictures of the hot filament ignition of Jet A sample #5 in the 1.8 liter vessel at initial conditions of p_0 = 58.5 kPa, T_0 = 323 K, the time interval between two frames is 17 ms. Test 784 of (Kunz 1998). 79

List of Tables

1 Discharge capacitor types. 18
2 Flashpoints of different fuels. 32
3 Flames speeds (S_u) deduced from 1180-liter vessel tests. 40
4 Propane-air flame properties. 43
5 Propane-air mixtures. 72
6 Hexane-air mixtures. 73
7 Jet A-air mixtures in 1.84-liter vessel. 74
8 Jet A-air mixtures in 1.84-liter vessel (continued). 75
9 Tests in the 1180-liter vessel. 76

1 Introduction

The purpose of the present testing is to provide basic data on ignition of mixtures of warm Jet A vapor and air. This study is part of the investigation into the crash of TWA 800 and is an extension of the previous study of Jet A properties reported in Shepherd et al. (1997). The accident investigation (NTSB 1997) has determined that the key factor in the loss of the airplane was an explosion within the center wing fuel tank (CWT). At the time of the explosion, the tank contained about 50 gallons (300 lbs) of aviation kerosene (Jet A). The fuel and air within the tank were heated by the air conditioning units (also known as the environment control system [ECS] or more simply, air packs) located directly under the center wing tank. This increased the evaporation of the liquid fuel and was a factor in creating a flammable fuel vapor-air mixture in the ullage of the tank.

The heating of the center wing tank occurs because the air packs are powered by hot (350°F) bleed air from either the main engines or the auxiliary power unit (APU). Flight testing (Bower 1997) indicates that at the time of the explosion, the temperatures in the air within the CWT ranged between 38 and 54°C (100 and 130°F), and the temperatures of the tank lower surface ranged between 38 and 60°C (100 and 140°F). Based on these temperatures, and vapor pressures measured at Caltech (Shepherd et al. 1997), the fuel vapor-air composition within the tank was estimated to be in the flammable range once the aircraft reached an altitute of 14 kft, with fuel-air mass ratios[1] between 0.040 and 0.072 (mole fractions between 0.0089 and 0.015). These estimates are corroborated by the vapor sampling of Sagebiel (1997), who measured fuel-air mass ratios between 0.048 and 0.054 (mole fractions between 0.010 and 0.012) at 14 kft. These values should be compared with a lean limit fuel-air mass ratio of 0.030 (mole fraction of 0.007) determined in previous testing (Nestor 1967; Ott 1970) on Jet A.

It is important to note that the combination of evaporation due to heating and the reduction in air pressure with increasing altitude created a flammable condition within the CWT. The finding that the fuel-vapor air mixture within the CWT was flammable at 14 kft should not be considered surprising in view of previous work (Nestor 1967; Ott 1970) on Jet A flammability. Flammability of fuel-tank ullage contents, particularly at high altitudes or with low flashpoint fuels, has long been considered unavoidable (Boeing et al. 1997). Experiments (Kosvic et al. 1971; Roth 1987) and simulations (Seibold 1987; Ural et al. 1989; Fornia 1997) indicate that commercial transport aircraft spend some portion of the flight envelope with the ullage in a flammable condition.

Aircraft manufacturers (Boeing et al. 1997) and regulatory agencies (FAA 1997) have long recognized the problem of airplane fuel-tank flammability. Extensive compilations of flammability properties of fuels (CRC 1983) and handbooks on fire and explosion (Kuchta 1985) attest to the awareness of and efforts to address this issue. Specific steps are taken to minimize the risk of fuel-tank explosions in commercial and military aviation. The commercial airplane industry practice is to provide engineering safety features such as current-limiting on the fuel quantity instrumentation system (FQIS), lightning-strike protection (Fischer and Plummer 1977), electrical bonding to prevent static buildup, anti-static (conductivity enhancing) additives for fuels

[1] In making these computations, we have used Sagebiel's estimated Jet A vapor composition of $C_{9.58}H_{17.2}$, which has an average molar mass of 132 g/mole.

(in some countries), and active explosion suppression systems at the wing-tip vents.

Military combat aircraft use these features plus more aggressive measures (Ball 1985) such as reticulated foams within the fuel tank, "self-sealing" tank liners, inerting by reducing or removing oxygen from the ullage, and active fire suppression systems. Ignition due to projectile penetration into the fuel tank is of particular concern for combat aircraft, and many of these features are designed to enhance combat survivability. Other successful efforts to reduce fuel flammability include introducing reduced flashpoint fuels, such as the Navy's use of JP-5, the switch by the Air Force from JP-4 to JP-8 (Beery et al. 1975), elimination of Jet B and JP4 in commercial transports in favor of Jet A. There was a long-term effort to develop viscosity-modifying additives as anti-misting agents (Kleug 1985) to reduce the hazard of fires in impact-survivable crashes, although this has never been implemented in other than research airplanes.

As a consequence of these efforts, the occurrence of fuel-tank explosions and fires has been reduced to a very low rate in commercial air transport. Nevertheless, fuel-tank ullages can often be flammable, and under exceptional circumstances, accidental ignition does result in fires or explosions (FAA 1997). The TWA 800 accident may have been one of these exceptional circumstances. What is at issue in the present case is the role that elevated temperatures and the nearly empty tank may have played in increasing the relative hazard of a fuel-tank explosion. The interest in the role of temperature is due to the a strong link between fuel volatility and explosion hazard that is observed in both experiments and airplane mishaps (Beery et al. 1975). Since the volatility of a fuel (Kanury 1988) is a strongly increasing function of temperature, fuel temperature relative to the flashpoint is the most important factor in determining the explosion hazard of a specific liquid fuel.

The concept of relative hazard emphasizes the fact that flammability limits are not absolute, but depend on the type and strength of the ignition source. Previous studies on flammability limits of hydrocarbon fuels have shown that the stronger the source of the ignition stimulus, the leaner the mixture that can be ignited. Following the established practice (Kuchta 1985) in explosion hazard evaluation studies (Ural et al. 1989), we use the spark ignition energy as a measure of ignition sensitivity of the fuel vapor-air mixture within the ullage. The ignition sensitivity is expected to depend on the following factors that appear to be prominent in the TWA 800 situation:

1. Effect of higher temperatures in the CWT associated with prolonged operation of the ECS on the ground prior to takeoff.

2. Effect of limited amount of liquid fuel in the CWT.

3. Effect of "weathering," i.e., exposure of fuel to the environment during flight and subsequent loss of low-molecular-weight components.

4. Specific Jet A fuel present in the CWT.

Of all of these factors, fuel temperature is the most important since the fuel vapor is created by evaporation of a liquid fuel and the amount of vapor, as determined by the vapor pressure, depends very strongly on temperature. We have focused on the first two factors, temperature and fuel amount, in the present study.

Our study extends the previous work (Nestor 1967; Ott 1970) on Jet A flammability. Those studies used a large (10 to 20 J), fixed ignition energy and large (1/4 to 1/2-full tank) quantities (mass loading) of fuel. We have examined two mass loadings: 200 kg/m^3, corresponding to a 1/4-full tank and 3 kg/m^3, corresponding to the conditions in TWA 800. The vapor conditions were a fixed pressure of 0.6 atm and temperatures ranged between 30 and 60°C. Most importantly, we varied the energy of the ignition source over five orders of magnitude, from 1 mJ to 100 J.

This report first presents some background material on spark ignition, followed by a discussion of our experimental facilities, ranging from 1.8 to 1180 liters in capacity. Spark ignition energies over a range of 1 mJ to 100 J have been determined for several hydrocarbon fuels and Jet A. In order to validate our technique, we measured the ignition energy of two pure hydrocarbon vapors, propane and hexane, in an 11.25-liter vessel. These data extends the results of previous researchers to a much wider range of compositions, particularly approaching the lean limit. Our results show that a strong variation of ignition energy (from less than 1 mJ up to 100 J) with composition is a universal feature of hydrocarbon combustion and the minimum ignition energy values of 0.2 mJ (2×10^{-4} J) typically quoted in textbooks are inappropriate for very lean mixtures.

2 Spark Ignition

One potential source of ignition in accidental fires and explosions is an electrical discharge or spark. Other possible sources include hot surfaces or adiabatic compression of fuel-air mixtures. The origin and characterization of common ignition sources are discussed at some length in the standard literature on fire and explosions (Kuchta 1985; Kuchta and Clodfelter 1985). In the present study, we have concentrated on capacitive spark discharges as a means for characterizing the potential for ignition of Jet A vapor in the ullage of an airplane fuel tank by accidental electrical discharges. Although the motivation for this work is the TWA 800 crash, at the present time, the source of ignition within the CWT is unknown and our use of spark sources is a matter of experimental technique. However, previous studies have shown that potential sources of sparks inside fuel tanks include static buildup (Lou 1986; NFPA 1993), lightning (Fischer and Plummer 1977), or malfunctioning electrical circuits (Magison 1978).

Following Magison (1978), it is convenient to categorize electrical ignition modes as follows:

1. Sparks created across a fixed or closing gap by energy stored in a capacitive circuit.
2. Arcs created across an opening circuit by energy stored in an inductor.
3. Opening or closing contacts in a purely resistive circuit.
4. Hot metal wires, particles, or surfaces created by ohmic heating of a circuit element, such as a wire strand.

All of these possibilities have been examined extensively in the context of explosion hazard prevention (Magison 1978), but the most often studied has been the capacitive spark. The standard way to characterize capacitive discharge sparks is in terms of the quantity of stored electrical energy, measured by the Joule (J). The actual amount of energy that is deposited in the gas by the discharge is lower but difficult to quantify, particular for short duration sparks. This issue is considered in more detail in the discussion section. It is found that for mixtures of a given fuel with an oxidizer such as air, there is a minimum spark energy required to cause ignition when the mixture falls in the range of flammable compositions. In this report, this energy will be simply referred to as the ignition energy.

Beginning with the work of Guest at the Bureau of Mines in the 1940s and continued by Blanc et al. (1947), an extensive series of tests (summarized in Lewis and von Elbe 1961) was carried out to determine ignition energy in hydrocarbon-air vapors. Ignition energy was found to be a function of fuel type and composition. For a given fuel, the ignition energy is a U-shaped function of composition with the vertical portions of the “U” occurring at the flammability limits and bottom of the “U” at some intermediate composition (see Fig. 1). The ignition energy for the most sensitive mixture is known as the Minimum Ignition Energy, or MIE. For both leaner and richer mixtures, the ignition energy increases sharply from the MIE. The MIE for hydrocarbon fuels in air has been measured for many common substances (Lewis and von Elbe 1961; Calcote et al. 1952) and is known to be on the order of 0.2 mJ and usually occurs for a rich composition. Examples of measured minimum ignition energy (Lewis and

von Elbe 1961) are shown in Fig. 1. Based on these results, the MIE for all petroleum-based fuels, including aviation kerosene is assumed to be on the order of 0.2 mJ.

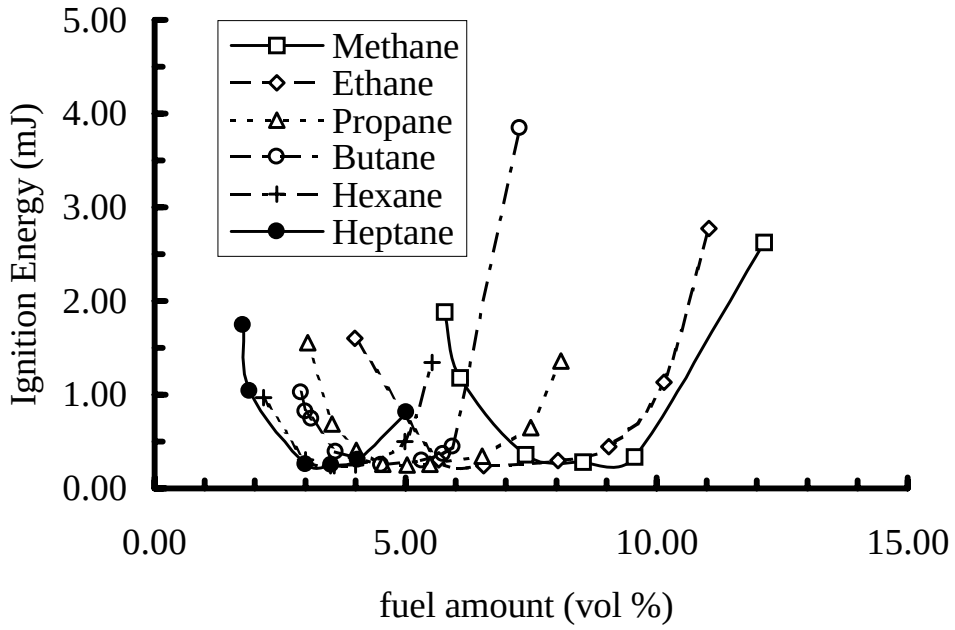

Figure 1: Classical results on ignition energy by Lewis and von Elbe (1961).

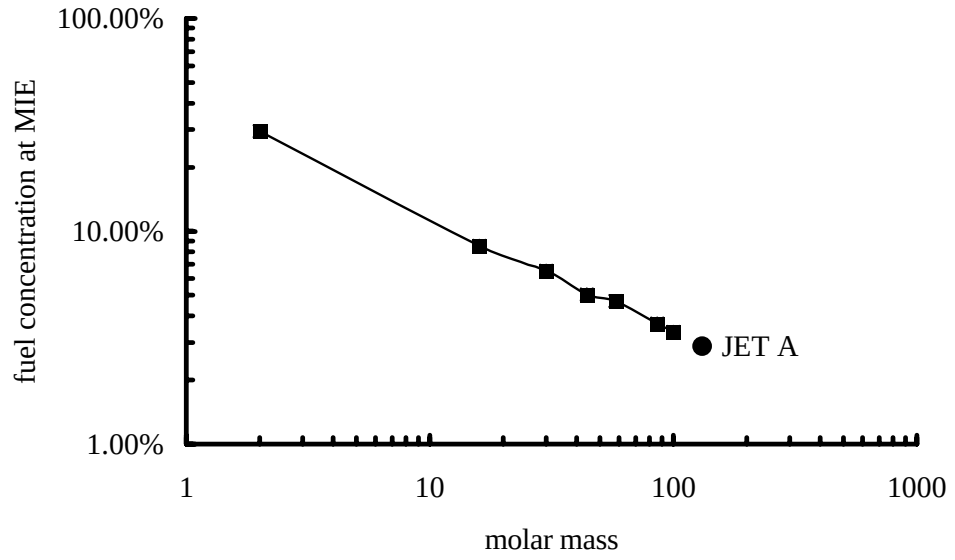

Figure 2: Dependence of composition at MIE (minimum ignition energy) on the molar mass of fuel. Based on the data of Lewis and von Elbe (1961) and following the treatment of (Ural, Zalosh, and Tamanini 1989).

As well as showing the strong dependence of the ignition energy on mixture composition,

these results also indicate that the MIE occurs at increasingly rich concentrations (Fig. 2) as the size of the fuel molecule (number of carbon atoms) increases. The results of Fig. 1 hint that the MIE increases as the fuel concentration is varied from the minimum ignition point. However, only a limited range of concentrations has been examined in the previous studies and these results conceal the very strong variation in ignition energy as the lean limit is approached.

The problem of ignition energy and flammability are closely related. Loosely speaking, flammability is the sensitivity of fuel-oxidizer mixture to ignition. A limiting concentration of fuel that will just result in ignition or flame propagation is referred to as the flammability limit. Traditional evaluations of explosion hazards rely on comparing the fuel concentration to the measured flammability limit.

However, the flammability limit depends on the choice of ignition method. Consequently, different methods of measuring the flammability have been devised such as the flashpoint test (ASTM D56 1988), spark ignition (ASTM E582 1988), temperature limit method (ASTM E1232 1991), and concentration limit method (ASTM E681 1985). Each of these uses different ignition methods: an open pilot flame in the flashpoint test; a capacitive spark in the spark ignition test; an electrically heated fuse-wire in the temperature limit test; and either a fuse wire or an electric arc in the concentration limit method. The most commonly used method of all, the flammability limit tube developed at the Bureau of Mines (Coward and Jones 1952; Zabetakis 1965; Zabetakis et al. 1951), has never been standardized. This method uses various ignition sources; one commonly employed is a quasi-continuous arc produced by a neon-sign transformer (20 kV, 30 mA) across a 0.25-in gap. Experience at Caltech with this type of source indicates that this is at least equivalent to a 100-J capacitive spark. Not surprisingly, all of these methods yield different results. This is illustrated for propane in Fig. 13. Since there is no fundamental theory of ignition or flammability limits, it is not possible to reconcile these various techniques.

2.1 Jet A Ignition Experiments

There are few reported values of Jet A vapor ignition energy in the open literature, but the MIE value of 0.2 mJ for hydrocarbon fuels is suggested in (CRC 1983) as being applicable to aviation fuels. The flammability limit measurements of Nestor (1967) and Ott (1970) use sparks with energies between 4 and 20 J. These values were used to create the standard flammability limit plots reported in most handbooks (CRC 1983); the results of Nestor (1967) are reproduced in Fig. 3.

We have not been able to identify any openly published data other than the Nestor and Ott data sets. However, after our initial experimental work was completed, we learned of experiments carried out in 1992 (Plummer 1992) with both propane and JP-8. The JP-8 was heated, vaporized, and mixed with air at temperatures between 150 and 190°F. The composition of the mixture was adjusted by varying the ratio of fuel-to-air flow rate and carrying out comparisons to a propane-air mixture. However, because not all of the fuel was vaporized and a mass balance was not carried out, the actual composition of the fuel-air mixture could not be determined.

The JP-8 experimental results were compared to a propane mixture had a concentration of

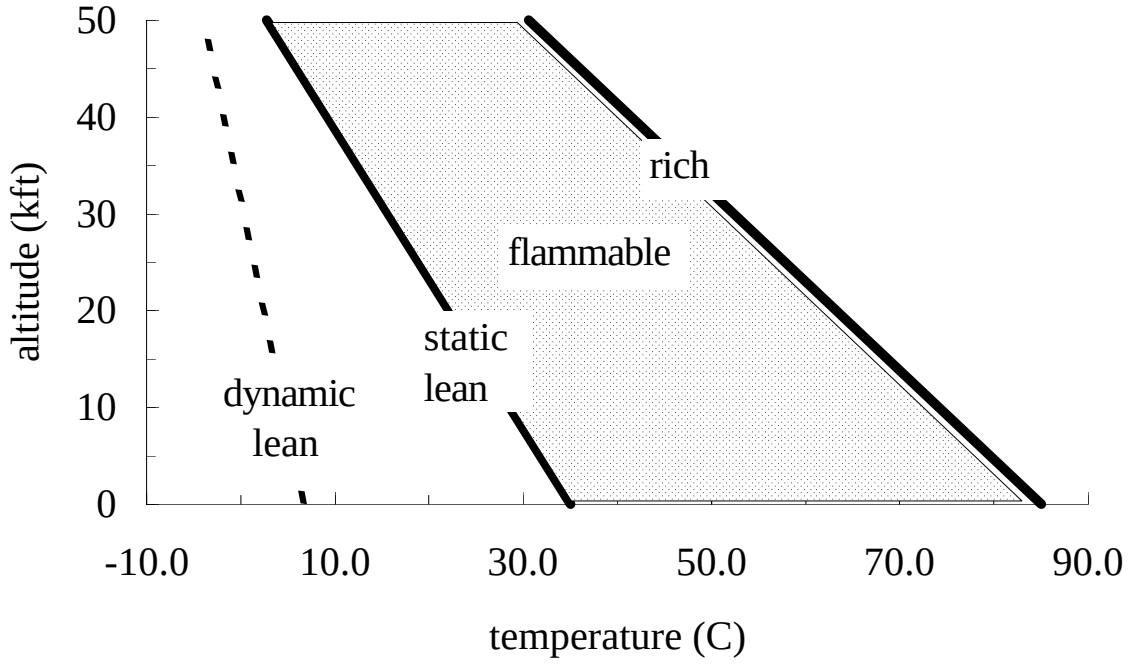

Figure 3: Flammability limits of Jet A in air in the standard representation of temperature vs. altitude (CRC 1983) based on Nestor (1967) measurements with a 20-J spark.

1.2 times stoichiometric, or approximately 4.8% fuel by volume. This is the composition at which the minimum ignition energy is observed and is frequently used as a test standard in military fuel-tank tests. By adjusting the JP-8/air mixture to have a similar ignition sensitivity as the reference propane mixture, it was assumed that the resulting JP-8/air mixture corresponded to the most sensitive mixture for spark ignition. The probability of ignition for a given energy was evaluated through multiple tests and found to vary from less than 5% at 400 μJ to 100% at 900 μJ for both the reference and JP-8 mixtures. The energy was computed from the capacitance and the charging voltage. The spark was created across a 2-mm gap with a secondary corona discharge to promote breakdown.

One other set of "data" deserves comment here. There is a published report (Frechou 1975) from the Concorde development team of ignition energy for both JP-4 and fuels characterized as "JP-1 and JP-5." This report provides a detailed, quantitative contour plot of ignition energy as a function of temperature and altitude. However, no information is given about the experimental technique or properties of the fuels. Further investigation reveals that these results were derived from estimates created by BAC (BAC 1972) using the Lewis and von Elbe data on propane shown in Fig. 1, and in fact consists of an estimated vapor pressure curve and some simple scaling ideas. There are a number of factors that make the analysis invalid:

1. The assumption that ignition-energy dependence on equivalence ratio is the same for propane as for Jet A or any other aviation fuel is incorrect.

2. The vapor pressures used in that analysis are a factor of three higher than Caltech mea-

surements and CRC reported values. The BAC memorandum refers to the vapor pressure as being appropriate for both Jet A and Jet B, although it is known that the vapor pressure of Jet B is substantially higher than Jet A.

3. The basic propane data are valid only up to 2 – 3 mJ but is extrapolated over three orders of magnitude, up to 25 J.

4. The scaling ideas are "believed to have been extracted from an FAA paper." There is no other justification or validation of the scaling.

The original 1972 BAC memorandum clearly identifies some of the limitations inherent in the original analysis, but these limitations have been disregarded in subequent applications to aircraft design.

The origin of these "data" has been further confused over the years since the label "JP-4" was substituted for "Jet B" and "JP-1 and JP-5" for "Jet A" when Frechou replotted the original estimates as a function of altitude instead of pressure. This plot has resurfaced recently (see Clodfelter 1997), and is now labeled as being characteristic of JP-8 with a 100°F flashpoint.

The only other published data are values of ignition energy measured by Kuchta et al. (1971) for mists (spray) of Jet A sprayed directly on electrodes (see Fig. 4). In discussing these data, the confusing and incorrect statement is made in the Handbook of Aviation Fuel Properties (CRC 1983, p. 74): "Likewise, if the fuel is present in the form of a mist or spray as opposed to a vapor, the ignition energy requirements will increase." However, this is clearly incorrect since spray ignition energies of 10 – 50 mJ are shown at conditions (1 atm, $-15 < T < +20$°C) for which the vapor cannot even be ignited with energies as high as 20 J. Studies of spray ignition (see discussions in Chapter 7 of Lefebvre 1983) have shown that when hydrocarbon fuel sprays are directly impinging on igniter electrodes, ignition can be obtained for much lower energies — or even for situations for which it is impossible to ignite the pure vapor phase created by equilibrium with the liquid. These data are clearly irrelevant to the problem of spark ignition energy in the pure vapor phase.

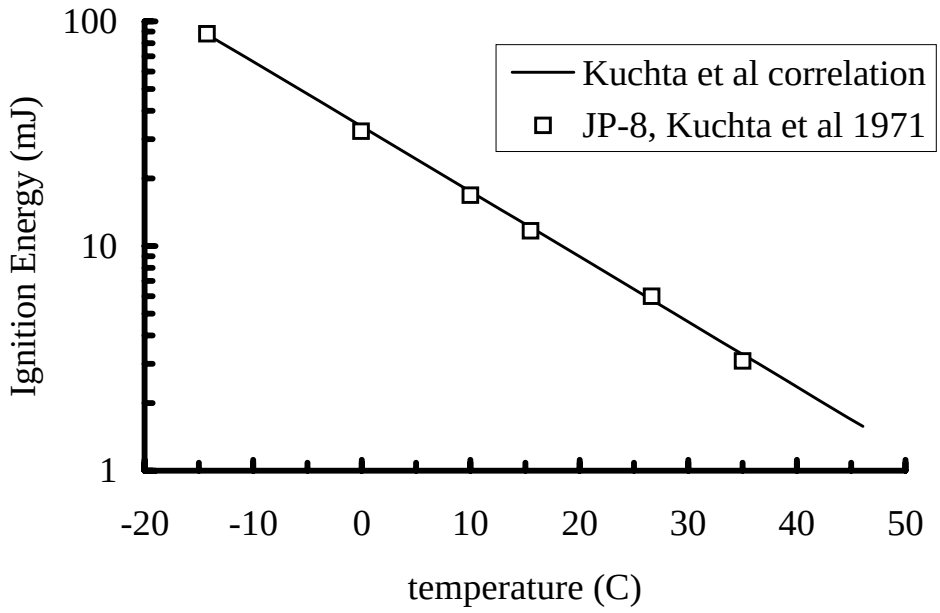

Figure 4: Dependence of ignition energy for Jet A sprays on fuel temperature (Kuchta et al. 1971).

3 Experimental Apparatus

Ignition energy measurements were performed in two different vessels with common electrical ignition and gas supply systems. For experiments conducted at ambient temperature with a purely gaseous mixture, an unheated 11.25-liter vessel was used. This vessel was used for initial calibration measurements with propane-air and hexane-air mixtures. For tests with Jet A in which the initial temperature of the system had to be precisely controlled, a heated 1.84-liter ignition vessel was used.

3.1 Gas Ignition Vessel

Ignition energy measurements on purely gaseous mixtures such as hexane-air and propane-air were performed in the gas ignition vessel. These tests were conducted primarily for verification of the ignition system and of the procedures used for flammability testing of Jet A.

3.1.1 Vessel

The gas ignition vessel consists of an 11.25-liter steel vessel with an approximately cubic interior of dimensions 19.0 cm $\times$ 20.3 cm $\times$ 30.5 cm as shown in Fig. 5. The vessel contains two circular windows on the front and back walls; this allows video documentation of the combustion phenomenon. A mixing fan inside the vessel ensures the homogeneity of the gaseous mixture. Liquid fuel such as hexane was introduced into the vessel under vacuum through the septum connected to the tank. The pressure history was recorded with a Kulite XT-190 gauge; the temperature history was recorded with a K-type thermocouple located about 5 cm from the vessel ceiling, near the center of the chamber. A high-precision Heise diaphragm pressure transducer was used to determine the initial pressure in the vessel.

The combustion process was captured using a color schlieren system. The schlieren images were recorded on video, allowing one to observe the details of the ignition process and flame propagation as well as infer flame speeds. The optical set-up is shown in Fig. 6. The light source is a mercury vapor lamp, and a mirror and lens system is used to obtain a parallel beam suitable for schlieren photography of the combustion event in the vessel. A three-color stop is used to provide the color schlieren effect, and the image is recorded using a CCD camera and a standard video recorder.

3.1.2 Gas-Feed System

The gaseous mixture in the vessel is controlled through the gas feed system shown in Fig. 7. The pneumatic valves of the system are activated from an external control panel such that the entire gas-loading procedure can be performed remotely. Gases can be evacuated through the vacuum pump, and various gases can be selected to fill the vessel. The mixture composition is determined by introducing the desired quantity of each gas through the method of partial pressures. In the case of hexane-air mixtures, liquid hexane was introduced into the evacuated vessel by a syringe through a septum located on the side of the vessel.

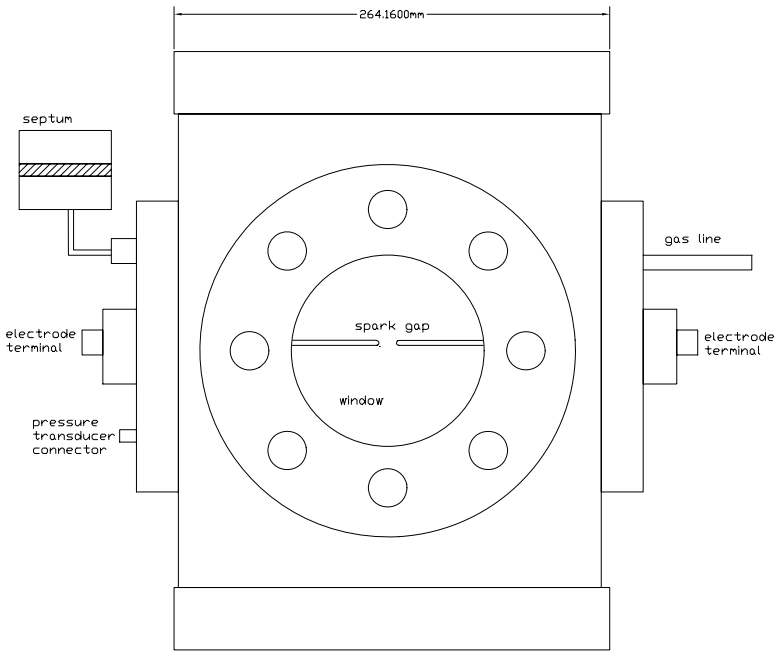

Figure 5: Schematic of the 11.25-liter vessel used for ignition energy measurements of hexane and propane with air.

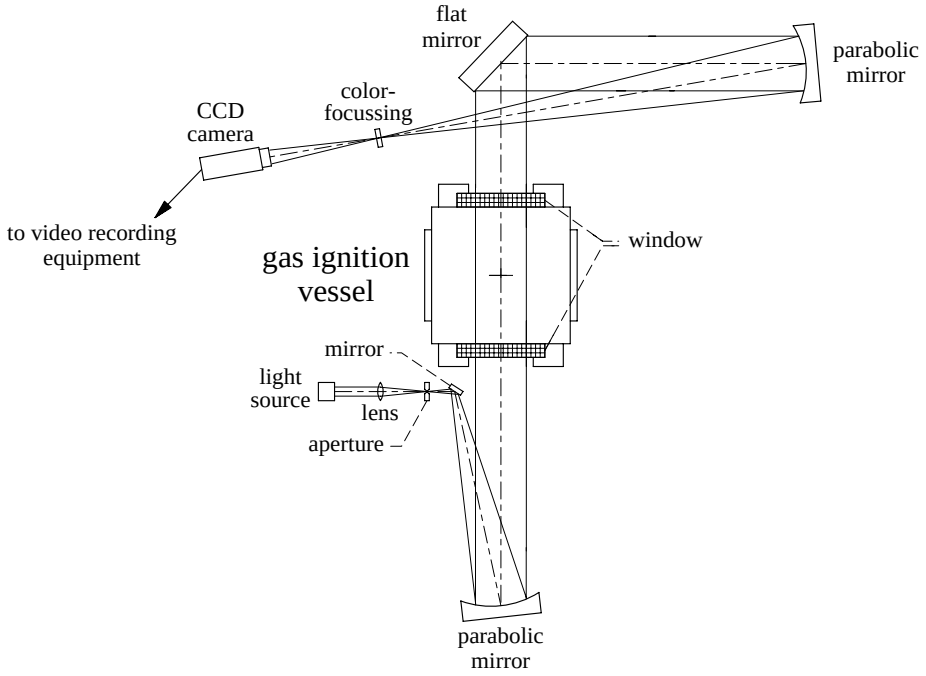

Figure 6: Schematic of optical arrangement used for color schlieren video recording of the combustion phenomena (shown with the 11.25-liter vessel).

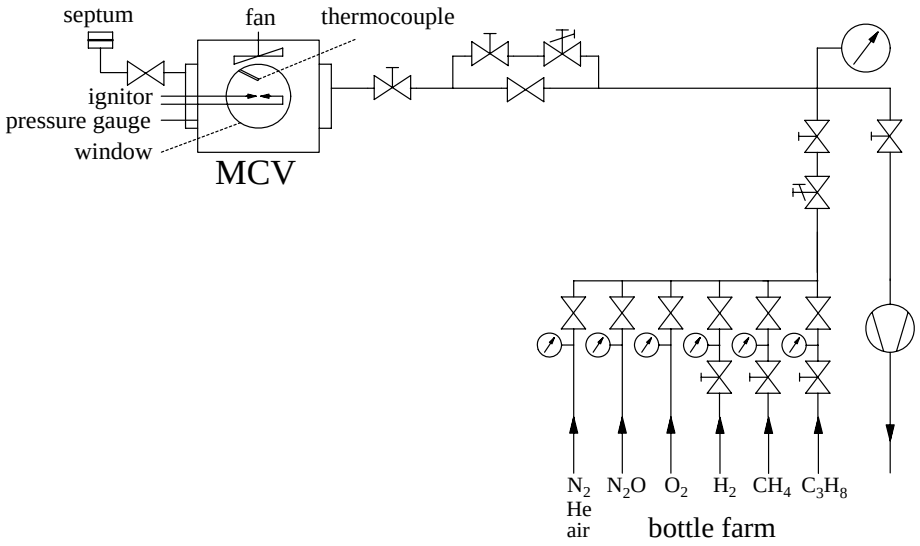

Figure 7: Schematic of the gas-feed system (shown here connected to the 11.25-liter vessel, labeled MCV).

3.1.3 Electrodes

The electrodes used for spark ignition of the gaseous mixture consisted of two 3.2-mm diameter stainless-steel rods inserted into opposite sides of the chamber such that the spark gap was located at the center of the chamber. The rods were insulated from the chamber wall with Teflon plugs and the electrode tips were rounded.

3.1.4 Experimental Procedure

In the first series of experiments, propane-air and hexane-air mixtures were tested. The tests with these mixtures were all conducted at approximately 22°C and an initial pressure of 1 bar. The propane used in the tests was commercial grade. The mixing fan was turned off during the tests so that the mixture was quiescent at the time of ignition.

The vessel was first evacuated, then filled to the desired fuel pressure. In the case of hexane, an appropriate quantity of liquid hexane was introduced into vessel through the septum. To ensure that no liquid residue remained, the hexane was limited to quantities such that the fuel partial pressure was always less than the vapor pressure. The chamber was left at low pressure with the mixing fan on for several minutes to allow the hexane to evaporate completely. Air was then added until the total pressure of the mixture in the vessel reached 1 bar. The mixture was stirred for several minutes with the fan before proceeding with the test.

The capacitor was charged to an energy between 1 mJ and 100 J and discharged across a 3.3-mm gap to create the igniting spark. If the mixture failed to ignite, the stored energy was increased until a flame was initiated. Since, in the case of ignition failure, the small amount of mixture burnt by the spark can contaminate the unburnt gases and influence the ignition limit of the mixture, a limited number of tests were performed with the same mixture. For tests at

low ignition energies (between 1 mJ and 500 mJ) for which only a small volume of mixture was burnt by the initiating spark, up to five tests were performed with the same mixture to find the ignition limit. For high-ignition-energy tests (between 1 J and 100 J), for which a larger volume of the mixture was burnt by the spark, no more than two tests were performed in succession without changing the mixture in the vessel. Ignition was determined by visual inspection of the video recording and by the recorded pressure signal.

3.2 Heated Ignition Vessel

3.2.1 Vessel

A 1.84-liter heated vessel was used for ignition energy measurements on the Jet A vapor and air mixture. This apparatus was designed to test the flammability of a combustible mixture created when fuel at the bottom of a partially-filled tank evaporates and mixes with the air in the space above (the ullage). Since the amount of Jet A vapor in the mixture depends primarily on the liquid fuel temperature, the initial temperature of the system was precisely controlled.

The heated ignition vessel is shown in Fig. 8. The vessel has an approximately cubic interior with a dimension of about 14 cm. A magnetic stirring rod ensures proper mixing of the liquid inside the chamber. The front and back walls of the vessel have circular windows through which the combustion process can be observed. We used the same color schlieren and video-recording system as the gas ignition vessel. The pressure history was recorded with a Kulite XT-190 gauge and the temperature history was recorded with a K-type thermocouple inserted from the top of the vessel into the gaseous section of the vessel above the liquid surface. An additional Baratron MKS diaphragm pressure transducer was used to determine the initial pressure in the vessel. The temperature of the vessel and its contents are controlled using 5-W/in^2 heating pads attached to the outside surface of the vessel. Power to the heating pads is supplied by a temperature controller unit which can monitor the vessel temperature through thermocouples on the top and bottom exterior surfaces as well as inside the vessel, at a point approximately 2 cm from the side walls. To maintain the vessel at the desired temperature during long periods of time, the entire vessel is placed inside a cubic wooden box with a dimension of about 25 cm. Natural convection in the air between the vessel and the box walls ensures thermal equilibration within 60 to 90 minutes.

3.2.2 Gas and Liquid Supply System

Liquid jet fuel is introduced into the vessel with a pipet through one of the inlets on top. The gas-feed system used for controlling the pressure in the vessel and evacuating the combustion products was the same as the one shown in Fig. 7 for the MCV vessel.

3.2.3 Electrodes

Two electrodes protrude into the vessel to provide a spark gap in the center of the chamber. The electrodes were made of 3.2-mm diameter stainless-steel rods with rounded tips. The gap

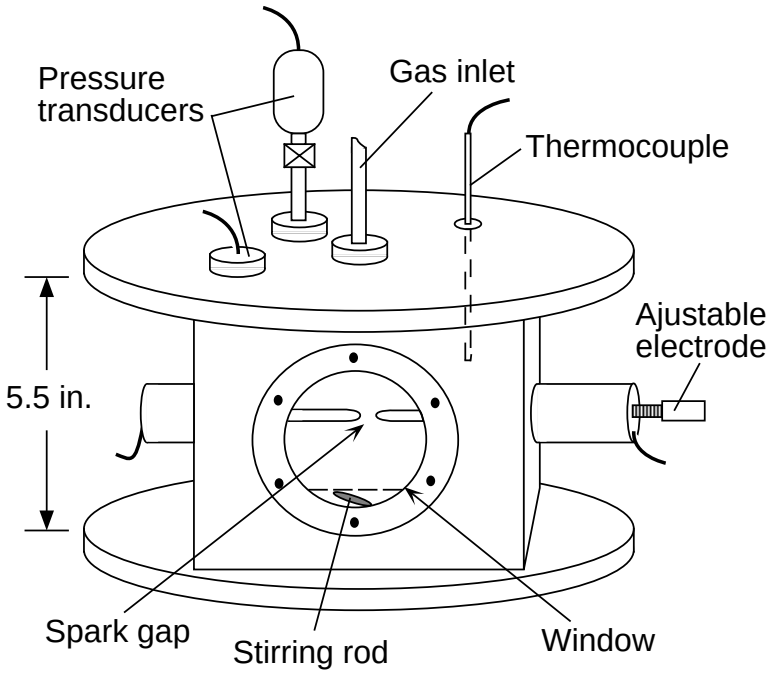

Figure 8: Schematic of the heated ignition vessel used for ignition energy measurements of Jet A vapor with air.

size determined by the electrode tip separation can be adjusted with a micrometer screw on one of the electrodes. The details of the electrode construction are shown in Fig. 9.

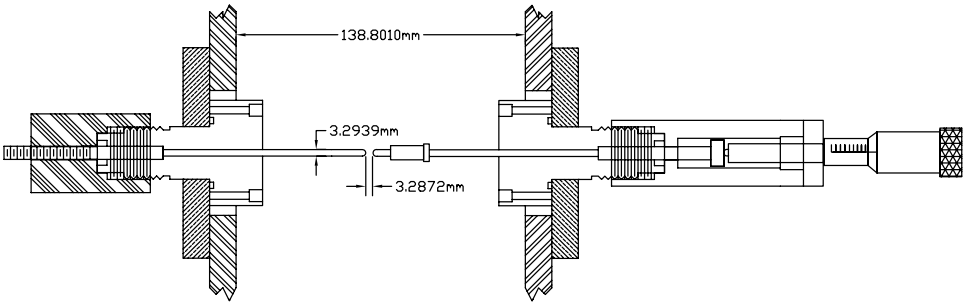

Figure 9: Schematic diagram of the adjustable gap electrodes used in the heated ignition vessel.

3.2.4 Experimental Procedure

The ignition energy was measured for commercial Jet A fuel obtained from local airports. Tests were done for two mass-to-volume ratios in the vessel: 3 kg/m^3, corresponding to 6.9 ml of fuel; and 200 kg/m^3, corresponding to 460 ml of fuel. The initial temperature of the mixture in the chamber was varied from 25°C to 55°C, and all tests were conducted at a pressure of 0.585 bar to match the atmospheric pressure at 13.8 kft.

For the tests at 3 kg/m^3, the empty vessel was first heated and allowed to stabilize at the desired temperature. The appropriate amount of fuel (6.9 ml) was then poured in carefully to avoid splashing onto the windows. After sealing the vessel, gas was evacuated until a pressure of 0.585 bar was reached. The magnetic stirring rod was turned on and the system was allowed to equilibrate over a period of about 30 minutes to 1 hour. During equilibration, the pressure rose due to the evolution of dissolved air and evaporation of the fuel. The vessel was periodically evacuated to reduce the pressure back to 0.585 bar. We proceeded with the ignition test when the pressure and temperature stabilized. The vessel was emptied and cleaned between each test.

A similar procedure was followed for tests at 200 kg/m^3, except that the same fuel was used for an entire series of tests over the temperature range 25°C to 55°C. The total amount of liquid fuel in the vessel was 460 ml. Between each test, the products of the previous combustion event were evacuated to approximately 6 mbar for a duration of several seconds. Fresh air was subsequently introduced into the chamber until the desired pressure of 0.585 bar was attained. The windows were cleaned between tests by heating the outside surfaces until the liquid droplets on the inside surface evaporated.

The fuel-air mixture in the vessel above the liquid layer was ignited using sparks created by discharging capacitors with stored energy between 10^{-3} J to 10^2 J across a 3.3-mm gap. This gap size was chosen to match the gap size used in previous ignition experiments done with hexane and propane. As in the gas-ignition vessel tests, the ignition limit was found by increasing the spark energy until ignition occurred for a given mixture. To minimize the influence of mixture contamination by spark-generated combustion products, no more than five successive tests (two for high spark energies) were performed with the same mixture. Inspection of the video recordings and pressure data was used to determine if a propagating flame was produced.

3.3 The 1180-Liter Vessel

Preliminary ignition energy tests were performed in a heated 1180-liter (1.18 m^3) vessel. The general features of this facility have been reported in Shepherd et al. (1997). This vessel was modified to use spark ignition. Due to its larger volume, the effects of vessel size on flame propagation rate and peak pressure could be investigated.

A schematic of the vessel is shown in Fig. 10. Previous experiments (Shepherd et al. 1997) were carried out with a jet ignition system. For the present study, the jet ignition was replaced by spark ignition, with the spark gap attached at the location where the jet nozzle was formerly attached. Only a limited number of tests were carried with propane, hexane, and Jet A to confirm the results obtained in the smaller vessels. Jet A tests were only carried out at a mass loading of 3 kg/m^3 due to the difficulty of handling and disposing of the large amounts of Jet A that would be required at higher mass loadings.

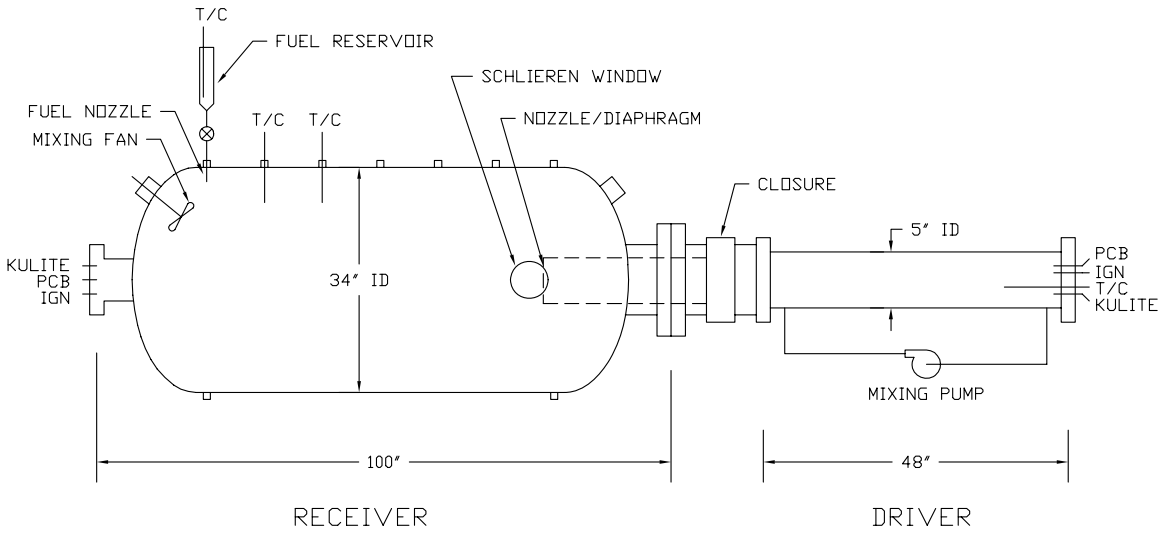

Figure 10: Schematic of the 1180-liter vessel.

3.4 Spark Discharge and Electrode Issues

Previous studies on spark ignition have shown that there is variability in results due to the dependence of ignition energy on the electrode construction and discharge circuit design. Quantifying the strength of a short-duration, low-energy capacitive spark ignition source has been found to be difficult (Strid 1973); thus a standard for spark energy has not been developed. The ASTM ignition energy test (ASTM E582 1988) follows the practice started by Lewis and von Elbe (1961) of reporting the stored energy rather than measuring the energy discharged into the spark. Some test procedures require flanges to be used on electrodes (ASTM E582 1988), while other researchers (Calcote et al. 1952; Crouch 1994) do not use flanges and find comparable ignition energies to studies done with flanges.

In the present study, we have reported the "energy stored" as the ignition energy and used unflanged electrodes. Some of the issues connected with these choices are explored in the next two sections. Ultimately, the validation of these choices and our experimental protocol was confirmed by doing control experiments with propane and hexane. Our values of ignition energy compare favorably with those of previous researchers for the overlapping ranges near the MIE, and interpolate smoothly between the lean limit and the MIE values.

3.4.1 Spark Energy

In the present study, the ignition energy reported is actually the energy stored in the capacitor used to create the electrical discharge. The stored energy was varied by using different combinations of capacitors and different charging voltages from 1 kV to 15 kV. Voltage was measured as the capacitor was charged, and the spark was triggered when the desired charging voltage was reached and stabilized. The energy stored in the capacitor was computed from the

standard relationship

$$E = \frac{1}{2}CV^2 \tag{1}$$

where E is the stored energy (J), C is the capacitance (F), and V is the charging voltage (V). With a fixed gap size (3.3 mm) and a constant pressure (0.585 bar), a minimum voltage of about 6 to 8 kV is needed to cause spontaneous electrical breakdown across the gap. This necessitated using various sizes of capacitors, ranging from 30 pF to 1 μF, for tests at different energy ranges (see Table 1).

Table 1: Discharge capacitor types.

Capacitance (nF)	Voltage (kV)	Type
500	15	Oil dielectric (2)
5	30	Mylar dielectric
0.0581	6	59 cm of RG-8A/U coaxial cable
0.0317	6	31 cm of RG-8A/U coaxial cable

In our arrangement, the residual energy remaining in the capacitor after the discharge was less than 1%. However, due to the finite impedance of the circuit and the complex nature of electrical arcs, it is not possible to draw any conclusions about the amount of energy deposited into the arc. In order to do that, it would be necessary to determine the actual energy dissipated within the arc

$$E_{arc} = \int_0^\infty v(t)i(t)\mathrm{d}t \tag{2}$$

which requires measuring the voltage $v(t)$ across the arc and current $i(t)$ through the arc as a function of time. Various arrangements have been proposed to do that; a review is given by Strid (1973). However, a short-duration (less than 1 μs) spark created by discharge of a small capacitor directly into an air gap is difficult to quantify in this fashion. The capacitance and resistance introduced by the measuring circuit can be substantial. Since the spark is of very short duration, careful circuit design is needed to eliminate the effects of the frequency response (phase shifts) introduced by the measurement circuit. Finally, the efficiency for converting electrical energy into work on the surrounding gas is known to have a strong dependence on spark duration but quantitative details are unknown.

It is possible to measure the energy dissipated by a spark directly if the spark energy is high enough and a pulse-shaping circuit is used to substantially increase the duration of the discharge. Recent studies (Ronney and Wachman 1985; Kono et al. 1976; Ballal and Lefebvre 1975) have used more sophisticated circuits to lengthen and measure the electrical pulse in order to report measured (Eq. 2) rather than stored (Eq. 1) energy. Critics (Grenich and Tolle 1983) of the "energy stored" method suggest that as little as 10% of the stored energy gets into the spark, but they were unsuccessful at actually measuring the energy deposited by short-duration sparks. Other researchers (Eckhoff 1975) have found that a substantial fraction

of the stored energy is deposited into the gas by a long-duration spark. Parker (1985) examined the effect of pulse duration and discharge circuitry on igniting a 2.7% propane-in-air mixture. A short-duration, constant-power pulse circuit was able to ignite this mixture using a 4-mm gap with a minimum energy of 0.3 mJ. This is about an order of magnitude lower than Lewis and von Elbe (1961) found with a capacitive circuit. Parker speculated that this difference was due to the much greater efficiency of coupling electrical to thermal energy for the pulse circuit as compared to straight capacitive discharge systems. However, if resistance elements are added to a capacitive discharge circuit, Parker suggests that the electrical-to-thermal conversion efficiency is increased. Resistance elements in series with capacitive discharges are used by one flammability testing organization in the USA (Dahn 1998). This is primarily to create an overdamped circuit in order to use conventional probe techniques and slow data acquisition systems to record the voltage-current characteristics used for computing energy. A recent project (Crouch 1994) to construct a standard test rig for lightning protection studies did not attempt to directly measure the spark energy but relied on the "energy stored" concept with a purely capacitive discharge circuit.

Direct measurements of a voltage and current of the spark were performed by Eckhoff (1975) using a circuit similar to our "trigger spark" device. The resulting measured energies were compared to the calculated estimate using stored capacitor energy (Eq. 1). For a calculated spark energy of 0.1 mJ, the measured energy was ten times higher (1 mJ). This is due to the energy of a trigger spark circuit. The difference between the two decreases as the spark energy increases, and at energies between 10 mJ and 100 mJ, the calculated and measured energies are the same. Above 100 mJ, the measured energy is lower than the calculated energy and is about a factor two lower for a calculated energy of 10 J.

3.4.2 High-Voltage Switching

In our experiments, the spark was triggered by one of two methods: a mechanical switch consisting of contacts closed by a metallic bar, or a 30-kV trigger spark provided by a TM-11A trigger module. The circuit for the mechanical switch is shown in Fig. 11. When the switch is in the normal position, the capacitor charges through the 1.9-MΩ resistor. When the switch is pressed, the capacitor discharges through the spark gap. This circuit was generally used

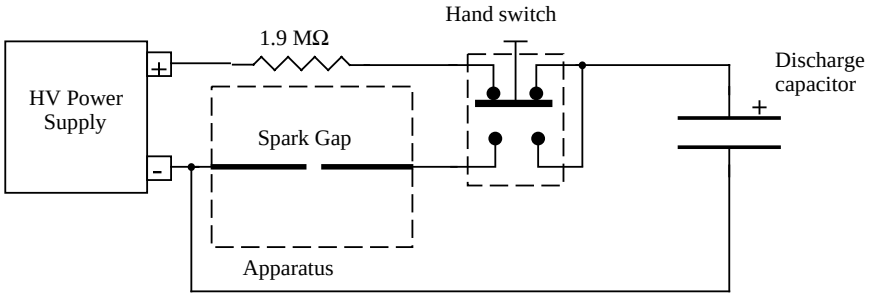

Figure 11: Circuit diagram for the high-voltage mechanical switch spark system.

for spark energies less than 1 J. For higher spark energies, the trigger spark system (shown

in Fig. 12) was used. In this system, the breakdown across the electrode gap is initiated by a

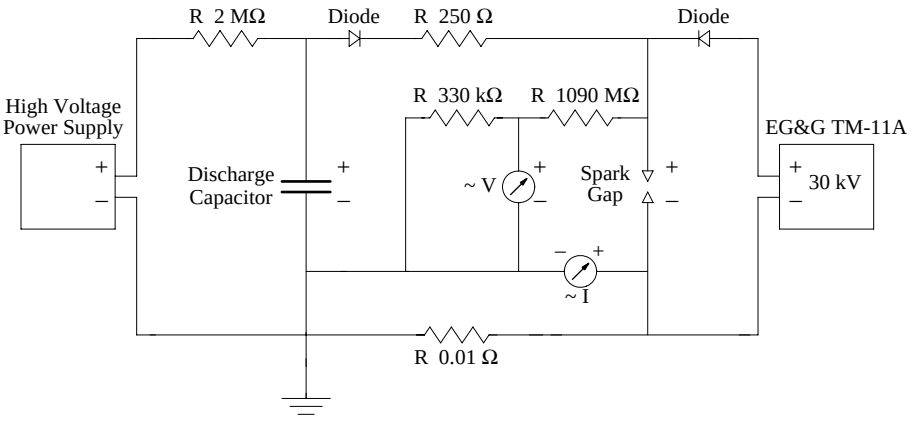

Figure 12: Circuit diagram for the trigger spark system.

low-energy (40 mJ), high-voltage (30 kV) spark from the TM-11A trigger module. Just before firing, the capacitor is charged by increasing the high-voltage power supply to the desired voltage through the 2-MΩ resistor. Ignition-energy measurements with 450-mJ sparks were performed on propane-air mixtures for both the mechanical switch and the trigger spark systems. For the mechanical switch system, a mixture of 2.6% propane ignited while a 2.5% propane mixture did not (Fig. 13). For the trigger spark system, the ignition limit was found to be slightly richer, as a mixture of 2.7% propane ignited while a 2.6% propane mixture did not. This discrepancy is well within the accuracy of the Kulite pressure gauge used to measure the composition of the mixture. We therefore conclude that the two spark generation systems are equivalent within the experimental error of the experiment.

3.4.3 Circuit Reactance

Stray circuit reactance in the discharge circuit and in the electrodes can have an effect on the time constant of the spark. Specifically, the reactance consists of resistance in the wires and contacts, stray capacitance in the electrodes, and inductance in various parts of the circuit. The reactance can change the rate of energy deposition or power as well as the spark duration. An underdamped discharge circuit can lead to an oscillatory spark energy release while an overdamped circuit can result in a lower-power, but longer-duration spark. Inductance is generally found to have little influence on the measured spark ignition energy (Magison 1978), but the series resistance on the electrodes is sometimes used to change the spark power (Ronney 1985).

The circuit inductance for the experimental arrangement used in this work was found to be approximately 1.5 μH. The resistance was a few ohms for the case of the mechanical switch. A resistance of 250 Ω was deliberately added to the spark trigger circuit in order to increase the duration of the discharge. Preliminary measurements of the spark duration showed it to be less than 5 μs. Previous work by Kono et al. (1976) showed that for propane-air mixtures at concentrations between 3.0% and 3.5%, the ignition energy varies by less than 1 mJ for spark

durations less than 50 μs. Hence stray reactance is likely to have a negligible influence on ignition energy measurements with the present discharge circuit.

At low spark energies however, smaller discharge capacitors are used, and the stray capacitance cannot be neglected. We measured the capacitance of our circuit and found values of approximately 20 pF to 40 pF, which is comparable to the lowest capacitor sizes (Table 1). At a spark voltage of 6 kV, however, the stray capacitance may produce a variation in the spark energy of up to 7 mJ. The present circuit is therefore not well suited for low ignition energy measurements.

3.4.4 Electrode Type

The electrodes used in this study were not of the flanged type described by the ASTM standard (ASTM E582 1988). When the electrodes are flanged, the flame kernel generated by the spark can be quenched by the flanges. This phenomenon was investigated by Calcote et al. (1952) and Lewis and von Elbe (1961) who found that the minimum ignition energy is generally higher with flanged electrodes. For flanged electrodes, the ignition energy was found to increase sharply as the spark gap was decreased to within 0.2 mm of the quenching distance of the combustible mixture; and the mixture was not ignitable at all if the gap was less than the quenching distance. Without flanges, the ignition energy increases a modest amount with decreasing gap size. By using unflanged electrodes, we were able to carry out tests over a large range of compositions without having to continuously adjust the gap size in order to stay above the so-called quenching distance.

The main advantage of this is that the voltage needed to breakdown the gap and produce a spark is relatively fixed and the energy input can be adjusted by simply changing the amount of capacitance. For a given dielectric, the breakdown voltage is proportional to the product of gap distance and pressure (Paschen's Law), so that the spark trigger voltage has to be increased with increasing gap distance. The drawback of working with a fixed gap distance is that the losses to the electrodes increase as the stored energy and consequently the flame kernel size increase. This results in ignition energies that are higher than the minimum value for the highest values of stored energy, which are encountered near the lean flammability limit. Further study is needed to quantify the magnitude of this effect.

4 Validation Tests

4.1 Propane Combustion

The first set of validation tests was carried out with propane-air mixtures. The propane used was from a small commercial cylinder of the type supplied for a hand-held plumbing torch. The exact composition is not known, but the HD-5 fuel specification is for at least 95% propane with the balance being lighter compounds such as propylene and butane. The initial conditions and key results are given in Table 5 of Appendix A.

4.1.1 Ignition Energy

Our ignition energy results for propane-air mixtures are shown in Fig. 13 along with previously reported data. The present data extend from 2.2% propane (LFL) up to 3.5% propane. The minimum ignition energy of approximately 0.2 mJ occurs at 5% propane as determined by Lewis and von Elbe (1961) and Calcote et al. (1952). The ignition energy increases continuously by a factor of 10^5 as the concentration is decreased from stoichiometric to the lean limit of 2.1% propane. Mixtures with less than 2% propane cannot be ignited even with a 20 J spark. The present data are consistent with the previously measured ignition limit between 2.1% and 2.3% propane given by Kuchta (1975) and Coward and Jones (1952).

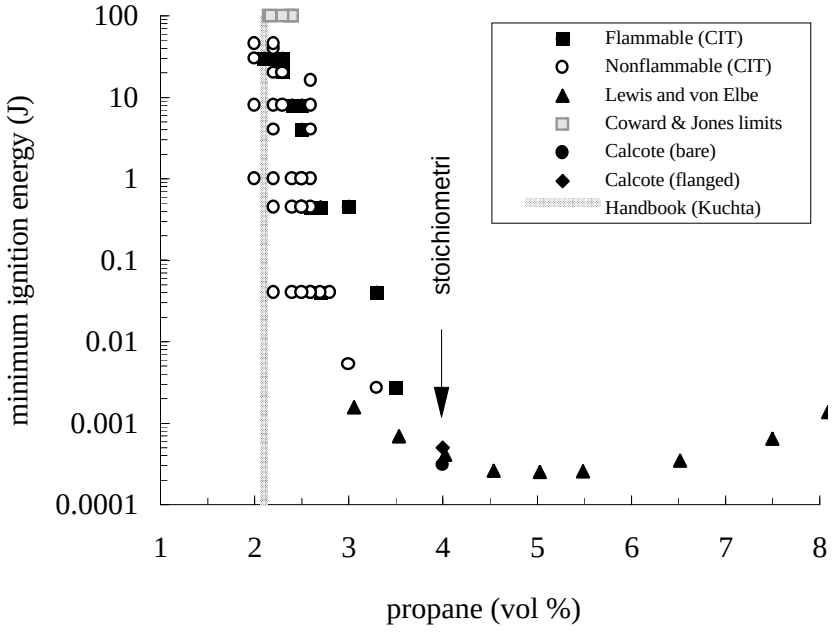

Figure 13: Measured ignition energy for propane-air mixtures, initial pressure 1 atm, initial temperature 295 K.

4.1.2 Combustion Pressure

The pressure-time histories were also recorded to confirm that the mixture had been ignited and burned. Selected results (Fig. 14) show that the leaner the mixtures, the slower the pressure rise. This agrees with the known dependence of burning speed on mixture strength. The burning speed S_u and the pressure rise coefficient K_g were calculated from the pressure-time profiles by the techniques discussed in (Shepherd et al. 1997). These values are shown in Table 5 of Appendix A.

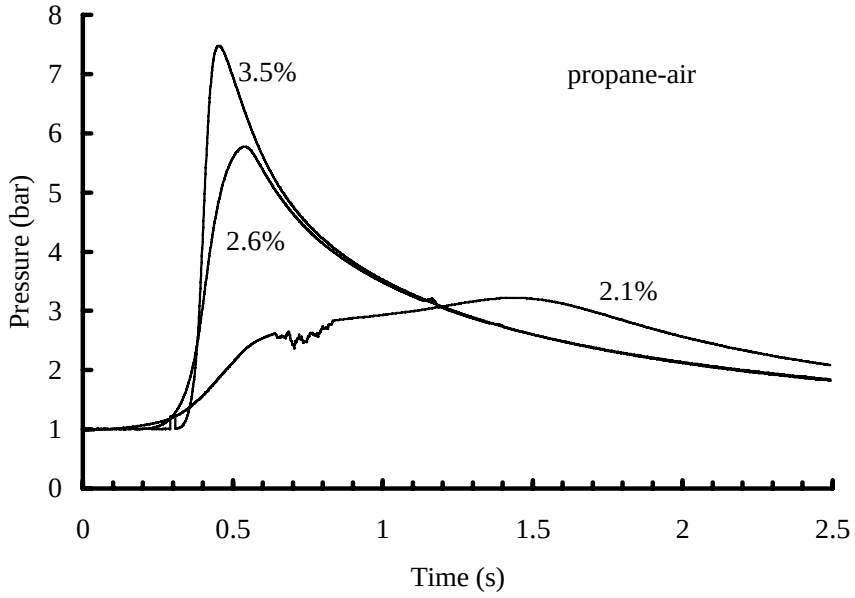

Figure 14: Measured pressure histories for propane-air combustion, initial pressure 1 atm, initial temperature 295 K.

The peak pressures for the various mixtures are shown in Fig. 15 along with the calculated maximum pressure for adiabatic, constant-volume combustion (AICC). The measured pressures are lower than the calculated values due to energy losses caused by radiative and convective heat transfer during the burn. This effect is stronger for leaner mixtures, for which the burning speed is lower. For very lean mixtures, less than about 2.6% propane, buoyancy prevents the flame from burning downward and the discrepancy between computed (AICC) peak pressure and measured peak pressure becomes even larger. This can also be observed qualitatively in the 2.1% propane case shown in Fig. 14. The pressure history in this near-limit case has a plateau between 0.6 and 1.5 s, which corresponds to a very slow combustion process in the upper portion of the vessel (this can be observed on the schlieren system). Contrast this with the 2.6 and 3.5% propane cases, which correspond to flame propagation throughout the vessel with a minimum buoyancy effect. Data from the 1180-liter vessel is also shown in Fig. 15. The peak pressures obtained in the two facilities are essentially identical, given the spread observed from repeat testing at the same concentration in a given facility.

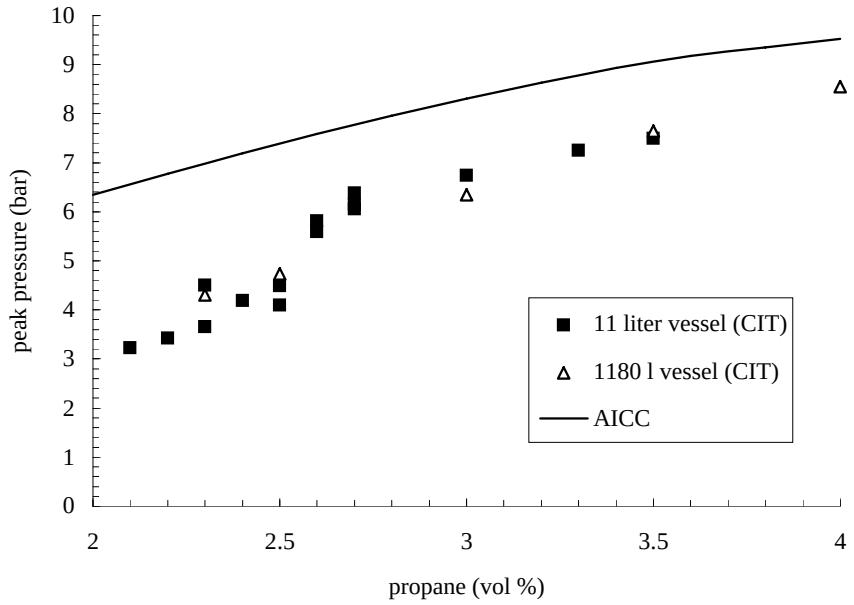

Figure 15: Measured peak pressure for propane-air mixtures, initial pressure 1 atm, initial temperature 295 K.

4.1.3 Flame Speeds

The burning speeds (Fig. 16) for the propane experiments were computed by the "t^3" pressure-trace analysis method described by Shepherd et al. (1997). We have compared our values with the previous measurements of Metghalchi and Keck (1980), Gibbs and Calcote (1959) and the computations of Göttgens et al. (1992). The present data are about 5 cm/s higher than the results of Metghalchi and Keck (1980) and in good agreement with both the computations of Göttgens et al. (1992) and the older data of Gibbs and Calcote (1959).

4.2 Hexane Combustion

Further ignition energy tests were conducted with hexane-air mixtures. The hexane used was UV grade (99.99%) hexane as supplied by Burdick and Jackson. The test conditions and key results are given in in Table 6 of Appendix A.

4.2.1 Ignition Energy

The results of the ignition trials are shown in Fig. 17 together with previously reported data. The present data covers the range of 1 to 2.2% hexane. As in the case of the propane-air mixtures, our results agree with previous studies at the lowest and highest energy levels tested. The studies of Lewis and von Elbe (1961) and Calcote et al. (1952) obtained the minimum ignition energy for mixtures of about 3.5% hexane. Our measured ignition limit of 1.2% hexane

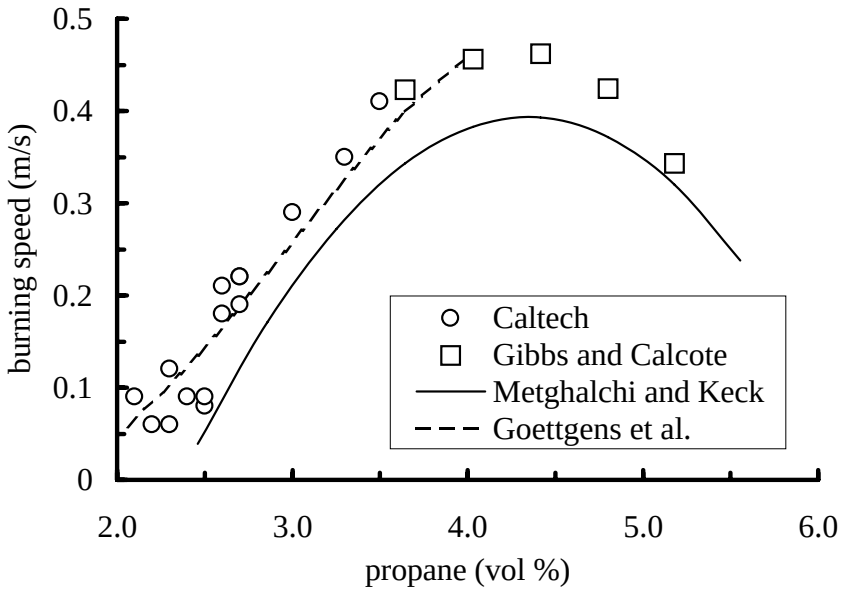

Figure 16: Effective burning speeds estimated from the pressure-time histories for propane-air mixtures, initial pressure 1 atm, initial temperature 295 K. Present measurements (Caltech) compared with previous data (Gibbs and Calcote 1959; Metghalchi and Keck 1980) and computations (Göttgens et al. 1992)

is in agreement with the values between 1.1% and 1.3% propane given by Kuchta (1975) and Coward and Jones (1952).

4.2.2 Combustion Pressure

The pressure-time curves (Fig. 18) are qualitatively similar to those for the propane-air case. The burning speed S_u and the pressure rise coefficient K_g were calculated from the pressure-time profiles by using the techniques discussed by Shepherd et al. (1997). The values are shown in Table 6 of Appendix A. The effect of buoyancy on the near-limit case (1.2% hexane) is not quite as dramatic as in the propane case, but the results have a lot of variability near the limits. This can be observed from the large spread in peak pressure values for the 1.2 and 1.5% cases shown in Fig. 19.

A few data points from the 1180-liter vessel are included on Fig. 19. Two of those experiments were carried out with the mixing fan running during the ignition event; the effect of convection and turbulence within the vessel can be observed to result in slightly higher peak pressure.

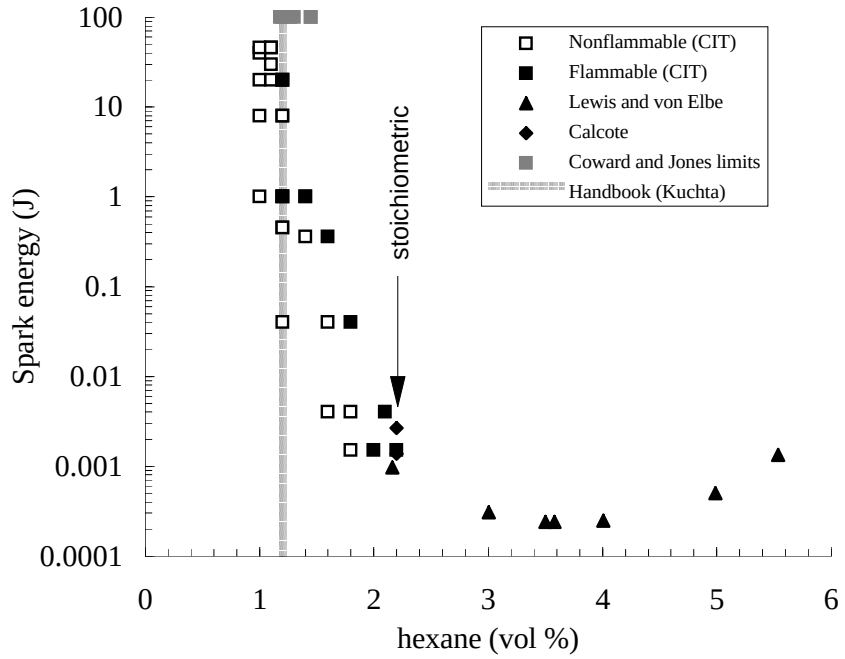

Figure 17: Measured ignition energy for hexane-air mixtures, initial pressure 1 atm, initial temperature 295 K.

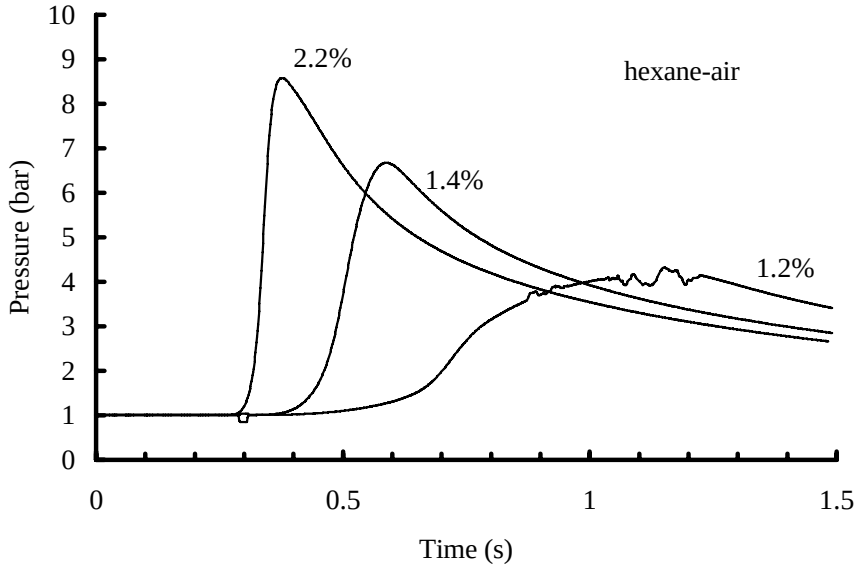

Figure 18: Measured pressure histories for hexane-air combustion, initial pressure 1 atm, initial temperature 295 K.

4.2.3 Flame Speeds

The burning speeds (Fig. 20) for the hexane experiments were also computed by the "t^3" pressure-trace analysis method described by Shepherd et al. (1997). There are no values

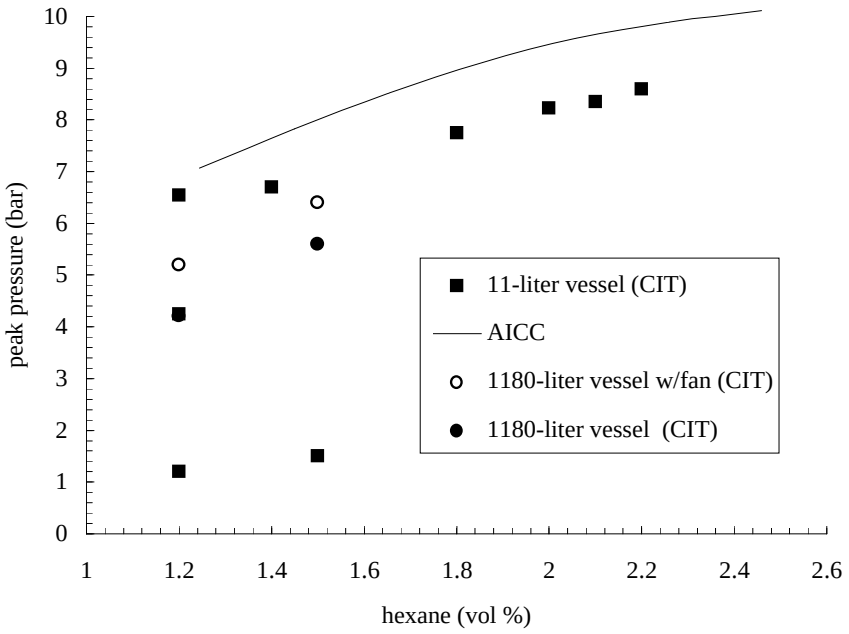

Figure 19: Measured peak pressure for hexane-air mixtures, initial pressure 1 atm, initial temperature 295 K.

for hexane-air burning speeds available in the open literature. However, the range of speeds is similar in magnitude to the range observed for propane, and varies with fuel concentration in a consistent manner. These speeds are comparable to those obtained for similar hydrocarbons like heptane (Gibbs and Calcote 1959; Gerstein et al. 1951).

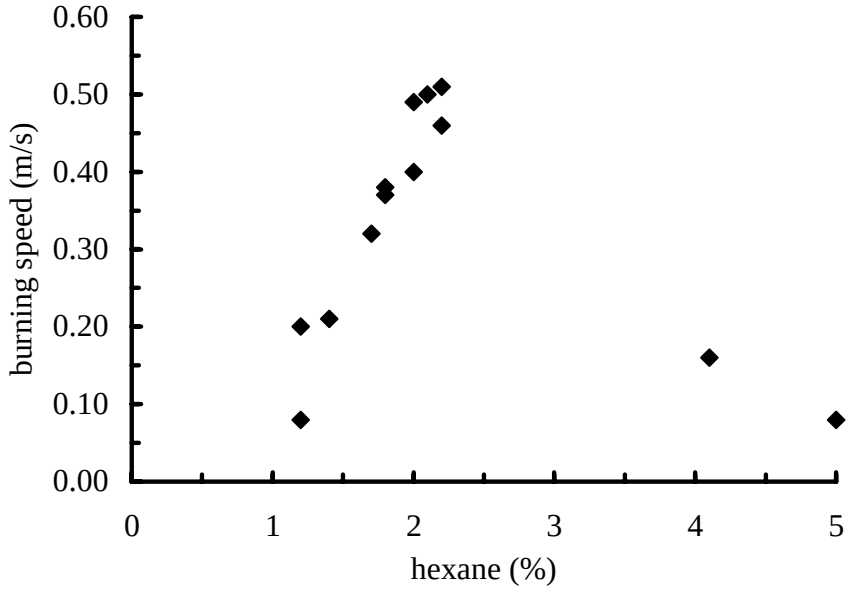

Figure 20: Effective burning speeds estimated from the pressure-time histories for hexane-air mixtures, initial pressure 1 atm, initial temperature 295 K.

5 Jet A Combustion

Following the validation testing with the hexane-air and propane-air mixtures, tests with Jet A were carried out. All these tests were carried out in the 1.84-liter vessel, with the exception of six tests performed in the 1180-liter vessel. The ignition energy was measured at two mass loadings, 3 kg/m^3 and 200 kg/m^3, for temperatures between 25 and 60°C. The initial conditions and key results are given in Tables 7 and 9 of Appendix A.

5.1 Flashpoint Measurements

In order to characterize the Jet A used in this study, we measured the flashpoint with a Tag closed-cup tester using the ASTM D56 (1988) method. These tests were conducted at an ambient pressure of about 99 kPa, and the flashpoints were corrected to an atmospheric pressure of 101.3 kPa as required by the method. Several other fuels, including hardware-store kerosene and single-component hydrocarbons were also measured in order to validate our procedures. The results of these tests and NTSB results on a Jet A sample from Athens, Greece are shown in Table 2.

Ignition energy tests were primarily performed with Jet A fuel obtained from Los Angeles International Airport (LAX). The fuel was stored at 20°C in a closed gas container to minimize the effects of fuel weathering, namely the loss of the low-molecular-weight components in the fuel. A single batch of fuel was used over a period of 3 to 4 months. Preliminary tests were also performed with Jet A fuel from El Monte airport. These tests were numbers 30, 31, and 31b shown in Table 7 of Appendix A. The results of these tests indicate that the El Monte fuel is indistinguishable from the LAX fuel in terms of ignition energy.

The El Monte and LAX fuel flashpoints ranged between 45 and 48°C, essentially identical given the intrinsic variability of the measurement technique. These values can be compared to the minimum flashpoint given in the specification (ASTM D1655 1997) of 38°C (100°F), which is chosen to coincide with the division between flammable and combustible liquids (Benedetti 1996). The NMAB report (NRC 1997) suggests that the processing used to refine and blend Jet A is often shared with the production of home heating oil (No. 2 Fuel Oil) which has a minimum flashpoint of 49°C (120°F). As a consequence, some Jet A flashpoints are similar to or greater than this value (see p. 7 of the NMAB report, NRC 1997). Surveys of the U.S. and world supply of Jet A indicate that the extremes range from flashpoint values of 100°F to 150°F.

The flashpoint is the standard (Benedetti 1996) figure-of-merit to classify the fire and explosion hazard of liquid fuels. For pure substances (Affens 1966) and simple mixtures, e.g., alkanes (Affens and McLaren 1972), the flashpoint can be uniquely related to the flammability limit of the vapor through the vapor pressure dependence on temperature. The flashpoint is found to be correlated closely to the temperature at which the vapor concentration reaches the lower flammability limit value. In terms of the fuel-air mass ratio f, this is

$$f_{LFL} \approx \frac{W_{fuel}}{W_{air}} \frac{P_\sigma(T_{flash})}{P_a} \tag{3}$$

Table 2: Flashpoints of different fuels.

Fuel	Flashpoint (°C)	Flashpoint (corrected) (°C)	Description
Jet A (sample 1)	47	48	LAX
Jet A (sample 2)	44	45	LAX
Jet A (sample 3)	47	47	LAX
Jet A	47	48	El Monte
Jet A	–	45	Athens
kerosene	56	57	commercial (1-K)
octane	13	14	technical grade
dodecane	80	80	technical grade

where W_{fuel} is the average molar mass of fuel vapor, about 130 g/mole, W_{air} is the molar mass of air, 29 g/mole, P_σ the vapor pressure of the fuel, and P_a is the ambient pressure.

For complex mixtures like Jet A, the flashpoint test only provides an indication of the relative flammability between different fuels. In the case of Jet A, ignition measurements with spark sources indicate that ignition can be obtained at temperatures that are lower than the flashpoint (Nestor 1967; Ott 1970). This has been ascribed variously as due to the method of ignition, the procedure used in the flashpoint test, lack of adequate mixing between fuel vapor and air, and the difference between upward and downward propagation of flames. It appears that the complex nature of the chemical composition must play a role in this effect since simple mixtures obey the relationship expressed in Eq. 3 (Affens and McLaren 1972).

A test of the relationship between flashpoint and vapor pressure is shown in Fig. 21 using the vapor pressure measurements and flashpoint measurements for Jet A carried out at Caltech (Shepherd et al. 1997). The vapor pressure used in this comparison was obtained at a high mass loading (400 kg/m^3) and is representative of what might be obtained in a flashpoint-type test, but not for a nearly empty fuel tank such as in TWA 800. Shown in this figure are two curves, one representing the fuel-air mass ratio at sea level and the other at 14 kft. The usual rule-of-thumb for flammability is that $f_{LFL} \approx 0.030$ to 0.035; it is plotted as the shaded bar.

Note that the flashpoint of 47°C is slightly higher than the intercept of the standard flammability limit range of f = .030 to .035. The reduction in the flashpoint and flammability limit temperature with increasing altitude is clearly illustrated by the 14 kft curve. This simple estimate indicates that at 14 kft, the mixture should be flammable for any temperature higher than about 30°C. This is roughly in accord with the observations discussed in the next section and the previous studies on Jet A (Nestor 1967; Ott 1970).

5.2 Ignition Energy Results

As demonstrated by the results for propane and hexane, the key factor in determining ignition energy is the composition and concentration of fuel vapor. The concentration of fuel vapor in

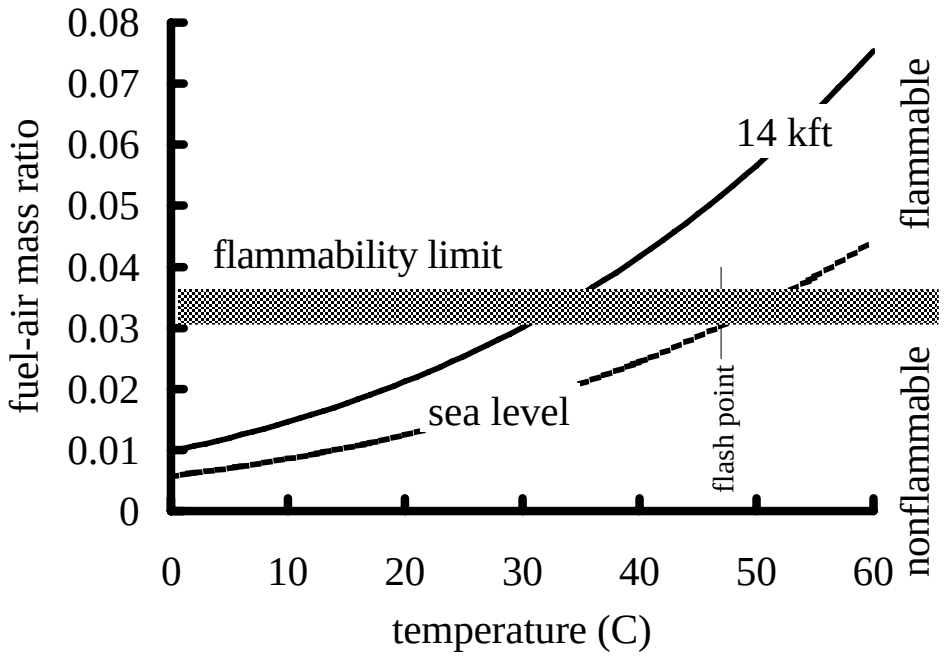

Figure 21: Fuel-air mass ratios estimated from Caltech 3-kg/m^3 vapor pressure measurements using a fuel-vapor molar mass of 130 g/mole.

equilibrium with a liquid fuel is proportional to the fuel vapor pressure $P_{\sigma,fuel}$ and inversely proportional to the ambient pressure P_a

$$X_{fuel} = \frac{P_\sigma(T_{fuel})}{P_a} \ . \tag{4}$$

The vapor pressure of fuel will in turn (Shepherd et al. 1997) depend primarily on the fuel liquid temperature T_{fuel} and secondarily on the amount of liquid and the history of handling. In previous flammability experiments (Nestor 1967; Ott 1970), the vapor pressure and the fuel concentration were not measured. Instead, with Eq. 4 in mind, the results of these experiments were simply presented as a function of temperature. We follow that practice here in the presentation of the data. The possibility of combined ignition and vapor pressure measurements to present the data in terms of concentration is discussed in the following section. In addition to examining the temperature dependence, we have studied the dependence on fuel loading by testing two situations, one with a 1/4-full tank (200 kg/m^3) and the other with a nearly empty tank (3 kg/m^3).

Quarter-full tank (200 kg/m^3) The ignition energy (Fig. 22) was measured for temperatures between 30°C and 60°C at a pressure of 0.585 bar and a mass-to-volume ratio of 200 kg/m^3. The pressure corresponded to the ambient pressure at 14 kft, and the mass-to-volume ratio corresponded to a tank 1/4-full of liquid, similar to previous experiments. In the 1.8-liter vessel,

this was about 450 ml of liquid fuel, which formed a layer about 3 mm deep on the bottom of the vessel. Below 30°C, the ullage mixture cannot be ignited even with spark energies of up to 100 J. The ignition energy decreases rapidly as the temperature increases. Above 50°C, the mixture can be ignited with spark energies on the order of 1 to 10 mJ. Typical pressure histories for tests at different temperatures are shown in Fig. 24.

Nearly empty tank (3 kg/m^3) One significant factor for TWA 800 was the very small mass of fuel in the CWT. At low mass-to-volume ratios, Jet A vapor pressure decreases due to depletion of the more volatile components in the fuel (Shepherd et al. 1997). This results in leaner fuel-air mixtures in the ullage and possibly, higher ignition energies. In order to examine this possibility, ignition energy (Fig. 23) was also measured for a mass-to-volume ratio of 3 kg/m^3 and temperatures between 30°C and 60°C at a pressure of 0.585 bar. This condition corresponds to that estimated for TWA 800 at the explosion altitude of 14 kft. In the 1.8-liter vessel, this was about 7 ml of liquid fuel, which formed a layer that just wetted the bottom of the vessel.

The results of our ignition energy tests with this mixture are shown in Fig. 23, and indicate a dependence on temperature very similar to the 200 kg/m^3 case (Fig. 22). The expected mass-loading effect is not obvious. Below 30°C, the ullage mixture cannot be ignited even with spark energies of up to 100 J. The ignition energy decreases rapidly as the temperature increases. Above 50°C, the mixture can be ignited with spark energies on the order of 1 to 10 mJ. Typical pressure histories for tests at different temperatures are shown in Fig. 24.

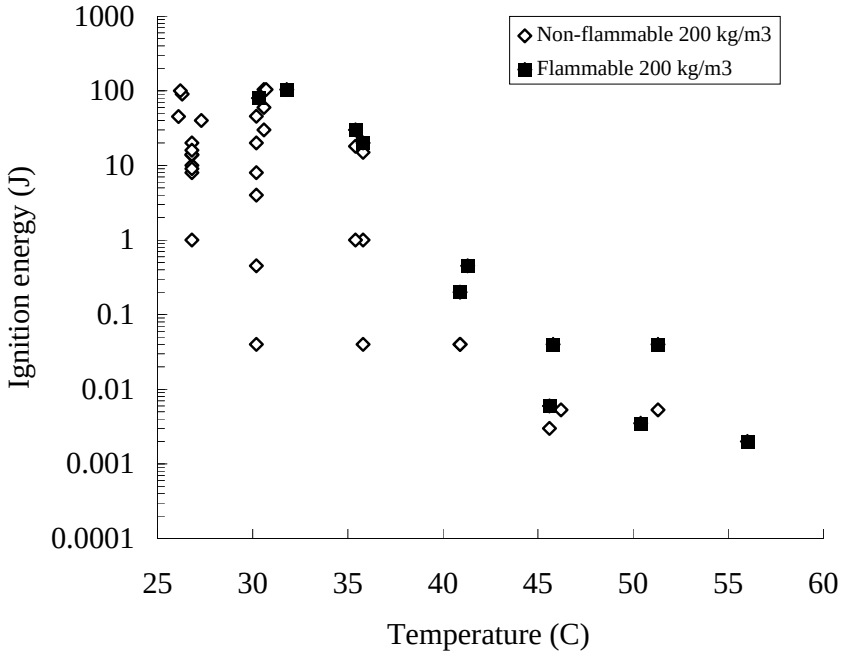

Figure 22: Measured ignition energy for Jet A vapor-air mixtures, mass loading of 200 kg/m^3 and an initial pressure 0.585 bar.

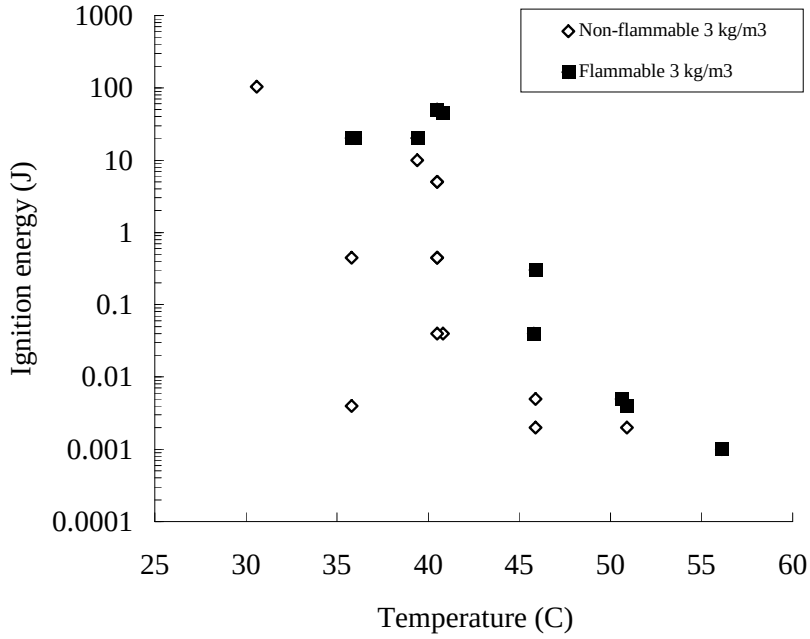

Figure 23: Measured ignition energy for Jet A vapor-air mixtures, mass loading of 3 kg/m^3 and an initial pressure 0.585 bar.

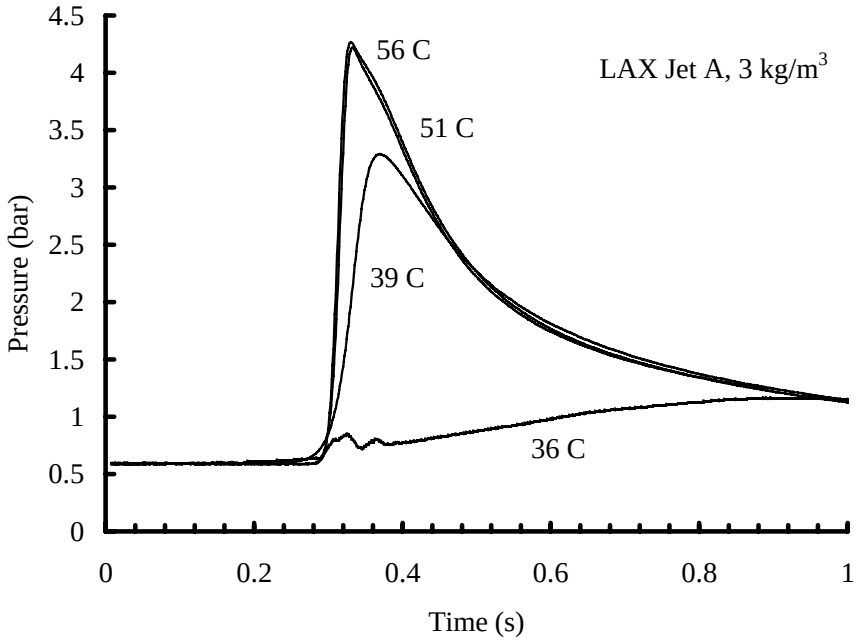

Figure 24: Pressure histories for Jet A-air mixtures (3 kg/m^3) in the 1.8-liter vessel.

5.3 Peak Combustion Pressure

The peak pressure rise data (maximum measured pressure minus the initial pressure) for the current Jet A combustion tests are shown in Fig. 26. The values of peak pressure rise ranged

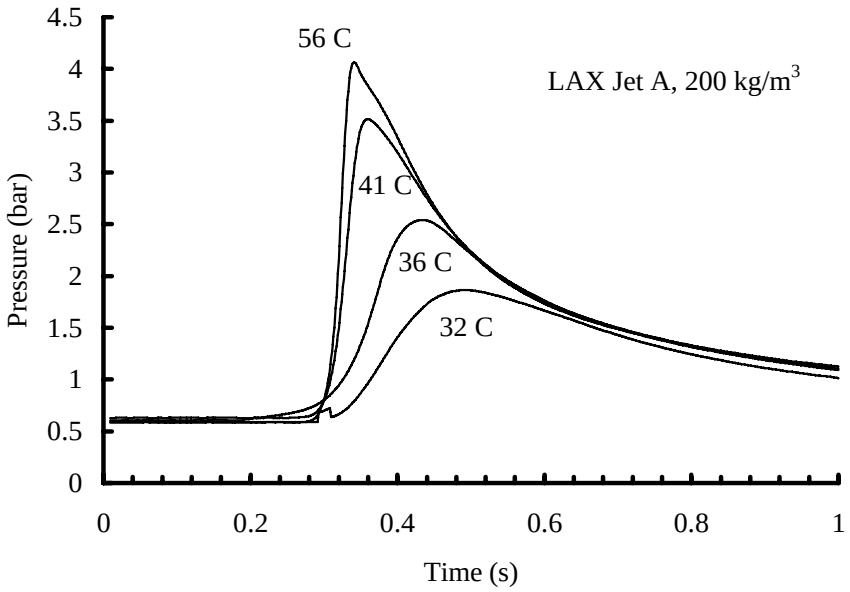

Figure 25: Pressure histories for Jet A-air mixtures (200 kg/m^3) in the 1.8-liter vessel.

from about 0.5 near the lean limit up to 3.5 bar for mixtures with temperatures between 45 and 60°C. As the temperature decreases, the peak pressure rise decreases due to the lower energy content, lower burning speed, and increasing heat transfer losses of leaner mixtures. The results also show that the peak pressures are reasonably independent of the vessel volume. Note that peak pressure rise between the two levels marked RS and SWB3 is consistent with the observed early damage in the TWA 800 CWT explosion. The two levels shown correspond to the estimated overpressure required for structural failure of the rear spar (RS) and spanwise beam 3 (SWB3) of the 747-100 center wing tank (Shepherd et al. 1997). Comparison of the present data with the previous results of Ott (1970) show that they are in reasonable agreement (Fig. 27) if the initial pressure (0.6 bar) of the present tests is taken into account.

Comparisons of the measured peak pressure rise with estimated adiabatic, isochoric, complete-combustion (AICC) pressures are shown in Fig. 28. These estimates were developed by using the Jet A composition and vapor pressures (see Fig. 36) measured by Woodrow and Seiber (1997) and Shepherd et al. (1997). The hydrogen-to-carbon ratio of the fuel was measured to be approximately 1.8. The molar mass of the vapor (discussed in Fig. 38) depends on the temperature and mass loading but in general ranges between 119 and 126 g/mole for mass loadings between 3 and 364 kg/m^3. Selecting a nominal value of 126 g/mole and the hydrogen-to-carbon ratio of 1.8, we obtain a composition of $C_{9.1}H_{16.4}$. For the purposes of the AICC computation, this was rounded to C_9H_{16}, which has a molar mass of 124 g/mole. In order to carry out the AICC computation, the heat of formation must be specified. In general, the heat of formation depends on the details of the molecular structure and for a mixture, the exact composition. Rather than attempting to account for all these details, a representative value was back calculated by assuming that the heat of combustion was 43 MJ/kg, typical of many hydrocarbon fuels. In this fashion, a heat of formation of -6124 kJ/mole was determined

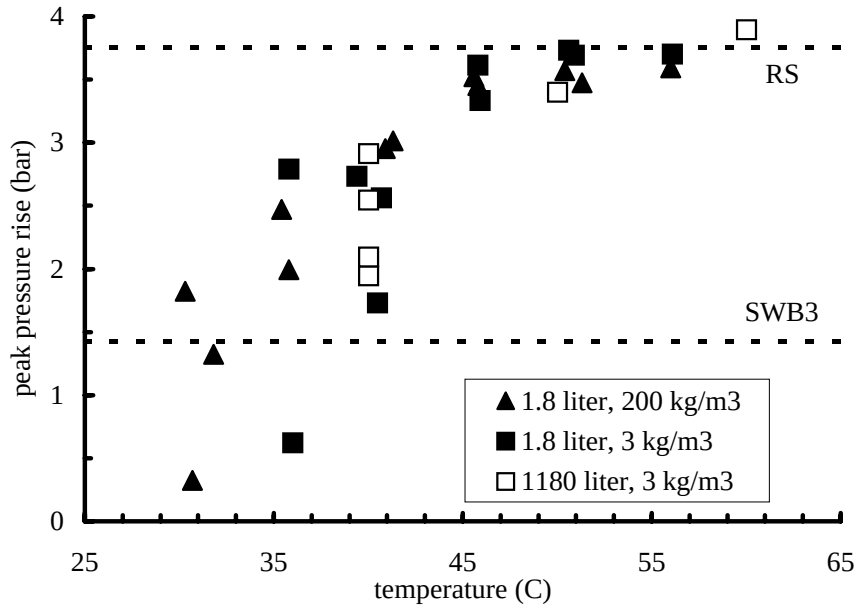

Figure 26: Measured peak pressure rise for Jet A-air mixtures, initial pressure 0.585 bar. Estimated overpressure required for structural failure of rear spar (RS) and spanwise beam 3 (SWB3) of 747-100 center wing tank are also shown (see Shepherd et al. 1997 for discussion of these values).

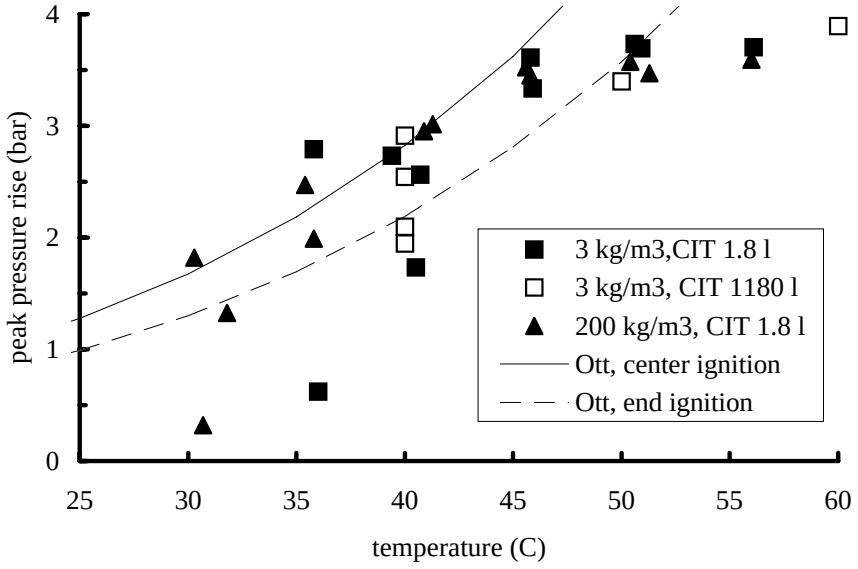

Figure 27: Measured peak pressure rise for Jet A-air mixtures at 0.585 bar initial pressure, compared with previous data of Ott (1970).

for Jet A vapor.

Finally, in order to plot the results as a function of temperature, the concentration of Jet A

had to be computed from the measured vapor pressure using Eq. 4. The results for two different mass loadings and both sets of vapor pressure data are shown in Fig. 28. Only one set of results for the higher mass loading is shown since both vapor pressure measurements gave the same results at this condition.

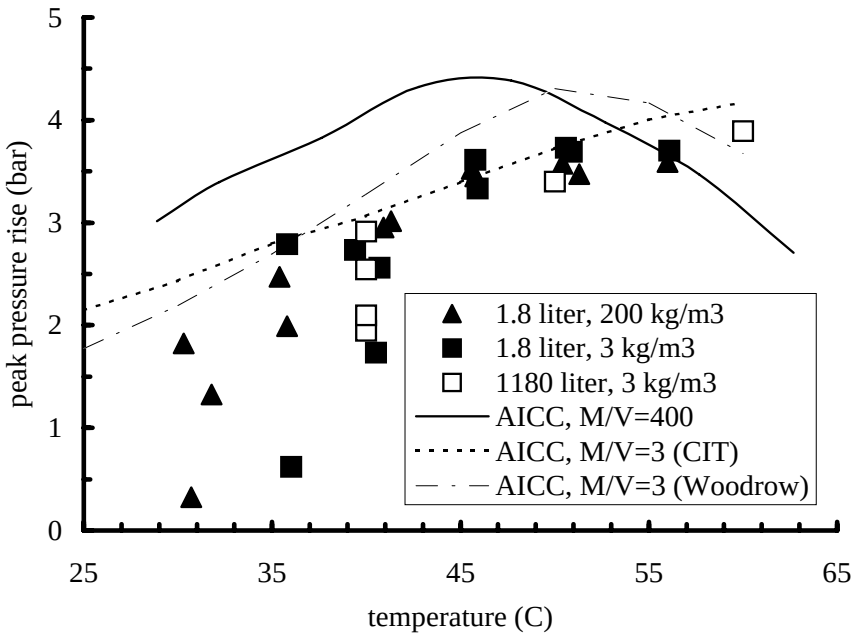

Figure 28: Measured peak pressure rise for Jet A-air mixtures, compared with AICC estimates of peak explosion pressure. Initial pressure 0.585 bar in all cases.

5.4 Burning Speed

The burning speed for the Jet A mixtures (Fig. 29) were computed from the tests carried out in the 1.84 and 1180-liter vessels using the "t^3" method discussed in Shepherd et al. (1997). Burning speeds can be found in Table 7. There is more scatter in the Jet A burning speed than in the propane and hexane burning speeds, but some clear trends are present. The range of values is comparable to that observed in the propane and hexane tests with a maximum of 60 cm/s and a minimum of 8 cm/s.

The values from the 3 kg/m^3 tests in the 1.84-liter vessel are consistently lower than the 200 kg/m^3 tests in the same vessel. The simplest explanation for this effect is that the vapor pressure is lower in the 3 kg/m^3 case and therefore the concentration of fuel molecules is lower. There may be poorer mixing of the vapor space in the 200 kg/m^3 case since the magnetic stirrer is completely submerged in that case.

The values for the 1180-liter vessel are comparable to those obtained in the 1.84-liter vessel at the same temperature and mass loading. There are several differences between the experiments in the 1.84 and 1180-liter vessels that could affect the burning speed. The pressure-reduction technique measures the effective value of the burning speed; the flame is turbulent

for a much greater portion of the time in the 1180-liter vessel than the 1.8-liter vessel. At the lowest burning speeds (8 to 15 cm/s), buoyancy is clearly a significant factor and will be more important in the larger vessel than in the smaller one. However, the procedure for heating and mixing the Jet A vapor is also different in the two vessels and this could be a factor in the observed differences.

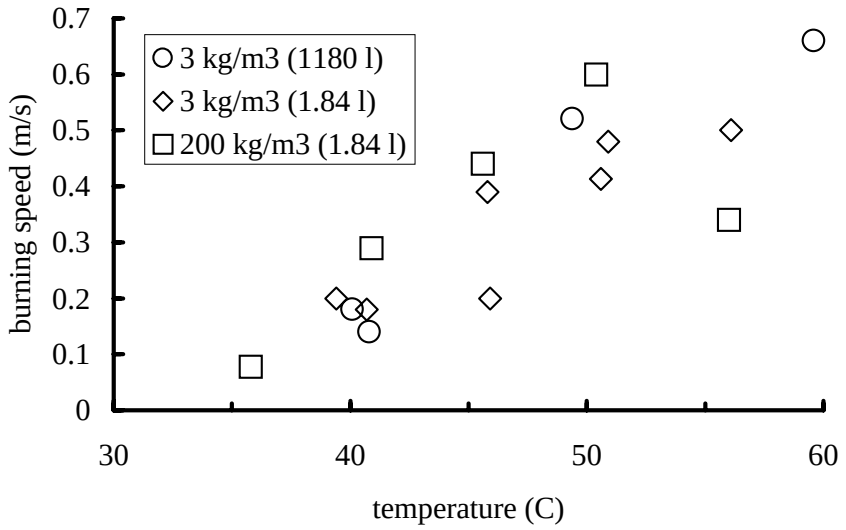

Figure 29: Effective burning speeds in Jet A-air mixtures as measured in the 1.8-liter vessel.

5.5 Ignition in the 1180-Liter Vessel

Preliminary ignition energy tests were also performed in the 1180-liter vessel. These tests are listed in Table 9. The procedure was to pour the fuel (about 4.4 liters) into the bottom of the heated tank and then evacuate the vessel to about 450 mbar. The fuel was allowed to evaporate and mix with the air in the tank over the next four hours. For 20 minutes each hour, the fan was run in the ullage. At the end of this period, air was added to bring the pressure up to 585 mbar and the fan was run for final 10-minute period. Ignition was through either a spark discharge system similar to that described in Fig. 12 or a neon-sign transformer between electrodes spaced 10 mm apart. One significant issue with these experiments was disposing of the waste fuel remaining in the tank following the combustion experiment. The procedure was to pump the fuel out of the bottom of the tank and then to burn off the remaining vapor using oxygen enrichment.

The pressure histories measured in the 1180-liter vessel are shown in Fig. 30. The peak pressures are compared in Fig. 26 with the peak values obtained in the 1.8-liter vessel. The effective burning speeds (Table 3) are compared in Fig. 29 with the values obtained in the 1.8-liter vessel.

The ignition energies obtained in 1180-liter vessel were generally higher than those obtained in the gas ignition vessel and the heated ignition vessel. Tests 466, 464, and 470 were

carried out with a 10-mm gap width and the continuous arc created by a neon sign transformer. Test 487 used a 10-mm gap width and a 0.5 μF capacitor charged to 7.7 kV (14 J stored energy). All of these cases required much higher energies than the corresponding temperature situations in the the 1.8-liter vessel. Possible causes for these higher values include the lack of liquid fuel stirring, different spark-gap distances, different discharge circuitry, and different vessel geometry. Since the experiments were time consuming, very few data points were obtained in the 1180-liter vessel and these systematic differences were not further examined.

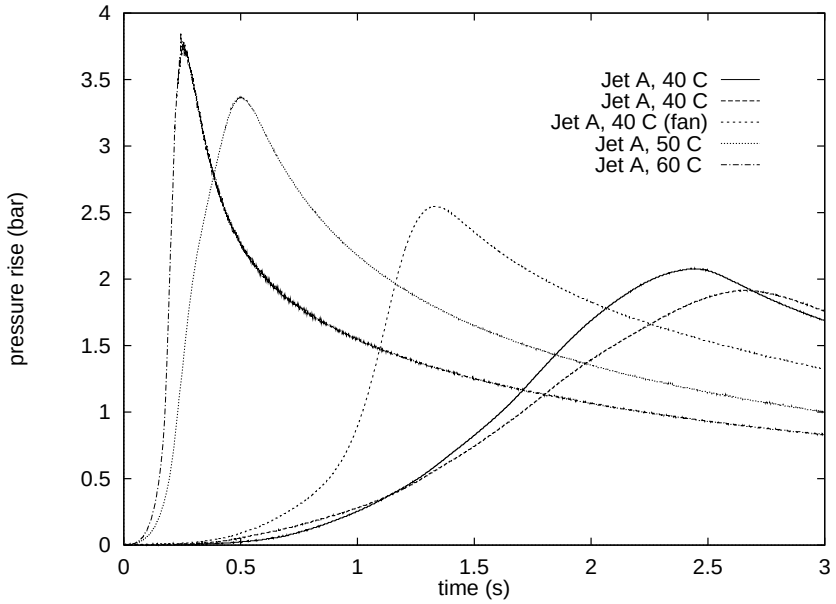

Figure 30: Pressure histories for Jet A-air mixtures (3 kg/m^3) in the 1180-liter vessel.

Table 3: Flames speeds (S_u) deduced from 1180-liter vessel tests.

Test	T (°C)	S_u (m/s)
466	40.1	0.18
464	40.8	0.14
470	49.4	0.61
487	59.6	0.66

6 Discussion

The results of the ignition energy tests raise a number of issues that merit extended discussion. The key issues we consider are: (1) theories or correlations that can be used to predict ignition limits; (2) relationship of previously measured flammability and ignition limits to those measured in this report; (3) effect of mass loading (amount of Jet A liquid in the fuel tank) on ignition energy; (4) weathering effects on ignition energy limits; (5) pressure dependence of ignition energy; (6) effects of flame propagation, temperature gradients, condensation, and ignition location. In the subsequent sections, we consider each of these issues in depth.

6.1 Ignition-Energy Prediction

Ignition by an electrical discharge is a surprisingly complex process. Experimental studies (Kono et al. 1988; Borghese et al. 1988) of rapid (nanosecond duration) discharges reveal that the process proceeds in several stages: (i) $t < 0.2\mu$s, deposition of electrical energy to create an ionized channel of hot gas between the electrodes; (ii) 0.2 to 10 μs, expansion of the hot gases and creation of a shock wave; (iii) 10 to 40 μs, recirculation of fresh gases into the channel; (iv) 40 to 200 μs, turbulent mixing of hot and cold gases. If the discharge occurs over an extended period of time then the distinction between these stages is blurred and effects such as buoyancy may also come into play. As a result of these processes, the kernel of hot gas created in the discharge region initiates reaction in the surrounding cooler gas. If the ignition energy is sufficiently large, then a propagating flame emerges from the vicinity of the kernel of hot gas after about 100 to 200 μs.

Because the process is so complex, there are no first-principle theories for the prediction of ignition energy. Several ideas (Lewis and von Elbe 1947; Litchfield 1960) have been proposed to correlate ignition energy with other combustion parameters. These ideas are all based on the notion of a *critical flame kernel* or *bubble*. Experiments (Litchfield et al. 1967) reveal that the initial disturbance created by the electrical discharge must exceed a minimum volume in order for the flame to become self-sustaining. Experimental observations (Kono et al. 1988) show that this volume is often toroidal in shape for a spark generated between bare electrodes. However, this shape is idealized as cylindrical or spherical by simple models.

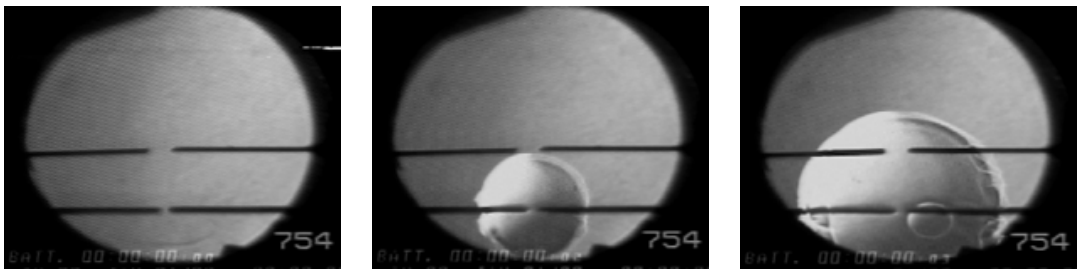

(a) (b) (c)

Figure 31: Ignition and growth of a flame in 7% H_2, 1.4% C_3H_8 Jet A simulant mixture at 295 K and 0.83 atm: (a) before spark; (b) 17 ms; (c) 34 ms. From Kunz (1998).

The first model for ignition was developed by Lewis and von Elbe (1947) and was based on the notion of a balance between heat generation and loss for a critical size kernel. In order for a spherical flame to be initiated, the spark energy must be at least as large as the *excess enthalpy* contained within the flame:

$$E \geq \int_0^\infty 4\pi r^2 \rho (h - h_0) \mathrm{d}r \tag{5}$$

where h is the specific enthalpy and ρ is the mass density. This integral is evaluated by recognizing that the main contribution occurs within the flame, a region of width δ_f, for a critical kernel of radius r_c:

$$E \geq 4\pi r_c^2 \rho c_p (T_b - T_u) \delta_f \tag{6}$$

where we have approximated $h - h_0 \approx c_p(T_b - T_u)$. The subscript u refers to the unburnt gas and b to the burnt gas.

The critical kernel size is identified with the so-called quenching distance, which was measured by Blanc et al. (1947) in ignition experiments, and measured for propagating flames by many other researchers and summarized in Potter (1960). The quenching distance δ_q is defined to be the smallest spacing between two plates that will allow a flame to propagate. Experimentally, the quenching distance is found to be correlated with fuel type and composition through a critical value of the Peclet number, Pe:

$$Pe \sim \frac{\delta_q S_u}{\kappa} \qquad \text{at quenching} \qquad 30 < Pe < 50 \tag{7}$$

where κ is the thermal diffusivity of the unburnt gas. Dimensional analysis suggests that the quenching distance is approximately proportional to flame thickness:

$$\delta_q = A \delta_f \ . \tag{8}$$

The flame thickness δ_f can be evaluated by carrying out numerical simulations of the flame structure (Göttgens et al. 1992) and using the maximum slope of the temperature-distance curve to define the thickness:

$$\delta_f \approx \frac{(T_b - T_u)}{\left.\frac{\mathrm{d}T}{\mathrm{d}x}\right|_{max}} \ . \tag{9}$$

The thermal theory of flame propagation links the flame thickness to the burning speed S_u and the thermal diffusivity κ:

$$\delta_f \sim \frac{\kappa}{S_u} \tag{10}$$

where the diffusivity has to be evaluated at some temperature intermediate to the unburnt T_u and burnt T_b values, as discussed in Göttgens et al. (1992). This idea is completely consistent with Eqs. 7 and 8 if we recognize the diffusivity is a smoothly varying function of temperature, $\kappa \sim T^{0.7}$ at fixed density. For hydrocarbon fuel-air mixtures, the diffusivity is close to that of air. At room temperature, the diffusivity of air is 2.25×10^{-5} m^2/s; at a typical intermediate temperature of 1000 K, the diffusivity is about 5×10^{-5} m^2/s.

Values of the burning speed (Lewis and von Elbe 1961), quenching distance (Lewis and von Elbe 1961), and flame thickness (Göttgens et al. 1992) are given for selected propane-air

Table 4: Burning speeds, quenching distances, flame thickness, and adiabatic flame temperatures for propane-air flames at normal temperature and pressure.

Fuel (%)	S_u (cm/s)	δ_q (mm)	δ_f (mm)	δ_q/δ_f	T_b (K)
2.86	28	4.2	0.25	17	1880
3.64	35	2.4	0.14	17	2190
4.02	40	1.9	0.12	16	2270
5.08	27	1.7	0.16	10	2120
5.52	17	2.0	0.33	6	2050
5.91	12	2.5	0.47	5	1970

mixtures in Table 4. Note that the quenching distance is between 5 and 20 times the flame thickness for these mixture conditions, supporting the concept of Eq. 8.

If we approximate the relationship between quenching distance and flame thickness as strictly proportional and identify the critical radius with one-half the quenching distance, $r_c = \delta_q/2$, the Lewis and von Elbe model for ignition energy yields:

$$E = C\delta_f^3 \rho c_p (T_u - T_b) \qquad C = \pi A^2 \; . \tag{11}$$

We have evaluated this relationship using available data on propane-air burning speed (Fig. 16) and the results are shown in Fig. 32 as the lines labeled "Kernel." The method outlined in Göttgens et al. (1992) is used to evaluate the flame thickness. The choice of the constant C is somewhat arbitrary since the ratio between quenching distance and flame thickness is not constant over the mixture range studied. On the basis of comparisons between the model and the data at near-stoichiometric conditions, we chose a value of $C = 60$ for the Metghalchi and Keck (1980) burning speed data and $C = 100$ for the Göttgens et al. (1992) burning speed data. These choices are consistent with $4.4 < A < 5.6$. The computed adiabatic flame temperatures were used for T_b.

A somewhat simpler model by Litchfield (1960) postulates that there is a minimum amount of work that must be done by the spark discharge on the surrounding gas in order for a flame to occur. The ignition energy is taken to be the mechanical work $P_0 V$ required to displace a volume V of fuel-air mixture equivalent to a sphere which has a diameter equal to the quenching distance.

$$E = P_0 V = P_0 \frac{4}{3}\pi \left(\frac{\delta_q}{2}\right)^3 \tag{12}$$

where P_0 is the ambient pressure. We have evaluated this model using Eq. 8 and a value of $A = 10$ for the Göttgens et al. (1992) burning speed data. In Fig. 32, the results are compared with the Lewis and von Elbe model and also the experimental data.

Both models reproduce the qualitative trend found experimentally. The ignition energy is predicted to have a "U"-shaped dependence on concentration. For slightly lean conditions, 3

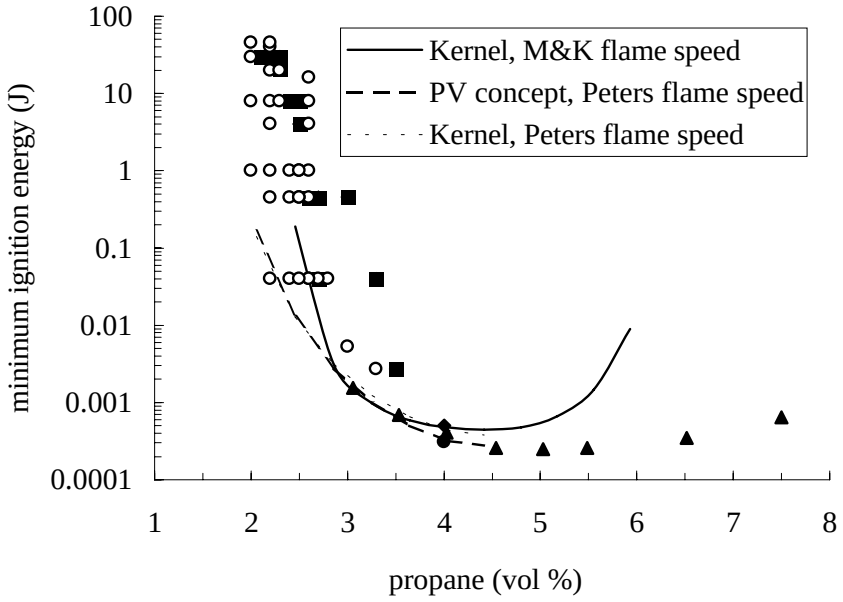

Figure 32: Comparison of propane-air ignition energy results with correlations. Kernel concept is the Lewis and von Elbe model. PV concept is the Litchfield work-done model. See Fig. 13 for the key to symbols.

to 4% propane, the models provide a reasonable description of ignition energy variation with fuel concentration. However, for very lean mixtures, less than 3% propane, the ignition energy is substantially underpredicted by both models. For rich mixtures, greater than 4% propane, the models substantially overpredict the ignition energy. There are a number of issues in both the experimental technique and the models which need to be studied in order to improve the agreement between models and experiment. The application to Jet A vapor mixtures is limited both by a lack of confidence in the models and the lack of reliable flame speed data.

The predicted functional dependence of ignition energy on flame thickness does provide a useful framework for understanding why ignition energy is such a strong function of composition near the lean limit. If we use the simple thermal model of flames to estimate the flame thickness, we can convert the Lewis and von Elbe model to the scaling relationship:

$$E \sim P_0 \frac{q}{RT_0} \left(\frac{\kappa}{S_u} \right)^3 \tag{13}$$

where we have substituted the mixture heat of combustion $q = c_p(T_b - T_u)$ and used the ideal gas law $P = \rho RT$ to eliminate the density. All other factors being the same, the ignition energy is predicted to vary inversely with the third power of the burning velocity,

$$E \sim S_u^{-3} \, . \tag{14}$$

Since the burning speed varies by at least one order of magnitude between stoichiometric (50 cm/s) and the lean limit (5 cm/s), the ignition energy is predicted to vary by a factor of 10^3. In

fact, the observed variation is approximately a factor of 10^5. A challenge for future research is to understand this discrepancy.

6.2 Previous Data

Previous work on Jet A vapor combustion has examined a very limited range of ignition energies. Nestor used two energy levels, 20 J and 4 J. Ott used a continuous arc that cannot be simply characterized, but for the purposes of comparison we have assigned a value of 100 J, based on our experience with neon sign transformer arcs at Caltech. The ignition energy results of the present work are shown in Fig. 33, along with previously reported Jet A flammability data (Nestor 1967; Ott 1970; Kuchta and Clodfelter 1985). The results are consistent with Nestor's flammability limit data and with the limited data of Ott. The band indicates the ignition energies of Jet A measured in the present work.

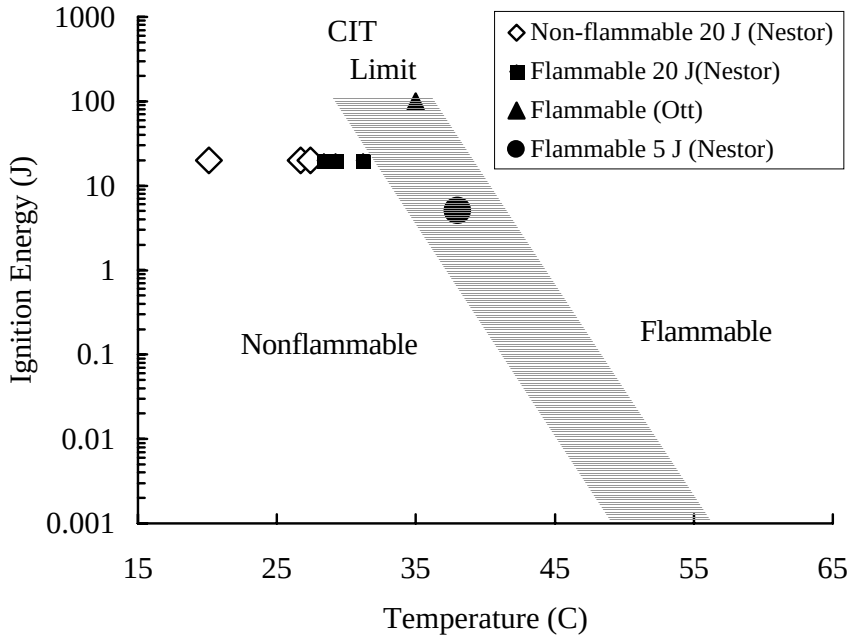

Figure 33: Comparison of present ignition energy results with previously reported data.

Closer comparison with the data of Nestor (1967) shows that the present data are located within the range of flammability represented in the altitude (pressure) – temperature plane (Fig. 34). Only two ignition energies were used in Nestor's work: 20 J as represented by the straight solid lines, and 4 J as represented by the curved dashed line. The region between the solid lines represent conditions at which jet fuel can be ignited by a 20 J spark. The region contained within the dashed line represents conditions at which jet fuel can be ignited by a 4 J spark. In this graph, the results of Fig. 22 would be located along a horizontal line at 14 kft which would intersect the region of flammability. In particular, they would correspond to points along this line from 86°F to 140°F. The intersection between the 14 kft line and the

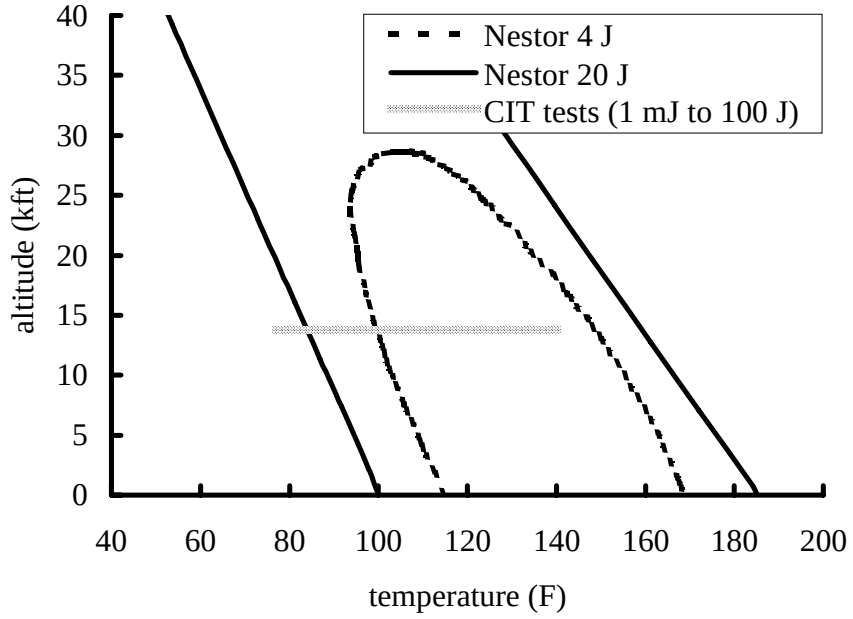

Figure 34: Flammability curves for Jet A by (Nestor 1967) and the range of the current experiments at Caltech.

lower temperature 20 J limit shows that Jet A at 85°F or 29°C has an ignition energy of 20 J. This value is lower than the 80 J obtained in the present work (Fig. 22), but can probably be attributed to differences in Nestor's apparatus and experimental procedure. Nestor's curve also shows an ignition energy of 4 J at 38°C, which is in complete agreement with the present work.

The present ignition energy results can also be compared to measurements performed on fuel mists in air (Kuchta et al. 1971). The discussion in CRC 530 indicates that the ignition energy of fuel mist is higher than the corresponding pure vapor mixture. However, comparison of Kuchta's data (Fig. 4) with the fuel vapor-air results of Nestor (1967), Ott (1970), and the present authors show that at a given temperature and pressure, mists can be ignited at much lower energies (by a factor of 10^3) than pure vapor. Indeed, Kuchta's data shows that mists can be ignited at temperatures that are up to 40°C less than the flammability limit temperatures for fuel vapor-air mixtures (Figs. 21 and 34). This can be attributed to the action of the spark heating of droplets directly within the spark channel. Vaporization and subsequent ignition of the hot vapor occurs when a droplet is sufficiently close to or within the high-temperature spark channel. A flame front may then propagate through a droplet cloud and produce overpressures that are comparable to gaseous combustion.

6.3 Fuel Mass Loading

One of the key results of the present tests is the limited influence of the fuel mass-to-volume ratio or mass loading on the ignition energy. This is illustrated in Fig. 35, in which the data from experiments with a mass loading of 3 and 200 kg/m^3 are plotted together. It is apparent

that in this representation, there is little to distinguish the two sets of data. This evaluation must be tempered by the lack of a crisp ignition boundary, primarily due to the limited number of data points.

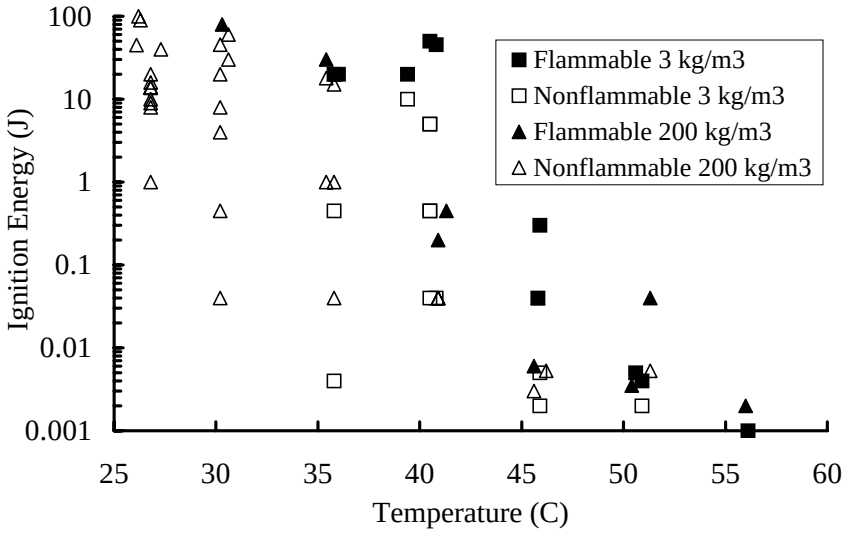

Figure 35: Ignition energies for Jet A vapor at 0.585 bar pressure, equivalent to 13.8-kft altitude. Combined data plot for both 3-kg/m^3 and 200-kg/m^3 mass loading.

This weak dependence of the ignition energy on mass-to-volume ratio is surprising since the vapor pressure (Fig. 36) at 3 kg/m^3 is significantly lower than the vapor pressure at a mass loading of 400 kg/m^3 (Woodrow and Seiber 1997; Shepherd et al. 1997). For example, at 50°C and 3 kg/m^3 loading, the Caltech physical measurements of LAX fuel (Shepherd et al. 1997) give a vapor pressure of 7 mbar and the University of Nevada, Reno (UNR) measurements of Reno fuel give a vapor pressure of 10 mbar. Both measurement techniques give a vapor pressure of about 14 mbar at 50°C when applied to a mass loading of about 400 kg/m^3. This variation in vapor pressure together with Eq. 4 imply that at a given temperature, the vapor concentration may be as much as 50% lower for the 3 kg/m^3 mass loading as compared to the 200 to 400 kg/m^3 loading situation. The ignition energy (Figs. 1, 17, and 13) for lean hydrocarbon fuels is strongly dependent on the mixture composition, suggesting that the leaner mixtures created by reducing the mass-to-volume ratio should have substantially higher ignition energies. This is not reflected in the present ignition data for Jet A. There are several possible explanations for the contradictory effects of mass loading:

1. The Caltech vapor pressure measurements are inaccurate for the 3 kg/m^3 mass loading. The Woodrow and Seiber (1997) measurements predict a much smaller decrease in vapor pressure with mass loading.

2. The ignition energy of Jet A vapor is not a function of vapor pressure or fuel concentration alone.

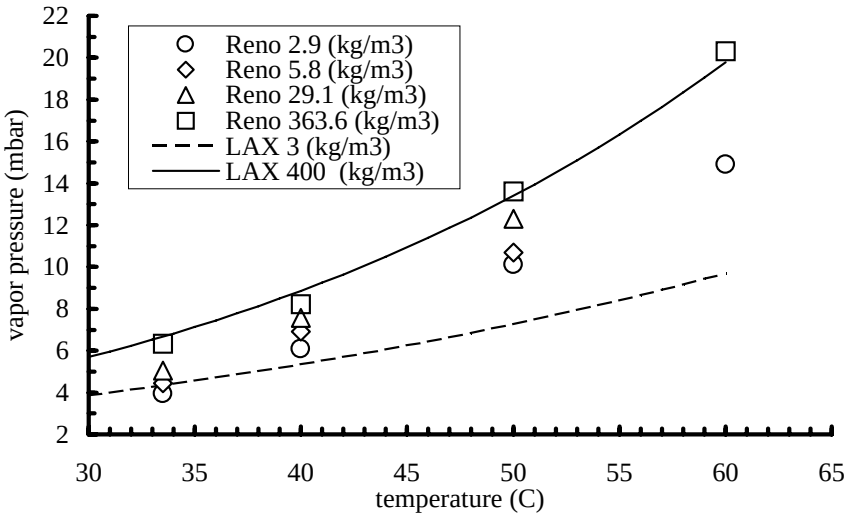

Figure 36: Vapor pressure vs. temperature for Reno Jet A (Woodrow and Seiber 1997) and LAX Jet A (Shepherd et al. 1997). Data for Reno fuel at intermediate fuel mass loadings (5.8 and 29.1 kg/m^3) were not obtained at 60°C.

(a) There is a strong dependence of average fuel composition on mass loading.

(b) Ignition energy limits are determined by a subset of the components of Jet A which are independent of the mass loading.

The first possibility is very plausible given the imprecise character of the ignition energy limits and the large differences between the Caltech and UNR measurements of the vapor pressure at low mass loading. The Caltech measurement is susceptible to many errors at extremely low mass loadings and the UNR measurements may be more reliable under these conditions. Another important element here is that the two fuel samples were obtained from different batches of Jet A that were also subjected to uncharacterized handling and weathering effects. Further studies are needed with well-characterized fuel from a common source before any definite conclusions can be drawn.

The second possibility is that even with well-controlled samples, the ignition energy could simply be relatively insensitive to the mass loading. This insensitivity could be a consequence of the multi-component nature of Jet A. The chemical analysis carried out at UNR (Woodrow and Seiber 1997) indicates that the vapors contain a mixture of molecules with between 5 and 15 carbon atoms. The relative amounts of the various components vary with the temperature and mass loading, as illustrated in Fig. 37 for Reno fuel. This data shows that as the mass-to-volume ratio changes, the concentration of the individual fuels in the mixture changes, with a strong decrease in lower molecular weight fuels as the mass-to-volume ratio decreases. However, only a modest change in the mean molar mass of the vapor (Fig. 38) is produced by changes in temperature and mass loading. This is consistent with insensitivity of the high-molecular-mass component concentrations to changes in the mass-to-volume ratio.

Since the ignition energy appears to be only weakly dependent on the mass-to-volume

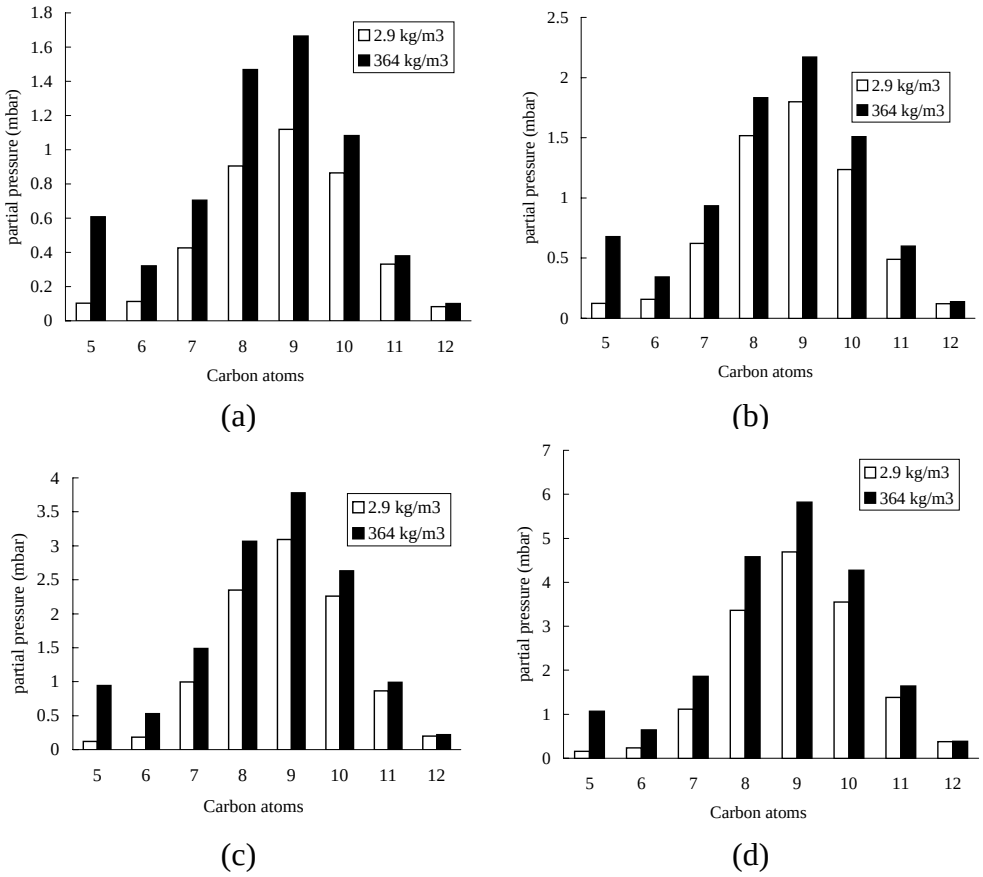

Figure 37: Partial pressure vs. number of carbon atoms in fuel molecules of Reno Jet A at two mass loading ratio: (a) 30°C, (b) 40°C, (c) 50°C, (d) 60°C (Woodrow and Seiber 1997). Note the change in vertical scale for each plot.

ratio, this suggests that the high-molecular-mass components may play a dominant role in the ignition process. Data on pure hydrocarbons (Figs. 1, 13, and 17) indicate that at a given fuel concentration (lean), the ignition energy is lower for a fuel with a higher molecular mass. The minimum ignition energy (MIE) location also shifts (Fig. 2) to lower fuel concentrations with increasing fuel molar mass. If the fuel-air mixture in the tank ullage contains a sufficient concentration of high-molecular-mass components, they may dominate the ignition process. Consequently, changes in the concentration of low-molecular-mass components may not have a strong influence on ignition energy.

Since the vapor pressure of a multi-component fuel is largely dominated by the volatile low-molecular-mass components, vapor pressure or flash point may not be a good indicator of the spark ignition hazard of the fuel. Instead, it may be necessary to develop a hazard index that reflects the dominant role of heavy species in determining the ignition energy. Further investigation of spark ignition in multicomponent mixtures is needed in order to develop a predictive capability for ignition energy.

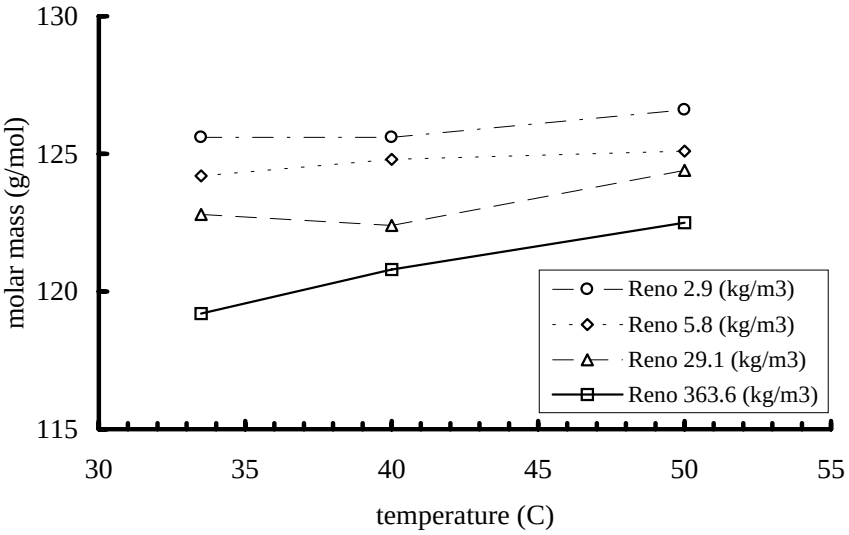

Figure 38: Molar mass vs. temperature for Reno Jet A (Woodrow and Seiber 1997).

6.3.1 Fuel Weathering

One concern in applying the present data to ignition of fuel vapors in the TWA 800 CWT is the issue of weathering. Weathering is the cumulative effect of environmental conditions on liquid fuel. Successive heating and cooling as well as changes in ambient pressure due to altitude changes can preferentially deplete certain components in the fuel, thus changing its composition. These variations in composition can in turn have an effect on fuel volatility and vapor flammability. The fuel in the CWT of TWA 800 was the residual of fuel that had been loaded over 15 hours earlier in Athens, Greece, and had been cycled through substantial excursions in pressure and temperature. A discussion of the issues and a preliminary evaluation of the effect of weathering was given in Shepherd et al. (1997). After the publication of that report, more extensive flight tests were carried out (Bower 1997) and chemical analyses of ullage vapor (Sagebiel 1997) and liquid fuel (Woodrow and Seiber 1997) were performed.

The results of these tests can be used to make a more quantitative evaluation of weathering on fuel flammability. The fundamental issue is the difference in the vapor composition at the time of the explosion as compared to that of the original fuel. There are two effects to consider. First, even without weathering, vapor created by evaporation from a limited mass of fuel liquid will have a different composition than the liquid (Shepherd et al. 1997). Second, weathering will further shift the composition due to the preferential evaporation of light components from the liquid.

The difference between liquid and vapor composition is illustrated in Fig. 39. Since liquid composition was not actually measured, the values of liquid mole fraction y_i shown here were inferred from measured (Woodrow and Seiber 1997) vapor composition mole fractions x_i and pure species vapor pressures $P_{\sigma i}$ by Raoult's law:

$$x_i = \frac{P_i}{P} \qquad P_i \approx y_i P_{\sigma i} \; . \tag{15}$$

The pure-species vapor pressures for each of the carbon atom groups was chosen to be that of the normal alkane. Figure 39 illustrates the dramatic difference between liquid and vapor compositions. It is clearly important to account for this difference in studying the flammability of these fuels.

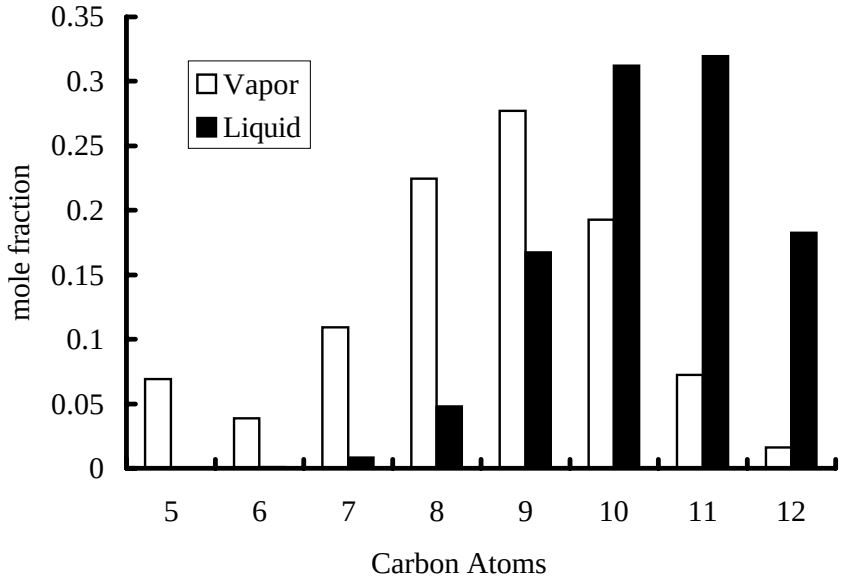

Figure 39: Mole fraction vs. number of carbon atoms in fuel molecules of Reno Jet A at temperature of 50°C and a mass loading of 364 kg/m^3. Vapor data is from Woodrow and Seiber (1997), and liquid value is inferred from Raoult's law.

The variation in composition of the fuel vapor was examined by analyzing (Woodrow and Seiber 1997) Jet A liquid used in flight testing (Bower 1997). Approximately 50 gal of Jet A was repeatedly exposed to cycles of heating by the air packs and evacuation by climbing to altitudes of 17.5 to 35 kft. Details of the liquid fuel sampling are given in Table 2 of Woodrow and Seiber (1997) and other details about the flight are given in Table 2-1 of Sagebiel (1997). Headspace gas chromatography was used to characterize the vapor evaporated from samples at a 3 kg/m^3 mass loading (appropriate for TWA 800) and temperatures between 40 and 60°C. Selected results from Woodrow and Seiber (1997) are shown in Fig. 40 as a function of the sample number for 50°C. Sample No. 1 was the initial fuel loaded into the CWT. Sample No. 2 was obtained after one cycle of operation (flight of 7-14-97), samples No. 3 and 4 after the second cycle of operation (first flight of 7-15-97), sample No. 5 after the third cycle (second flight of 7-15-97), sample No. 6 after the fourth cycle (first flight of 7-16-97), and sample No. 7 after the fifth cycle (second flight of 7-16-98).

The main results of this study are: (a) the increase in molar mass with successive cycles of fuel weathering; (b) the decrease in vapor pressure with successive cycles of fuel weathering; (c) the shift from lower molar mass to higher molar mass components with increasing number

of cycles. On each cycle, the pumping action of ascending to cruise altitude removes some fraction of the light components. This is what gives rise to the weathering.

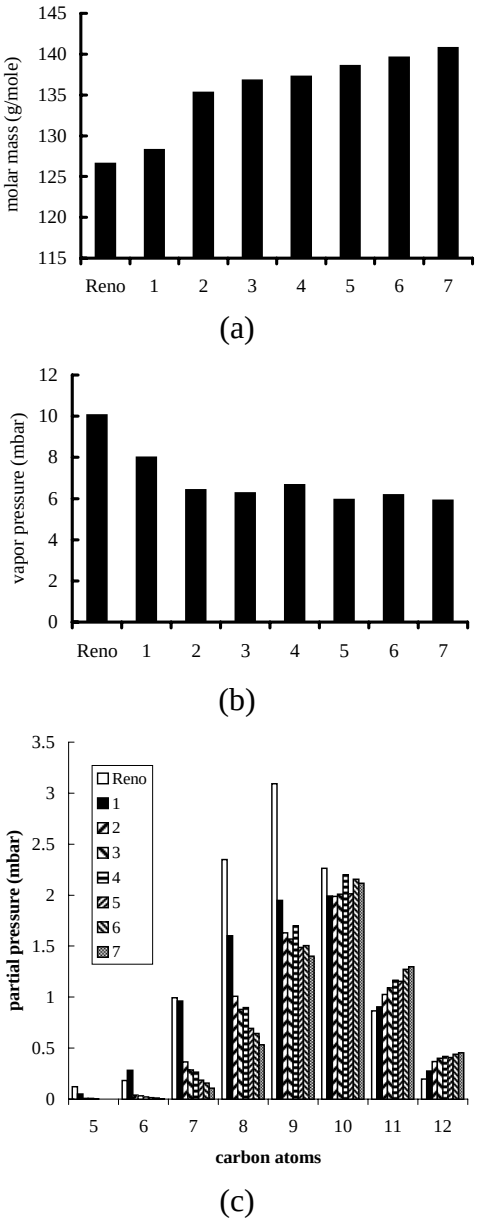

Figure 40: Effect of weathering on: (a) molar mass; (b) vapor pressure; (c) subsection partial pressures. Data labeled “Reno” is from fuel obtained at the Reno airport. All other samples were from the fuel originating in Athens and used in the flight test carried out by the NTSB in July 1997. All results were obtained at 50°C and a mass loading of 2.9 kg/m^3 (Woodrow and Seiber 1997)

.

It is not clear what effect this shift in composition will have on the ignition energy. Fur-

ther tests are needed to systematically study the effect of weathering on the ignition energy characteristics of these fuels. Preliminary results (Kunz 1998) indicate that the effect is to shift the ignition energy vs. temperature curve for weathered fuel to the higher temperatures at a given ignition energy. The effect of weathering appears to be more pronounced than the effects of mass loading. However, these results are preliminary and more carefully controlled experiments are needed to draw firm conclusions.

Weathering was also a concern in the present tests with fresh Jet A. Because the same sample of fuel was used for a series of tests at 200 kg/m^3, there is a possibility that the fuel properties changed slightly during the course of the series. One series typically involved 6 to 8 tests at different temperatures. A set of tests was performed by increasing the temperature from test to test in a staggered manner to see if the ignition energy dependence on temperature would become staggered. The tests in the series (shots 21 to 29 in Table 7) were performed in the following order of temperatures: 56°C, 47°C, 36°C, 41°C, 26°C, 31°C, 50°C, and 31°C. Despite of the non-sequential order of the initial test temperatures, the results show that the ignition energy follows a relatively smooth monotonic curve (Fig. 22). Moreover, the results of this series were consistent with those of a previous series performed on a different fuel sample (shots 715 to 723 in Table 7). We conclude that the effect of repeated tests on the 460-ml fuel sample used in the 200-kg/m^3 series was negligible since little or no influence on the ignition energy was observed.

6.4 Pressure Dependence

The experiments carried out in the present study have all been performed at a constant pressure, 1 bar in the case of propane and hexane and 0.585 bar in the case of Jet A. The fuel concentration (or in the case of Jet A, temperature), was shown to have a very significant effect on ignition energy. However, evaluation of explosion hazards during airplane operation requires considering the effect of changing altitude and the associated change in pressure. It is known from studies with pure hydrocarbons (Lewis and von Elbe 1961) that minimum ignition energy can be a strong function of pressure, even if the composition (fuel-air ratio) is kept fixed. There is no data available for Jet A ignition-energy pressure dependence.

Both Ott and Nestor obtained data on flammability limits for Jet A vapor as function of pressure but at a fixed energy. Figure 41 shows the lean flammability limit (for 20-J sparks) measured by Nestor (1967) represented as a fuel-air mass ratio as a function of the pressure. It is apparent that the LFL is essentially independent of pressure from 1 bar to 0.2 bar. For richer mixtures with lower ignition energies, there is apparently a stronger dependence of the ignition energy on pressure. For hydrocarbon fuel-air mixtures with a fixed composition (fuel-air ratio), a power-law dependence of ignition energy E on pressure P

$$E = E_0(P/P_0)^{-n} \tag{16}$$

is often quoted (Ural et al. 1989) where E_0 is the reference ignition energy for the composition of interest and the pressure P_0. This relationship is supported by data (Lewis and von Elbe 1961) for methane, ethane, and propane near the minimum ignition point. The coefficient n is nominally about 2 for most hydrocarbon fuels (Kuchta 1975; Gerstein and Allen 1964). A

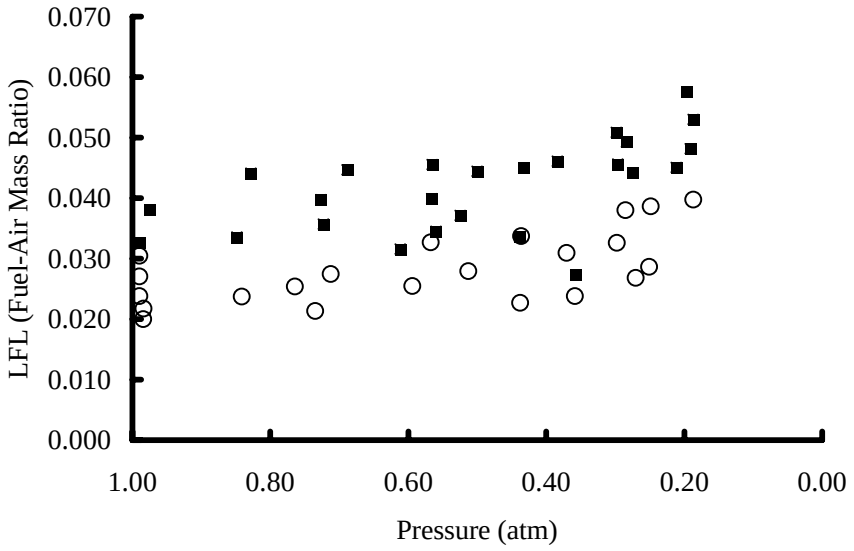

Figure 41: The LFL of Jet A from (Nestor 1967) shown in terms of the ambient pressure.

curve fit to the data of Lewis and von Elbe (1961) shown in Fig. 42 yields a value of n = 1.8. This dependence is based on measurements for mixtures close to or at the MIE, and ignition energies lower than 100 mJ. The observed pressure dependence implies that the minimum ignition energy of these small hydrocarbons increases from about 0.2 mJ at sea level to about 2.2 mJ at 35 kft altitude (0.25 bar). For leaner mixtures, the ignition energy is apparently not so sensitive to pressure variations. Ronney (1985) observed that for methane-air mixtures between 4.5% and 5% fuel (near the lean limit) the ignition energies are essentially independent of pressure.

There is no theory for the ignition energy dependence on pressure. We can develop some simple estimates from the ignition energy models discussed previously. The key issues are how the quenching distance and burning speed vary as a function of pressure. For near-MIE mixtures, the quenching distance increases with decreasing pressure (Gerstein and Allen 1964), approximately represented by $\delta_q \sim P^{-1}$. The flame-thickness dependence on pressure can be estimated by using the relationship given by the thermal flame model:

$$\delta_f = \frac{k}{\rho C_p S_u} \, . \tag{17}$$

Inserting this into Eq. 6, we have

$$E = \pi k \Delta T \delta_q^2 S_u^{-1} \tag{18}$$

where the thermal conductivity k is a function of temperature only for ideal gases. In general, the burning speed S_u dependence on pressure varies widely depending on the fuel-oxidizer system, equivalence ratio, and ambient temperature. Empirically, it is observed that a relationship of the form

$$S_u = S_u^0 \left(\frac{P}{P^0} \right)^m \left(\frac{T}{T^0} \right)^2 \tag{19}$$

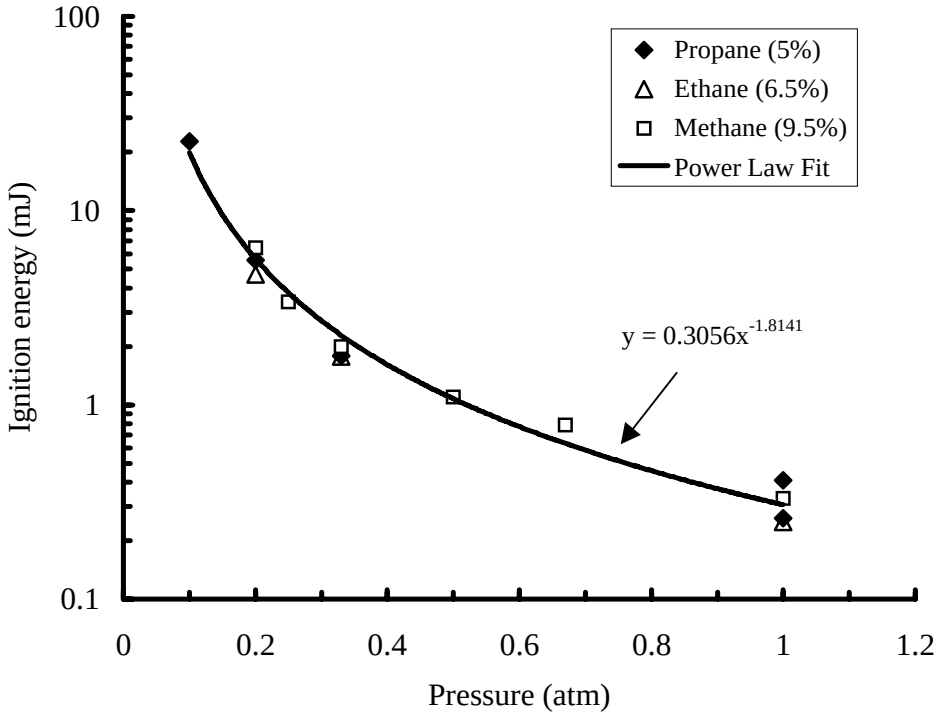

Figure 42: The dependence of ignition energy on mixture pressure for various hydrocarbon fuels at fixed composition (Lewis and von Elbe 1961).

can described the dependence of burning speed on initial pressure and temperature, the values with the supercript $(\ )^0$ are reference values. The exponent m has been correlated with the burning speed itself (Gaydon and Wolfhard 1979), high burning speeds (greater than 50 cm/s) are associated with positive values of m, low speeds with negative values of m.

If the burning speed is approximately independent of pressure, then Eq. 6 predicts that $E \sim P^{-2}$, in rough agreement with the near-MIE measurements of Fig. 42. For other mixtures, we can use the general burning speed dependence (Eq. 19) and estimate the quenching distance using Eq. 8. Substituting in either the Lewis and von Elbe or Litchfield ignition model, we obtain the scaling relationship

$$E \sim P^{-2-3m} \, . \tag{20}$$

For very lean mixtures with low burning speeds, the speed will increase with decreasing pressure; and as $m \to -2/3$, the ignition energy will be independent of pressure. Therefore we expect that as the lean limit is approached, the ignition energy will become less dependent on pressure. Values of m for burning speeds of 5 cm/s, appropriate to the lean limit, are not available from experimental data. Extrapolation of the data in Gaydon and Wolfhard (1979) indicates that a value $-0.7 < m < -0.6$ would be representative of mixtures with burning speeds between 5 and 10 cm/s. This same data set indicates a value of $m \approx 0$ for burning speeds of 40 to 50 cm/s, appropriate for near-MIE mixtures. Computations by Göttgens et al. (1992) for stoichiometric propane-air mixtures show a weak dependence (with slightly nega-

tive values of $m \sim -0.1$) of burning speed on ambient pressure for initial states close to normal atmospheric pressure and temperature.

The pressure dependence of ignition energy has not been measured for Jet A but we can make some bounding estimates using limiting values of the burning-speed pressure exponent m suggested by the previous discussion. Using the data of the present investigation for the reference ignition energy E_0 at a reference pressure of $P_0 = 0.585$ bar, we can use the simple scaling relationship Eq. 16 to predict the energy at other pressures, assuming that the value of E_0 is a function of fuel concentration only. The fuel concentration is determined as a function of temperature by using our equilibrium vapor pressure measurements (Fig. 36) and Eq. 4. The results are shown in Fig. 43 for $n = 0$ ($m = -2/3$), and $n = -1.7$ ($m = -0.1$).

The two sets of estimates in Fig. 43 are very similar and suggest that the pressure dependence of the ignition energy for Jet A at a fixed temperature (fuel amount) is dominated by the shift in composition with ambient pressure for a given temperature, rather than the modest pressure dependence given by Eq. 16. This follows simply by considering that the energy will at most vary by a factor of 4 due to the pressure difference alone for a fixed composition. On the other hand, variations over a range of 10^5 are produced by varying the composition from the lean limit to the MIE point.

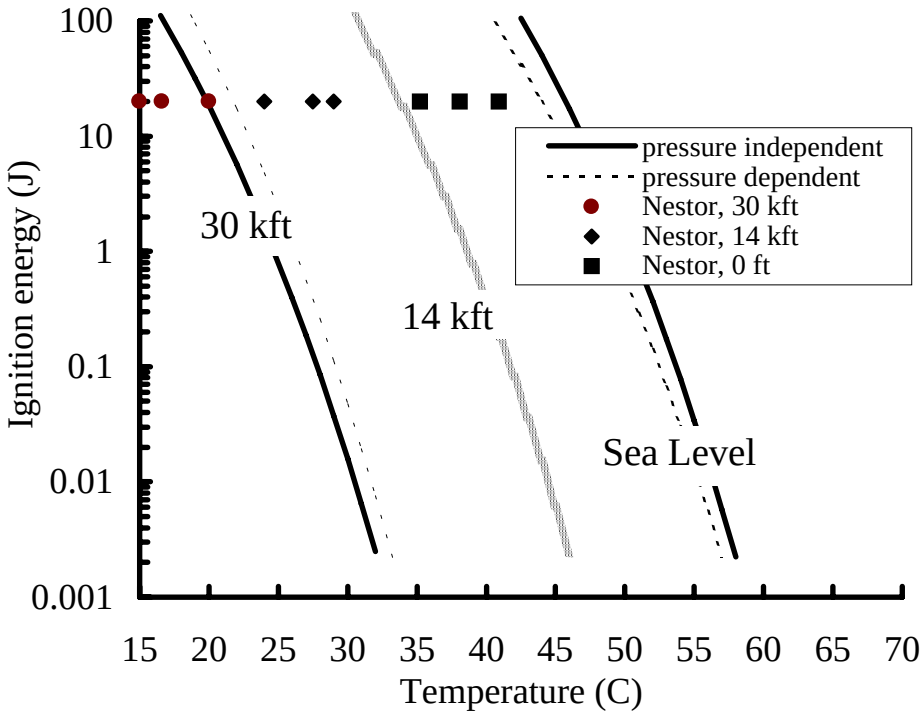

Figure 43: The ignition energy of Jet A estimated at three altitudes: sea level, 14 kft, and 30 kft. Estimation based on Caltech measurements of ignition energy and vapor pressure as discussed in the text.

Shown on Fig. 43 are several data points taken from the work of Nestor. These points show

the same trend as our predictions but the temperatures are up to 5°C lower than the our estimates. This reflects differences in fuel properties, ignition source, and experimental technique. The shift in temperature between our data and Nestor's is consistent and provides limited support for our estimation technique. We conclude that ignition energy dependence on pressure is dominated by the effect of ambient pressure on composition at a given temperature. The effects of altitude on the ignition energy vs. temperature curve can be estimated by ignoring the small dependence of ignition energy on pressure and only accounting for the shift in composition. Experimental studies are needed to obtain the data necessary to test and refine this model. Measurements are needed of ignition energy vs. temperature for at least two additional pressures corresponding to sea level and cruise altitude.

6.5 Miscellaneous Issues

Here we consider a variety of issues that are not central to our results but have arisen in the course of our investigation.

6.5.1 Near-Limit Behavior

Flammability limits are determined by the competition between chemical reactions that release energy and chemical or physical mechanisms that absorb or divert energy from contributing to flame propagation. Near the flammability limit, flames can exhibit a wide range of behavior. Consequently, there has been much debate as to the actual definition of the flammability limit. For low values of the Lewis number (Le), a near-limit flame can propagate upward in a very erratic fashion. This is particularly true of very lean hydrogen-air mixtures which have an ill-defined flammability-limit region between 4 and 9% hydrogen. Within this composition range, flammability is strongly influenced by geometry, turbulence level, and ignition type. In some cases, the flame appears to propagate spherically, then suddenly extinguish (Ronney and Wachman 1985; Ronney 1985). These near-limit flames have been called upward-propagating flames or self-extinguishing flames (Abbud-Madrid and Ronney 1990). However, this type of behavior does not appear to be relevant to the present experiments.

For the present Jet A mixtures, sparks above the ignition energy generate pale blue flame bubbles that grow steadily from the spark gap. This flame is identified by visual inspection through the window as well as by observation of the schlieren video recording. Furthermore, a flame propagation was confirmed by a rapid pressure rise within less than a second and a peak pressure close to the adiabatic, constant-volume combustion pressure. When the spark energy was less than the ignition energy of the ullage mixture, the spark-generated flame bubble extinguished itself immediately in almost all cases. Only in test 28 (Table 7) were the conditions close enough to the limit to observe an upward-propagating flame. The ignition limit was therefore unambiguous for our Jet A tests.

6.5.2 Temperature Nonuniformity

Although measures were taken to control the temperature in the test vessel, it was difficult to eliminate all the sources of nonuniformity. These variations in temperature within the vessel

could affect the ignition-energy measurements in several ways. The most significant factor is that the jet-fuel vapor pressure is a sensitive function of fuel temperature (Shepherd et al. 1997). Variations in fuel temperature could lead to uncertainty in the fuel-vapor concentration, which we have shown is the primary factor in determining ignition energy. Localized regions of low temperature may cause condensation, removing some fuel vapor from the vapor mixture. This is of particular concern in the plumbing leading to and from the vessel.

These effects have not been systematically investigated, but precautions were taken to minimize the temperature variations within the vessel. Temperature nonuniformity can occur due to heat loss through conduction in the tubing of the gas-feed system or poor convection around the outside of the vessel. The characteristic time for thermal equilibration of the aluminum vessel itself is on the order of minutes, and approximately one hour was allowed for equilibration of the system before each test. The vessel was insulated, the liquid fuel was stirred, the heaters were controlled using a feedback controller, and the temperature monitored at several points on the vessel. Consequently, the vessel temperature is believed to be fairly uniform. Temperature variations are estimated to be less than 1 to 2 °C.

6.5.3 Condensation

At temperatures above 40°C, condensation of the fuel vapor onto the cooler surfaces in the vessel occurred. Consequently, the walls and tubing, but more importantly, the windows and electrodes, became covered by small droplets of fuel. A small droplet of liquid fuel on the electrode tip may be ignited during the discharge, and thus influence the measured ignition energy limit. Preliminary observations seem to indicate that condensation of jet fuel on the electrodes may lower the ignition energy. If the vicinity of the electrode is cooler than the surroundings, it is also possible that a local cloud of fuel mist forms. According to fuel-mist experiments (Kuchta et al. 1971), this may lower the ignition energy. However, no evidence of such mists have ever been found in the present experiments.

6.5.4 Spark Location

If the spark gap is located too close to the surface of the liquid fuel, the ignition-energy measurement could be biased due to the localized heating of the liquid. Creation of a liquid mist or a fuel-rich region surrounding the electrodes could substantially lower the ignition energy. We do not believe that there were any effects of this type in the present experiments. In both vessels used in this work, the spark gap was far from the liquid surface, and inspection of the video footage showed that the initial spark-generated flame bubble did not come into contact with the liquid surface except in the case of ignition. In the 1.8-liter vessel, the spark gap was located about 5 cm above the liquid surface in the 200-kg/m^3 loading case. In the 1180-liter vessel, the spark gap was located about 45 cm above the liquid surface. No evidence of a surface disturbance or fuel spray was seen in the 1.8-liter vessel when the spark discharge occurred.

6.5.5 Relevance to Airplane Fuel Tanks

In airplane fuel tanks, a continuous variation in temperature has been observed both in the horizontal and vertical directions. This variation not only results in a variation in fuel vapor concentration above the liquid but also induces convective flows within the fuel tank. These flows cause mixing which stir the vapor and tend to reduce the variations in concentration resulting from the variation in temperature along the bottom of the tank. The effectiveness of convection in promoting mixing within the tank is still under evaluation.

The location of the spark within the vapor is unimportant as long as the vapor is well-stirred and the spark is not too close to any of the walls or liquid. In the case of actual fuel tanks, the ignition location may have an influence if the vapor is not well-stirred. In the case of TWA 800, flight and ground tests in 747 center wing tanks indicated that the natural convection within the center wing tank is very effective in mixing the vapor in the tank.

7 Summary and Recommendations

We have carried out a series of tests to determine the spark ignition energy for Jet A vapor as a function of fuel temperature at a pressure of about 0.6 bar (equivalent to 14 kft altitude). Previous flammability data has been obtained at a single energy level or else the ignition energy was not measured. Other than our own work, there exist only two unclassified sets of data obtained on Jet A vapor flammability; one sponsored by the military (Ott 1970) and the other by the FAA (Nestor 1967).

7.1 Key Results

The principal results of the present study are:

1. The temperature dependence of the ignition energy has been measured for LAX Jet A (flashpoint of 47°C). The energy varies from 100 J at 35°C to less than 1 mJ at 60°C for a pressure of 0.585 bar and fuel loadings between 3 and 200 kg/m^3.

2. Near the conventional flammability limit of Jet A, as determined by a standardized flash-point measurement, the ignition energy (measured as stored energy in a capacitor) is between 20 and 100 J.

3. Mass loading variations between 3 and 200 kg/m^3 have a very minor effect on the ignition energy vs. temperature relationship for Jet A vapor.

4. Measurements of ignition energy in hexane-air and propane-air mixtures also demonstrate a factor of 10^5 variation in ignition energy between the lean limit and the minimum ignition-energy point. Data obtained in our experiments agree with previous data on ignition energy in the region of overlap.

5. Existing models of ignition energy are in quantitative agreement with our propane-air results near the minimum ignition point. Away from the MIE, these models predict the qualitative trend of increasing ignition energy but are quantitatively incorrect. As the mixtures become progressively leaner, these models increasingly underpredict ignition energy.

6. The dependence of the ignition energy on ambient pressure has been estimated. For a fixed vapor composition (fuel-air ratio), existing data on hydrocarbon fuels suggests that the ignition energy will increase by up to a factor of 10 as the pressure is decreased from ambient to 0.25 bar (35 kft altitude equivalent). However, at a given fuel temperature with fuel vapor in equilibrium with liquid, the composition will vary rapidly, becomimg richer, with increasing altitude. The shift in the composition with altitude is anticipated to be much more significant in determining flammability since this can cause variations in ignition energy by factors of 10^5.

As shown in Figs. 33 and 34, our measured flammability limit temperatures are in reasonable accord with the earlier data of Ott (1970) and Nestor (1967) at 14-kft altitude pressure equivalent. As shown in Fig. 35, our measured ignition energies at 60°C and 14 kft indicate that the minimum ignition energy is less than 1 mJ, consistent with the industry assumption of 0.2 mJ minimum ignition energy for Jet A. As shown in Fig. 27, our measured peak pressures are consistent with those measured by Ott (1970) . We conclude that the present results are in agreement with the data of previous researchers and assumptions that have been made about Jet A flammability. In addition, we have demonstrated that our measured dependence of ignition energy on liquid fuel temperature, Fig. 35, is reasonable given the ignition behavior of other hydrocarbon fuels with variations in concentration (Figs. 13, 17, and 32) and the vapor pressure dependence on temperature (Fig. 36) for Jet A.

7.2 TWA 800 Crash Investigation

The most significant result of the present study is the demonstration of the dramatic effect fuel-tank temperature has in creating a flammability hazard within the center wing tank.

Experimental measurements were carried out on flames in Jet A vapor-air mixtures at conditions simulating those of the initial explosive event in the center wing tank of TWA 800. The conditions were those measured in NTSB flight tests, a pressure of about 0.6 bar (equivalent to 14 kft) and a temperature of 40 to 50°C. The amount of fuel was equivalent to the 50 gallons believed to be present in the CWT. The results of these experiments demonstrated that:

1. Spark ignition sources with energies between 5 mJ and 1 J would be sufficient to ignite the vapor, resulting in a propagating flame.

2. The peak pressure rise was between 1.5 and 4 bar (20 and 60 psi).

3. Thermal ignition sources created by discharging 15 J of electrical energy into a metal wire (hot filaments) are also sufficient to ignite the vapor, resulting in a propagating flame. See Appendix B for details of these tests.

4. Laminar burning speeds between 15 and 45 cm/s were measured.

7.3 Implications for Fuel-Tank Flammability Reduction

The rapid decrease in spark ignition energy with increasing temperature demonstrates that hot fuel tanks are significantly more hazardous than cool ones with respect to spark ignition sources. Prior to our study, there were no unclassified data available demonstrating the ignition energy dependence on fuel-tank temperature. Some classified data exists, but these data are inconclusive and have apparently never been a factor in commercial airplane fuel-tank design. A review of the Jet A flammability literature reveals that the minimum ignition energy data is based on extrapolation of single component hydrocarbon fuels.

The current design practice and Federal regulations (14.CFR.25, parts 954 and 981) reflect the practice of focusing on eliminating ignition sources rather than reducing flammability. Under these current regulations, fuel-tank temperatures as high as 390°F (198°C) are considered

acceptable. The FAA is reviewing this philosophy and is examining the NTSB recommendations of November 1996 (A-96-175 and -176) for reducing fuel-tank flammability. These recommendations include minimizing potential ignition sources, reducing tank temperature, inerting the ullage, and possibly raising fuel flashpoint. Each of these measures has some potential safety benefit and also, some economic cost. In order to evaluate the trade-offs between the safety benefits and cost, some quantitative analysis is required. The evaluation of these tradeoffs has been addressed by the Aviation Regulatory Advisory Committee (ARAC) Fuel Tank Harmonization Working Group (FTHWG).

As part of the FTHWG activity, fuel producers have been asked to consider the costs of various increments in flashpoint. However, this is in absence of any real data on the effectiveness of modest (10 to 20°F) flashpoint increases in reducing fuel-tank flammability. There is an implicit assumption that an increase in flashpoint is, degree for degree, equivalent to decreasing the fuel temperature. Indeed, the relationship between flashpoint and spark ignition hazard for a complex fuel such as aviation kerosene has never been explored in detail. Key issues that need to be addressed when considering changing the flashpoint specification of Jet A are:

1. How much does increasing the flashpoint by 10°F shift the ignition energy vs. temperature relationship?

2. Does increasing the flashpoint by some amount, say 40°F accomplish the same decrease in ignition energy as decreasing the tank temperature, e.g., from 140 to 100°F?

3. With modest increases in the flashpoint, do we also decrease the fire risk associated with impact-survivable crashes and improve aviation safety overall?

4. Would a combination of fuel temperature reduction and a modest minimum flashpoint increase be a more effective solution to fuel-tank flammability than changing only one of these factors?

Studies addressing these issues need to consider the context of a typical flight envelop that contains a range of fuel temperatures and ambient pressures.

Previous flammability testing on Jet A, including this study, has been opportunistic and used readily available fuels. A systematic effort is now needed to relate spark ignition hazards to flashpoint in order to make further progress in safety analyses. Some key issues that need to be addressed in future testing are:

1. Relationship between flashpoint and ignition energy.

2. Ignition energy vs. temperature as a function of altitude.

3. Effect of fuel weathering on ignition energy.

4. The effect of ignition source type on ignition limits.

7.4 Future Work

The present results have raised a number of issues relevant to the aviation safety community. For the purposes of application to the TWA 800 accident, the key unresolved issue is weathering. For the purposes of remediation, a key issue is the applicability of the present results to the worldwide supply of Jet A, which has a broad range of flashpoints, 100 to 150°F and the whole envelop of flight conditions. In order to address these issues and other questions that came up during our program, the following steps are recommended:

1. Characterize the amount of energy in the spark that is actually deposited in the gas.
2. Repeat the Jet A ignition-energy measurements using several levels of ambient pressure to simulate the effect of altitude.
3. Repeat the measurements using samples of Jet A with various flashpoints.
4. Characterize the fuel used in the ignition tests by headspace gas chromatography.
5. Measure the ignition energy of weathered fuel.
6. Use alternate techniques such as burners to measure burning speed.
7. Use a experimental protocol and statistical analysis such as the up-down or Bruceton method (Dixon and Massey Jr. 1983), or the “One-Shot” test (Langlie 1962) to quantify the median value of ignition energy.

We plan to address some of these issues in the next series of tests. In addition, there are fundamental issues in ignition that need to be addressed:

1. Determine which chemical properties and species are most important in determining the ignition energy.
2. Develop a fundamental model of ignition energy that can be used to predict the effects of compositional changes and flashpoint variation.

These are long-term research problems that will require a concentrated effort by the combustion community in order to make progress.

Acknowledgments

Julian Lee was partially supported by a fellowship from FCAR of Quebec, Canada. Uli Pfahl and Oliver Kunz assisted on some ignition experiments.

References

Abbud-Madrid, A. and P. Ronney (1990). Effects of radiative and diffusive transport processes on premixed flames near flammability limits. In *Twenty-Third Symp. (Intl) Combustion*, pp. 423–431. The Combustion Institute, Pittsburgh, PA.

Affens, W. A. (1966). Flammability properties of hydrocarbon fuels. *J. Chem. Eng. Data 11*(2), 197–202.

Affens, W. A. and G. W. McLaren (1972). Flammability properties of hydrocarbon solutions in air. *J. Chem. Eng. Data 17*(4), 482–488.

ASTM D1655 (1997). *Standard Specification for Aviation Turbine Fuels*. American Society for Testing and Materials.

ASTM D56 (1988). *Standard Test Method for Flash Point by Tag Closed Tester*. American Society for Testing and Materials.

ASTM E1232 (1991). *Standard Test Method for Temperature Limit of Flammability of Chemicals*. American Society for Testing and Materials.

ASTM E582 (1988). *Standard Test Method for Minimum Ignition Energy and Quenching Distance in Gaseous Mixtures*. American Society for Testing and Materials.

ASTM E681 (1985). *Standard Test Method for Concentration Limits of Flammability of Chemicals*. American Society for Testing and Materials.

BAC (1972, March). An assesment of the spark ignition risk in aircraft fuel tanks. part a. electrical sparks. Memorandum, Systems Engineering Department, Commercial Aircraft Division, Britsh Aircraft Corporation Limited.

Ball, R. E. (1985). *The Fundamentals of Aircraft Combat Survivability Analysis and Design*. AIAA.

Ballal, D. and A. H. Lefebvre (1975). Ignition. *Combust. Flame 24*, 99.

Beery, G. T., R. G. Clodfelter, G. W. Gandee, J. L. Morris, J. R. McCoy, D. M. Spear, D. C. Wright, J. K. Klein, and T. O. Reed (1975). Assessment of JP-8 as a replacement fuel for the air force standard jet fuel JP-4. Technical Report AFAPL-TR-75-71, Air Force Aero Propulsion Laboratories, Wright-Patterson Air Force Base, Ohio.

Benedetti, R. P. (Ed.) (1996). *Flammable and Combustible Liquids Code Handbook*. National Fire Protection Association.

Blanc, M. V., P. G. Guest, G. von Elbe, and B. Lewis (1947). Ignition of explosive gas mixtures by electric sparks: I. minimum ignition energies and quenching distances of mixtures of methane, oxygen and inert gases. *J. Phys. Chem. 15*, 798–802.

Boeing, Airbus, et al. (1997). Industry response to faa on fuel system safety. Technical report, Boeing Commercial Airplane Group, http://www.boeing.com/news/techissues/pdf/FAARESPONSE.PDF. Authored by industry consortium: ATA, AEA, AAPA, EAAI, AIA.

Borghese, A., A. D'Alessio, M. Diana, and C. Venitozzi (1988). Development of hot nitrogen kernel, produced by a very fast spark discharge. In *Proc. 22nd Symp. (Intl) on Comb.*, pp. 1651–1659.

Bower, D. (1997, November). Flight test chairman's factual report. Accident DCA-96-Ma-070, NTSB Docket SA-516 Exhibit 23, National Transportation Safety Board.

Calcote, H., C. G. Jr., C. Barnett, and R. Gilmer (1952). Spark ignition-effect of molecular structure. *Industrial and Engineering Chemistry 44*(11), 2656–2662.

Coward, H. F. and G. W. Jones (1952). Limits of flammability of gases and vapors. Bulletin 503, Bureau of Mines.

CRC (1983). Handbook of aviation fuel properties. CRC Report 530, Society of Automotive Engineers, Warrendale, PA.

Crouch, K. (1994). Aircraft fuel system lightning protection design and qualifications test procedures development. Technical Report LT-94-1067, Lightning Technologies, Inc.

Dahn, C. J. (1998, March). Private communication. Safety Consulting Engineers, Schaumberg, Il.

Dixon, W. J. and F. J. Massey Jr. (1983). *Introduction to Statistical Analysis*. McGraw-Hill.

Eckhoff, R. (1975). Towards absolute minimum ignition energies for dust clouds. *Combust. Flame 24*, 53–64.

FAA (1997, April). Fuel tank ignition prevention measures. *Federal Register 62*(64), 16014–16024. Notice of Request for Comment on National Transportation Safety Board recommendations.

Fischer, F. A. and J. A. Plummer (Eds.) (1977). *Lightning Protection of Aircraft*, Chapter Fuel System Protection, pp. 115–184. Number RP-1008. NASA.

Fornia, T. (1997, October). Thermal modeling to predict fuel tank flammability. In *Transport Fuel Flammability Conference*. SAE/FAA.

Frechou, G. (1975). Inertage des etudes avions de carburant (in french). In *Aircraft Fire Safety*, Number 166 in AGARD Conference Proceedings, pp. 5–1. NATO.

Gaydon, A. G. and H. G. Wolfhard (1979). *Flames*. Chapman and Hall.

Gerstein, M. and R. D. Allen (1964). Fire protection research program for supersonic transport. Technical Report APL TDR-64-105, Air Force Aero Propulsion Laboratory, Wright-Patterson Air Force Base, Ohio.

Gerstein, M. A., O. Levine, and E. L. Wong (1951). Fundamental flame velocities of hydrocarbons. *Ind. Eng. Chem 43*(12), 2770–2772.

Gibbs, G. J. and H. F. Calcote (1959). Effect of molecular structure on burning velocity. *J. Chem. Eng. Data 4*(3), 226–237.

Göttgens, J., F. Mauss, and N. Peters (1992). Analytic approximations of burning velocities and flame thicknesses of lean hydrogen, methane, ethylene, ethane, acetylene and

propane flames. In *Twenty-Fourth Symposium (International) on Combustion*, pp. 129–135. The Combustion Institute.

Grenich, A. F. and F. F. Tolle (1983). Electrostatic safety with explosion suppresant foams. Technical Report AFWAL-TR-83-2015, Air Force Aero Propulsion Laboratories, Wright-Patterson Air Force Base, Ohio.

Kanury, A. M. (1988). *SFPE Handbook of Fire Protection Engineering*, Chapter Ignition of Liquid Fuels, pp. 1–315. NFPA.

Kleug, E. P. (1985). Antimisting fuel technology for transport category aircraft. In *Proceedings of the Fuel Safety Workshop*, pp. 11–60. Federal Aviation Administration.

Kono, M., S. Kumagai, and T. Sakai (1976). The optimum condition for ignition of gases by composite sparks. In *Proc. 16nd Symp. (Intl) on Comb.*, pp. 757–766.

Kono, M., K. Niu, T. Tsukamoto, and Y. Ujiie (1988). Mechanism of flame kernel formation produced by short duration sparks. In *Proc. 22nd Symp. (Intl) on Comb.*, pp. 1643–1649.

Kosvic, T., L. Zung, and M. Gerstein (1971). Analysis of aircraft fuel tank fire and explosion hazards. Technical Report AFAPL-TR-71-7, Air Force Aero Propulsion Laboratory, Wright-Patterson Air Force Base, Ohio.

Kuchta, J. M., , J. N. Murphy, A. L. Furno, and A. Bartkowski (1971). Fire hazard evaluation of thickened aircraft fuels. In *Aircraft Fuels, Lubricants and Fire Safety*, Volume 84 of *AGARD Conference Proceedings*, pp. 22–1 to 22–11.

Kuchta, J. M. (1975). Summary of ignition properties of jet fuels and other aircraft combustible fluids. Technical Report AFAPL-TR-75-70, U.S. Bureau of Mines.

Kuchta, J. M. (1985). Investigation of fire and explosion accidents in the chemical, mining, and fuel-related industries—a manual. Bulletin 680, U.S. Bureau of Mines.

Kuchta, J. M. and R. G. Clodfelter (1985). Aircraft mishap fire pattern investigations. Final Report APWAL-TR-85-2057, Aero Propulsion Laboratory.

Kunz, O. (1998, March). Combustion characteristics of hydrogen- and hydrocarbon-air mixtures in closed vessels. Technical Report FM98-4, GALCIT, California Institute of Technology.

Langlie, H. J. (1962). A test-to-failure program for thermal batteries. In *Sixteenth Annual Power Sources Conference*, pp. 117–120. PSC Publications Committee.

Lewis, B. and G. von Elbe (1947). Ignition of explosive gas mixtures by electric sparks. II. theory of the propagation of flame from an instantaneous point source of ignition. *J. Chem. Phys. 15*(11), 803–808.

Lewis, B. and G. von Elbe (1961). *Combustion, Flames and Explosions of Gases*. Academic Press.

Litchfield, E. L. (1960). Minimum ignition energy concept and its application to safety engineering. Report of Investigations 5671, Bureau of Mines.

Litchfield, E. L., M. H. Hay, T. A. Kubala, and J. S. Monroe (1967). Minimum ignition energy and quenching distance in gaseous mixtures. Report of Investigations 7009, Bureau of Mines.

Lou, H.-S. (1986). Experimental investigation of electrostatic fire and explosion accidents after aircraft landing and preventive design. In *ICAS Proceedings*, pp. 998–1009. American Institute of Aeronautics and Astronautics.

Magison, E. (1978). *Electrical Instruments in Hazardous Locations* (Third ed.)., pp. 69. The Instrument society of America.

Metghalchi, M. and J. C. Keck (1980). Laminar burning velocity of propane-air mixtures at high temperature and pressure. *Combust. Flame 38*, 143–154.

Nestor, L. (1967). Investigation of turbine fuel flammability within aircraft fuel tanks. Final Report DS-67-7, Naval Air Propulsion Test Center, Naval Base, Philadelphia.

NFPA (1993). *NFPA 77 Recommended Practice on Static Electricity*. National Fire Protection Association.

Ott, E. (1970). Effects of fuel slosh and vibration on the flammability hazards of hydrocarbon turbine fuels within aircraft fuel tanks. Technical Report AFAPL-TR-70-65, Fire Protection Branch of the Fuels and Lubrication Division, Wright-Patterson Air Force Base, Ohio.

Parker, S. J. (1985). *Electrical Spark Ignition of Gases and Dusts*. Ph. D. thesis, City University, London.

Plummer, J. A. (1992). Technical Report LT-92-764, Lightning Technologies, Inc.

Potter, A. E. (1960). Flame quenching. In *Progress in Combustion Science and Technology*, Volume 1, pp. 145–181. Peramon Press.

Ronney, P. (1985). Effect of gravity on laminar premixed gas combustion ii: Ignition and extinction phenomena. *Combust. Flame 62*, 121–133.

Ronney, P. and H. Wachman (1985). Effect of gravity on laminar premixed gas combustion ii: Flammability limits and burning velocities. *Combust. Flame 62*, 107–119.

Roth, A. J. (1987). Development and evaluation of an airplane fuel tank ullage composition model - volume II: Experimental determination of airplane fuel tank ullage compositions. Technical Report AFWAL-TR-87-2060, Volume II, Air Force Wright Aeronautical Laboratories, Wright-Patterson Air Force Base, Ohio.

Sagebiel, J. C. (1997, November). Sampling and analysis of vapors from the center wing tank of a test Boeing 747-100 aircraft. Final report for NTSB, Desert Research Institute.

Seibold, D. W. (1987). Development and evaluation of an airplane fuel tank ullage composition model - volume i: Airplane fuel tank ullage computer model. Technical Report AFWAL-TR-87-2060, Volume I, Air Force Wright Aeronuatical Laboratories, Wright-Patterson Air Force Base, Ohio.

Shepherd, J. E., J. C. Krok, and J. J. Lee (1997, June). Jet A explosion experiments: Laboratory testing. Explosion Dynamics Laboratory Report FM97-5, California Institute of Technology.

Shepherd, J. E., J. C. Krok, J. J. Lee, L. L. Brown, R. T. Lynch, T. M. Samaras, and M. M. Birky (1998, July). Results of 1/4-scale experiments, vapor simulant and liquid Jet A tests. Explosion Dynamics Laboratory Report FM98-6, California Institute of Technology.

Strid, K.-G. (1973). Experimental techniques for the determination of ignition energy. In *Oxidation and Combustion Reviews*, pp. 1–46.

Ural, E. A., R. G. Zalosh, and F. Tamanini (1989). Ignitability of jet-a fuel vapors in aircraft fuel tanks. In *Aircraft Fire Safety*, AGARD Conference Proceedings, pp. 14–4.

Woodrow, J. E. and J. N. Seiber (1997, November). The laboratory characterization of jet fuel vapors under simulated flight conditions. Final report for NTSB, Order No. NTSB12-97-SP-0255, University of Nevada, Reno, Nevada.

Zabetakis, M., G. S. Scott, and G. W. Jones (1951). Limits of flammability of paraffin hydrocarbons in air. *Ind. Eng. Chem. 43*(9), 2120–2124.

Zabetakis, M. G. (1965). Flammability characteristics of combustible gases and vapors. Bulletin 627, Bureau of Mines.

A Test Conditions

Table 5: Propane-air mixtures.

Date	Run	Fuel (%)	Gap (mm)	E (GO) (J)	E (NOGO) (J)	P_{max} (bar)	K_g (bar-m/s)	Su (m/s)	C (nF)	V (kV)	Trigger
6/29/97	679	3	3.3		0.0053				0.0581	13.5	switch
6/29/97	679	3	3.3	0.456		6.74	17.4	0.29	5	13.5	switch
6/29/97	680	2.8	3.3		0.04				*		TM-11
6/29/97	681	3.3	3.3		0.0027				0.0317	13.05	switch
6/29/97	681	3.3	3.3	0.04		7.25	22.6	0.35	*		TM-11
6/29/97	682	3.5	3.3	0.0027		7.5	31.0	0.41	0.0317	13.05	switch
6/30/97	684	2.5	3.3		1				500	2	TM-11
6/30/97	684	2.5	3.3	8		4.09	4.2	0.08	500	5.66	TM-11
6/30/97	685	2	3.3		1				500	2	TM-11
6/30/97	685b	2	3.3		8				500	5.66	TM-11
6/30/97	689	2.7	3.3	0.04		6.15	11.6	0.19	*		TM-11
6/30/97	690	2.4	3.3		0.04				*		TM-11
6/30/97	690b	2.4	3.3		0.45				500	1.342	TM-11
6/30/97	690c	2.4	3.3		1				500	2	TM-11
6/30/97	690c	2.4	3.3	8		4.19	4.6	0.09	500	5.66	TM-11
6/30/97	691	2.2	3.3		0.04				*		TM-11
6/30/97	691b	2.2	3.3		0.45				500	1.342	TM-11
6/30/97	691c	2.2	3.3		1				500	2	TM-11
6/30/97	691d	2.2	3.3		4				500	4	TM-11
6/30/97	691e	2.2	3.3		8				500	5.66	TM-11
6/30/97	692	2.7	3.3		0.04				*		TM-11
6/30/97	692	2.7	3.3	0.45		6.38	13.7	0.22	500	1.342	TM-11
6/30/97	693	2.6	3.3		0.04				*		TM-11
6/30/97	693b	2.6	3.3		0.45				500	1.342	TM-11
6/30/97	693c	2.6	3.3		1				500	2	TM-11
6/30/97	693d	2.6	3.3		4				500	4	TM-11
6/30/97	693e	2.6	3.3		8				500	5.66	TM-11
6/30/97	693f	2.6	3.3		16				500	8	TM-11
6/30/97	694	2.7	3.3	0.45		6.05	11.4	0.22	5	13.42	switch
6/30/97	695	2.6	3.3	0.45		5.81	10.4	0.21	5	13.42	switch
7/1/97	696	2.5	3.3		0.45				5	13.42	switch
7/1/97	696b	2.5	3.3		0.04				*		TM-11
7/1/97	696c	2.5	3.3		0.45				500	1.342	TM-11
7/1/97	696d	2.5	3.3		1				500	2	TM-11
7/1/97	696d	2.5	3.3	4		4.49	5.0	0.09	500	4	TM-11
7/1/97	697	2.6	3.3		0.04				*		TM-11
7/1/97	697	2.6	3.3	0.45		5.59	9.4	0.18	500	1.342	TM-11
7/1/97	698	2.3	3.3		8				500	5.66	TM-11
7/1/97	698b	2.3	3.3		20				500	8.9	TM-11
7/1/97	698b	2.3	3.3	20.5		3.65	2.6	0.06	500	9.1	TM-11
7/1/97	699	2.2	3.3		20				500	8.9	switch
7/1/97	699b	2.2	3.3		40				500	12.65	switch
7/1/97	699c	2.2	3.3		45.6				500	13.5	switch
7/7/97	709	2.3	3.3	30		4.5	5.0	0.12	500	10.95	switch
7/7/97	710	2.2	3.3	30		3.42	19.6	0.06	500	10.95	switch
7/8/97	712	2.1	3.3	30		3.22	15.5	0.09	500	10.95	switch
7/8/97	713	2	3.3		30				500	10.95	switch
7/8/97	713b	2	3.3		45.6				500	13.5	switch

* Spark energy from the TM-11A trigger module spark (30kV)

Table 6: Hexane-air mixtures.

Date	Run	Fuel (%)	Gap (mm)	E (GO) (J)	E (NOGO) (J)	P_{max} (bar)	K_g (bar-m/s)	Su (m/s)	C (nF)	V (kV)	Trigger
6/20/97	647	2.2	4?	0.04					*		TM-11
6/20/97	648	2	4?		0.04				*		TM-11
6/20/97	648b	2	4?		0.05				500	0.45	TM-11
6/20/97	648b	2	4?	0.1		7.7	27.6	0.40	500	0.63	TM-11
6/20/97	649	1.6	4?		0.1				500	0.63	TM-11
6/20/97	649b	1.6	4?		1				500	2.00	TM-11
6/20/97	649c	1.6	4?		8				500	5.66	TM-11
6/20/97	650	1.8	4?		1				500	2.00	TM-11
6/20/97	650	1.8	4?	8		7.44	23.3	0.37	500	5.66	TM-11
6/20/97	651	1.7	4?		1				500	2.00	TM-11
6/20/97	651	1.7	4?		8				500	5.66	TM-11
6/22/97	654	1.4	6	8					500	5.66	TM-11
6/23/97	655	4.1	6	0.04		8.11	18.8	0.16	*		TM-11
6/23/97	656	6.8	6		0.04				*		TM-11
6/23/97	657	6	6	0.04		2.74	3.4	0.13	*		TM-11
6/23/97	662	5.75	6		0.04				*		TM-11
6/23/97	663	5	6	0.04		3.06	3.5	0.08	*		TM-11
6/23/97	665	2.2	6	0.04		8	35.9	0.46	*		TM-11
6/23/97	666	1.7	6	0.04		7.6	25.2	0.32	*		TM-11
6/23/97	667	1.2	6		0.04				*		TM-11
6/26/97	668	1.4	6		0.04				*		TM-11
6/26/97	669	5.2	6	0.04					*		TM-11
6/26/97	670	2.1	3.3	0.004		8.35	43.0	0.50	0.058	11.73	switch
6/27/97	671	1.6	3.3		0.004				0.058	11.73	switch
6/27/97	672	1.8	3.3		0.004				0.058	11.73	switch
6/28/97	673	1.8	3.3	0.04		7.75	29.8	0.38	*		TM-11
6/28/97	674	1.6	3.3		0.04				*		TM-11
6/28/97	674	1.6	3.3	0.36					5	12.00	switch
6/28/97	675	1.4	3.3		0.36				5	12.00	switch
6/29/97	676	2.2	3.3	0.0016		8.59	50.8	0.51	0.032	10.00	switch
6/29/97	677	2	3.3	0.0016		8.23	39.9	0.49	0.032	10.00	switch
6/29/97	678	1.8	3.3		0.0016				0.032	10.00	switch
6/30/97	686	1.4	3.3	1					500	2.00	TM-11
6/30/97	687	1.2	3.3	1		6.54	13.8	0.20	500	2.00	TM-11
6/30/97	688	1	3.3		1				500	2.00	TM-11
6/30/97	688b	1	3.3		8				500	5.66	TM-11
7/1/97	700	1	3.3		20				500	8.94	switch
7/1/97	700b	1	3.3		40				500	12.65	switch
7/1/97	700c	1	3.3		45.6				500	13.50	switch
7/1/97	701	1.1	3.3		45.6				500	13.50	switch
7/1/97	701b	1.1	3.3		20				500	8.94	switch
7/1/97	702	1.2	3.3		0.45				500	1.34	TM-11
7/1/97	702b	1.2	3.3		1				500	2.00	TM-11
7/1/97	702c	1.2	3.3		8				500	5.66	TM-11
7/1/97	702d	1.2	3.3		20				500	8.94	TM-11
7/2/97	703	1.2	3.3		0.04				*		TM-11
7/2/97	703b	1.2	3.3		0.45				500	1.34	TM-11
7/2/97	703c	1.2	3.3		1				500	2.00	TM-11
7/2/97	703d	1.2	3.3		8				500	5.66	TM-11
7/2/97	703e	1.2	3.3		20				500	8.90	TM-11
7/2/97	704	1.4	3.3	1		6.7	14.9	0.21	500	2.00	TM-11
7/7/97	708	1.2	3.3	20		4.25	22.6	0.08	500	8.90	switch
7/7/97	711	1.1	3.3		30				500	10.95	switch
7/7/97	711b	1.1	3.3		45.6				500	13.50	switch

* Spark energy from the TM-11A trigger module spark (30kV)

Table 7: Jet A-air mixtures in 1.84-liter vessel.

Date	Run	M/V	T	P	Gap	E (GO)	E (NOGO)	P_{max}	K_g	Su	C	V	Trigger	Jet A
		(kg/m^3)	(^oC)	(Torr)	(mm)	(J)	(J)	(bar)	(bar-m/s)	(m/s)	(nF)	(kV)		
7/11/97	714	3	40.8	436.5	3.3		0.04				*		TM-11	LAX
7/11/97	714	3	40.8	436.5	3.3	45.6					500	13.5	switch	LAX
7/12/97	715	200	26.8	439	3.3		1				500	2.0	TM-11	LAX
7/12/97	715b	200	26.8	439	3.3		10				500	6.3	TM-11	LAX
7/12/97	715c	200	26.8	439	3.3		8				500	5.8	breakdown	LAX
7/12/97	715d	200	26.8	439	4		20				500	8.9	TM-11	LAX
7/12/97	715e	200	26.8	439	6		9				500	6.0	breakdown	LAX
7/12/97	715f	200	26.8	439	8		13.7				500	7.4	breakdown	LAX
7/12/97	715g	200	26.8	439	10		14				500	7.5	breakdown	LAX
7/12/97	715h	200	26.8	439	10		16				500	8.0	breakdown	LAX
7/12/97	715i	200	27.3	439	15		40				500	12.6	TM-11	LAX
7/13/97	716	200	26.2	438	3.3		100				*		neon transf. 1s	LAX
7/13/97	717	200	30.2	439.2	3.3		0.04				*		TM-11	LAX
7/13/97	717b	200	30.2	439.2	3.3		0.45				5	13.4	switch	LAX
7/13/97	717e	200	30.2	439.2	3.3		20				500	8.9	switch	LAX
7/13/97	717f	200	30.2	439.2	3.3		45.6				500	13.5	switch	LAX
7/13/97	717g	200	30.3	439.2	3.3	80		2.40			1000	12.6	switch	LAX
7/14/97	718	200	35.4	439.4	3.3		1				500	2.0	TM-11	LAX
7/14/97	718b	200	35.4	439.4	5		18				500	7.0	breakdown	LAX
7/14/97	718c	200	35.4	439.4	3.3	30		3.05			500	11.0	switch	LAX
7/14/97	719	200	41.3	438.2	3.3	0.45		3.59			500	1.3	TM-11	LAX
7/14/97	720	200	40.9	439.1	3.3		0.04				*		TM-11	LAX
7/14/97	721	200	45.8	438.9	3.3	0.04		4.03			*		TM-11	LAX
7/14/97	722	200	46.2	439	3.3		0.0053				0.058	13.5		LAX
7/14/97	723	200	51.3	438.5	3.3		0.0053				0.058	13.5		LAX
7/14/97	723	200	51.3	438.5	3.3	0.04		4.05			*		TM-11	LAX
7/15/97	724	3	35.8	438.7	3.3	0.45		3.37			5	13.4	switch	LAX
7/16/97	12	3	35.8	438.5	3.3		0.004				0.058	12.0	switch	LAX
7/16/97	12b	3	35.8	438.5	3.3		0.04				*		TM-11	LAX
7/16/97	12c	3	35.8	438.5	3.3		0.45				5	13.5	switch	LAX
7/16/97	12c	3	35.8	438.5	3.3	20					500	9.0	switch	LAX
7/16/97	13	3	36	439.4	3.3		5				1000	3.2	TM-11	LAX
7/16/97	13b	3	36	439.4	3.3	20		1.20	3.3	0.06	500	9.0	switch	LAX
7/17/97	14	3	40.5	438.8	3.3		0.04				*		TM-11	LAX
7/17/97	14b	3	40.5	438.8	3.3		0.45				1000	1.0	TM-11	LAX
7/17/97	14c	3	40.5	438.8	3.3		5				1000	3.1	TM-11	LAX
7/17/97	14d	3	39.4	438.8	3.3		10				1000	4.5	TM-11	LAX
7/17/97	14d	3	39.4	438.8	3.3	20		3.31	7.5	0.20	500	9.0	switch	LAX
7/17/97	15	3	45.8	438.8	3.3	0.04		4.19	17.0	0.35	*		TM-11	LAX
7/17/97	16	3	50.6	438.5	3.3	0.005		4.31	22.0	0.41	0.058	13.1	switch	LAX
7/18/97	17	3	56.1	439	3.3	0.001		4.28	21.0	0.50	0.058	11.2	switch	LAX
7/20/97	18	3	40.7	438.9	3.3		0.04				*		TM-11	LAX
7/20/97	18	3	40.7	438.9	3.3	1		3.14	9.0	0.18	1000	1.5	TM-11	LAX
7/21/97	19	3	45.9	438.8	3.3		0.002				0.032	11.2	switch	LAX
7/21/97	19b	3	45.9	438.8	3.3		0.005				0.058	13.1	switch	LAX
7/21/97	19c	3	45.9	438.8	3.3		0.04				*		TM-11	LAX
7/21/97	19d	3	45.9	438.8	3.3	0.3		3.91	16.0	0.20	5	10.8	switch	LAX
7/22/97	20	3	50.9	439	3.3		0.002				0.032	11.2	switch	LAX
7/22/97	20	3	50.9	439	3.3	0.004		4.27	20.0	0.48	0.058	11.7	switch	LAX
7/24/97	21	200	56	439	3.3	0.002		4.17	17.5	0.34	0.032	11.2	switch	LAX
7/24/97	22	200	45.6	438.9	3.3		0.003				0.032	13.8	switch	LAX
7/24/97	22	200	45.6	438.9	3.3	0.006		4.10	19.7	0.44	0.058	14.4	switch	LAX
7/24/97	23	200	35.8	438.9	3.3		0.04				*		TM-11	LAX
7/24/97	23b	200	35.8	438.9	3.3		1				1000	1.4	TM-11	LAX
7/24/97	23c	200	35.8	438.9	3.3		15				1000	5.5	TM-11	LAX

Table 8: Jet A-air mixtures in 1.84-liter vessel (continued).

Date	Run	M/V	T	P	Gap	E (GO)	E (NOGO)	P_{max}	K_g	Su	C	V	Trigger	Jet A
		(kg/m^3)	(^oC)	(Torr)	(mm)	(J)	(J)	(bar)	(bar-m/s)	(m/s)	(nF)	(kV)		
7/24/97	23c	200	35.8	438.9	3.3	20		2.57	3.1	0.08	500	8.9	switch	LAX
7/24/97	24	200	40.9	438.9	3.3		0.04				*		TM-11	LAX
7/24/97	24	200	40.9	438.9	3.3	0.2		3.53	9.9	0.32	5	8.9	switch	LAX
7/25/97	25	200	26.1	438.8	3.3		45				1000	10.0	switch	LAX
7/25/97	25b	200	26.3	438.8	3.3		90				1000	13.5	switch	LAX
7/25/97	26	200	30.6	438.9	3.3		30				500	11.0	switch	LAX
7/25/97	26b	200	30.6	438.9	3.3		60				1000	11.0	switch	LAX
7/25/97	26c	200	30.6	438.9	3.3		104				1000	14.4	switch	LAX
7/25/97	27	200	50.4	439	3.3	0.0035		4.15	19.0	0.60	0.032	14.9	switch	LAX
7/26/97	28	200	30.7	438.9	3.3		104	0.90			1000	14.4	switch	LAX
7/26/97	29	200	31.8	438.6	3.3	104		1.90			1000	14.4	switch	LAX
7/27/97	30	3	30.6	439	3.3		104				1000	14.4	switch	El Monte
7/27/97	31	3	40.5	438.9	3.3		0.45				1000	0.9	TM-11	El Monte
7/27/97	31b	3	40.5	438.9	3.3		5				1000	3.2	TM-11	El Monte
7/27/97	31b	3	40.5	438.9	3.3	50		2.31	11.1	0.10	500	14.1	switch	El Monte

* Spark energy from the TM-11A trigger module spark (30kV)

Table 9: Tests in the 1180-liter vessel.

Run	Date	Fuel	Quantity	T (C)	P (mbar)	Ignition	Fan	P_{max} (bar)	Proc
440	5 Jun 97	Hexane	100 ml	23.6	1000	TM-11, 2.3 mm		NO GO	A
441	6 Jun 97	Jet A	700 ml	39.2	585	.5µF, 6kV, 3 mm		NO GO	B
442	11 Jul 97	Propane	4%	22.9	1000	TM-11, 3.5 mm		8.55	A
443	13 Jul 97	Propane	2.1%	23.2	1000	1µF, 8 kV, 10 mm		NO GO	A
444	14 Jul 97	Propane	2.5%	24.0	1000	.5µF, 8 kV, 10 mm		long burn	A
445	14 Jul 97	Propane	2.5%	26.2	1000	.5µF, 8 kV, 10 mm		4.73	A
446	14 Jul 97	Propane	2.3%	28.0	1000	.5µF, 8 kV, 10 mm		4.31	A
447	14 Jul 97	Propane	2.2%	29.2	1000	.5µF, 8 kV, 10 mm	on	NO GO	A
448	14 Jul 97	Propane/H2	1/4%	31.0	1000	.5µF, 8 kV, 10 mm	on	3.28 (slow)	A
449	15 Jul 97	Propane/H2	1/6%	26.0	1000	.5µF, 8 kV, 10 mm		4.16	A
450	15 Jul 97	Propane/H2	0.5/6%	26.0	1000	.5µF, 8 kV, 10 mm		stabilized	A
451	15 Jul 97	Propane/H2	0.5/8%	28	1000	.5µF, 7.7 kV, 10 mm		4.04	A
452	15 Jul 97	H2	8%	28.6	1000	.5µF, 7.7 kV, 10 mm		stabilized	A
453	15 Jul 97	H2	10%	28.6	1000	.5µF, 7.7 kV, 10 mm		3.69	A
454	16 Jul 97	Jet A	4.4 liter	40.6	1000	.5µF, 7.7 kV, 10 mm		lost	C
456	18 Jul 97	Propane	2.5%	29.2	1000	.5µF, 7.7 kV, 10 mm	on	6.00	A
457	18 Jul 97	Hydrogen	10%	32.0	1000	.5µF, 7.7 kV, 10 mm	on	3.80	A
458	18 Jul 97	Methane	9.5%	32	1000	TM-11, 10 mm		7.61	A
459	19 Jul 97	Methane	9.5%	27.1	1000	TM-11, 10 mm	on	7.94	A
460	19 Jul 97	Hexane	1.5% (94.4 ml)	30.3	1000	.5µF, 7.7 kV, 10 mm		5.64	A
461	19 Jul 97	Hexane	1.5% (94.4 ml)	33.1	1000	.5µF, 7.7 kV, 10 mm	on	6.44	A
462	19 Jul 97	Hexane	1.2% (75.5 ml)	25.7	1000	xfmr, 10 mm		slow burn	A
463	20 Jul 97	Hexane	1.2% (75.5 ml)	28.3	1000	xfmr, 10 mm	on	5.14	A
464	26 Jul 97	Jet A	4.4 liter	40.8	585	xfmr, 10 mm		2.68	C
466	26 Jul 97	Jet A	4.4 liter	40.1	585	xfmr, 10 mm		2.53	C
468	26 Jul 97	Jet A	4.4 liter	40.4	585	xfmr, 10 mm	on	3.13	C
470	26 Jul 97	Jet A	4.4 liter	49.4	585	.5µF, 4 kV, 10 mm		3.9	C
472	1 Aug 97	Propane	3.5%	31.8	1000	Estes		7.65	A
473	1 Aug 97	Propane	3.0%	35.2	1000	Estes		6.34	A
474	1 Aug 97	Propane	2.3%	35.3	1000	Estes no, xfmr	on	4.93	A
475	4 Sep 97	Propane	2.3%	22.3	843	.5µF, 7.7 kV, 10 mm		NO GO	D
476	4 Sep 97	Propane	2.5%	26.2	834	.5µF, 7.7 kV, 10 mm		4.11	D
477	4 Sep 97	Propane/H2	2.5/10%	26.5	834	.5µF, 7.7 kV, 10 mm		6.71	D
478	5 Sep 97	Propane/H2	2.5/6%	25.1	834	.5µF, 7.7 kV, 10 mm		5.90	D
479	5 Sep 97	Propane/H2	2.5/6%	26.0	834	.5µF, 7.7 kV, 10 mm		5.93	A
480	8 Sep 97	Propane/H2	2.0/6%	22.9	834	.5µF, 7.7 kV, 10 mm		5.55	A
481	8 Sep 97	Propane/H2	1.8/6%	24.9	834	.5µF, 7.7 kV, 10 mm		5.30	A
482	9 Sep 97	Propane/H2	1.5/6%	24.3	834	.5µF, 7.7 kV, 10 mm		4.67	A
483	9 Sep 97	Propane/H2	1.4/8%	26.3	834	.5µF, 7.7 kV, 10 mm		4.77	A
484	9 Sep 97	Propane/H2	1.4/7%	27.6	834	.5µF, 7.7 kV, 10 mm		4.49	A
485	9 Sep 97	Propane/H2	1.3/7%	28.0	834	.5µF, 7.7 kV, 10 mm		4.62	A
486	10 Sep 97	Propane/H2	1.2/7%	25.2	834	.5µF, 7.7 kV, 10 mm		4.19	A
487	19 Sep 97	Jet A	4.4 l	59.6	585	.5µF, 7.7 kV, 10 mm		4.48	C
489	24 Sep 97	Propane/H2	1.4/7%	25.8	834	ΓM-11, drvr 1/2 quench		pass	A
490	24 Sep 97	Propane/H2	1.4/7%	27.4	834	ΓM-11, drvr 1/4 quench		fail	A
491	25 Sep 97	Propane/H2	1.4/7%	27.0	834	ΓM-11, drvr 1/4 quench		fail	A
492	26 Sep 97	Propane/H2	1.4/7%	24.3	834	Davey Fire		4.96	A
493	29 Sep 97	Propane/H2	1.4/7%	23.2	834	TM-11, spark plug	on	4.76	A

Procedures

A Inject fuels/gasses, mix 10 min, fire

B Inject fuel w/ fan on, wait 30 min w/ fan off, mix 10 min, fire

C Pour fuel, evac to 450 mb (approx), fan on 20 min per hour for four hours. Add air to 585 mb, mix 10 min, fire.

D Same procedure as A but using 50/50 O2/N2 instead of Air

B Hot Filament Ignition of Jet A

Five laboratory tests were carried out to investigate the hot filament ignition of Jet A. These tests are reported as shots 779, 782,783, 784, and 799 in the study of Kunz (1998). These tests duplicated the main features in the ignition circuit used in the tests carried out in the 1/4-scale facility experiments at Denver, CO and reported in Shepherd et al. (1998). Our circuit consisted of a 1300 μF capacitor charged to 150 volts and discharged through a mechanical relay into the filament of type 1156 light bulb with the glass envelope removed. A 1000 Ω series resistor was used between the capacitor and the power supply to limit current during charging phase. An 0.6 Ω resistor was used between the capacitor and the light bulb in order to simulate the resistance of the firing line used at Denver. Observation with a photodiode indicated that the filament reached a peak temperature rapidly after the current was applied. Visual observation and continuity measurements indicated that the filament remained intact and did not produce any molten fragments. This was important in the 1/4-scale tests in order to produce a repeatable initial condition. Even though 15 J of energy are deposited in the filament, no spark is created since the continuity in the circuit is never broken.

Four tests were carried out at a temperature of 50°C and one test was performed at 40°Cin the 1.8 liter vessel facilty. All tests used a mass loading of about 3 kg/m^3 and an initial pressure of 0.585 bar, simulating the conditions of the TWA Flight 800 accident. All tests resulted in ignition and a propagating flame. Figure 44 shows pressure and temperature traces for 6.9 ml of fuel sample #5 with air (test 784 of Kunz 1998) at initial conditions of p_0 = 58.5 kPa, T_0 = 323 K. Repeat tests using the filament and spark source indicated that the development of the flame was identical in two cases as demonstrated by the near coincidence of the pressure-time traces. This is shown in Fig. 45 using El Monte Jet A. Test 776 used 200 cc of Jet A in 0.585 bar of air at 50°C and the 40 mJ TM-11 source while test 779 had the same conditions but used the light bulb filament igniter. The only differences between the two traces are some "spikes" near t = 0.27 s. These are artifacts created by the ignition circuit electrical transient coupling into the data acquisition circuit. The difference in peak pressure between the two tests is typical of the experimental uncertainty in Jet A experiments.

Figure 46 shows the corresponding Schlieren video pictures. The time delay between two frames is 17 ms. The window has a diameter of about 60 mm. In picture (a), the light bulb setup can be seen just before the ignition. The two pairs of electrodes (one behind the other one) belong to spark ignition systems were not used in this experiment. As discussed in Kunz (1998), the fuel used in test 784 was a sample of Jet A from Athens that had been used in the flight tests at JFK and was "weathered" to a certain extent.

In the lower part of the picture, the socket of the light bulb can be seen. The glass of the bulb is removed. Wires are soldered to the socket to allow connection to the electrical system. The point of ignition is the filament just above the spark gap. The second picture (b) is taken 17 ms after the ignition. The light emission causing the image to "bloom" results from the incandescence of the filament. In the upper middle part of the emission, a small part of the flame surface can be seen. The third picture (c) shows the nearly spherical flame 34 ms after ignition. The influence of buoyancy can be seen as the flame propagates slightly faster in the upward than in the downward direction. In the last picture (d), only a small part of the flame

surface can be seen in the lower left corner.

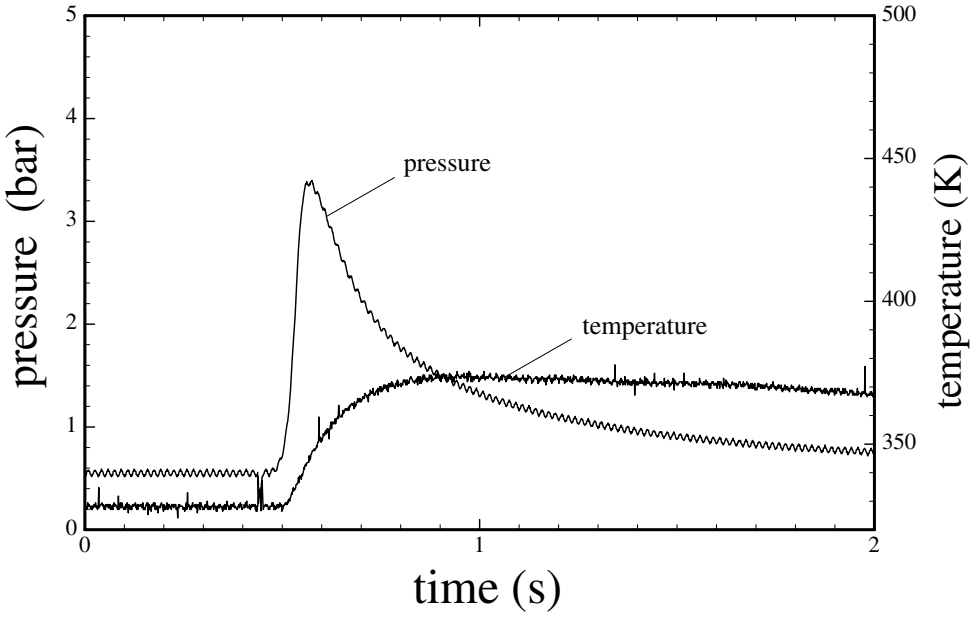

Figure 44: Pressure and temperature vs. time for 6.9 ml of Jet A sample #5 with air in the 1.8 liter vessel at initial conditions of p_0 = 58.5 kPa, T_0 = 323 K, hot filament ignition. Test 784 of (Kunz 1998).

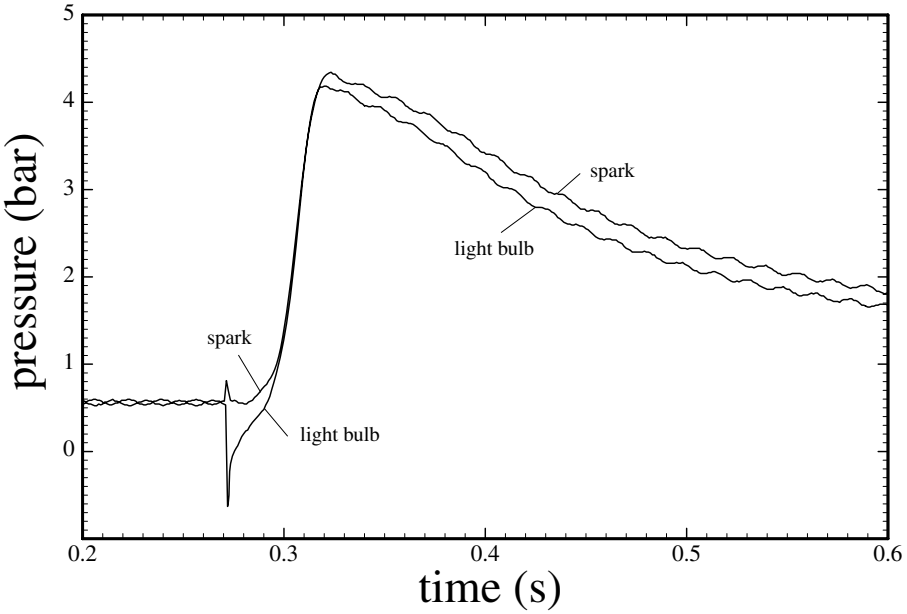

Figure 45: Pressure vs. time for 200 ml of Jet A (El Monte) with air in the 1.8 liter vessel at initial conditions of p_0 = 58.5 kPa, T_0 = 323 K Test 776 uses a 40 mJ spark ignition, test 779 uses hot filament ignition (Kunz 1998).

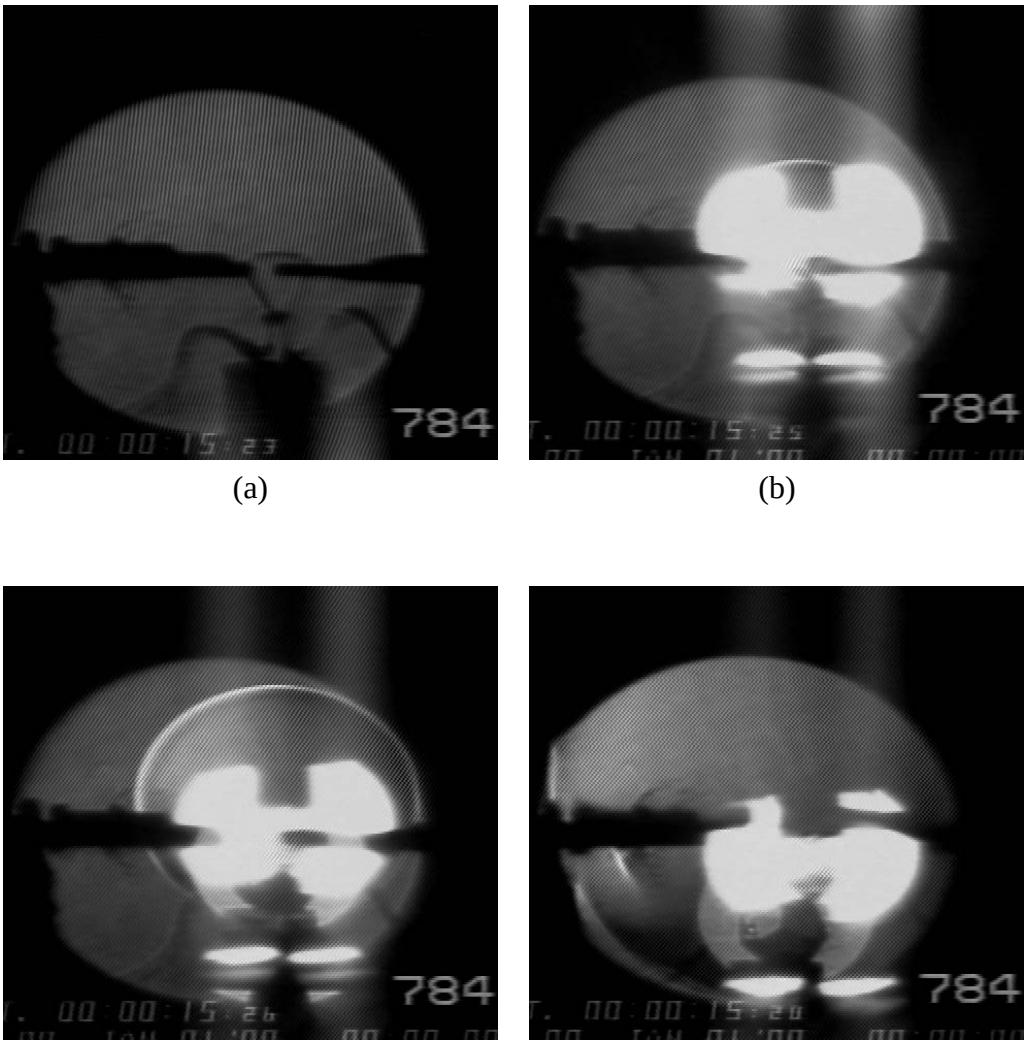

(a) (b)

(c) (d)

Figure 46: Video schlieren pictures of the hot filament ignition of Jet A sample #5 in the 1.8 liter vessel at initial conditions of p_0 = 58.5 kPa, T_0 = 323 K, the time interval between two frames is 17 ms. Test 784 of (Kunz 1998).